Fasting alters histone methylation in paraventricular nucleus through regulating of polycomb repressive complex 2

Ying Jiang

Dissertation submitted to the faculty of the Virginia Polytechnic Institute and State University in partial fulfillment of the requirements for the degree of

Doctor of Philosophy

In

Animal and Poultry Sciences

Michael D. Denbow

Cynthia J. Denbow

Mark A. Cline

Paul B. Siegel

7-16-2013

Blacksburg, VA

Keywords: Neuroscience, Epigenetics, Histone, Fasting, PVN, EZH2, PRC2, BDNF

Fasting alters histone methylation in paraventricular nucleus through regulating of polycomb repressive complex 2

Ying Jiang

ABSTRACT

The developing brain is highly sensitive to environmental influences. Unfavorable nutrition is one kind of stress that can cause acute metabolic disorders during the neonatal period [1,2,3] and severe diseases in later life [4,5]. These early life experiences occurring during heightened periods of brain plasticity help determine the lifelong structural and functional aspects of brain and behavior. In humans, for example, weight gain during the first week of life increased the propensity for developing obesity several decades later [5]. This susceptibility is, if not all, related to the dynamic reversible epigenetic imprints left on the histones [6,7,8], especially during the prenatal and postpartum period [9].

Histones are highly dynamic and responsive towards environmental stress [10,11]. Through covalent modification of the histone tail, histones are able to direct DNA scaffolding and regulate gene expression [10,12]. Thus far, various types of post translational modifications have been identified on various histones tails [12]. Among them, the methylation and acetylation on lysine residue (K) 27 on histone 3 (H3) has been tightly linked to gene repression [13,14] and activation [15], respectively. EZh2 (enhancer of zeste 2) in the polycomb repressive complex 2 (PRC2) is the only methyltransferase that has been linked to catalyze this methylation reaction. In addition, SUZ (suppressor of zeste) and EED (embryonic ectoderm development) are two other key proteins in PRC2 function core that help EZH2. As previous reported, increased H3K27 methylation was monitored after fasting stress during neonatal period in chicks' paraventricular nucleus (PVN). In this study, we investigated the detailed mechanism behind changes in H3K27 methylation following fasting stress.

After 24 hours fasting on 3 days-of-age (D3), chicks exhibited elevated mRNA levels of PRC2 key components, including EZH2, SUZ and EED, in the PVN on D4. Western blots confirmed this finding by showing increased global methylation status at the H3K27 site in the PVN on D4. In addition, until 38 days post fasting, SUZ and EZH2 remained inhibited. A newly identified anorexigenic factor, Brain-derived neurotrophic factor (BDNF), was used as an example of multiple hormones expressed in PVN to verify this finding. Both BDNF protein and mRNA exhibited compatible changes to global changes of tri- (me3) and di-methylated (me2) H327. Furthermore, by using chromatin immunoprecipitation assays (ChIP), we were able to monitor the changes of H3K27me2/me3 deposition along the *Bdnf* gene. Fasting significantly increased H3K27me2/me3 as well as EZH2 at the *Bdnf*'s promoter, transcription start site and 3'-untranslated region. These data show that fasting stress during the early life period could leave epigenetic imprinting in PVN for a long time. Next, we tried to understand the function of this epigenetic imprinting in the chicks' PVN. Thus, we compared naive chicks (never fasted) to chicks that received either a single 24 hour fast on D3 or two 24 hour fast on both D3 and 10 days-of-age (D10). We found that

the D3 fasted group significantly increased the level of PRC2 key components and its product H3K27me2/me3 compared to the naive group. However, D3 fasting and D10 fasting together decreased the surges of H3K27me2/me3, SUZ and EED (not EZH2) compared to the naive group. We called this phenomenon "epigenetic memory". The Western blot, qPCR and CHIP assay results from BDNF all confirmed the existence of "epigenetic memory" for PRC2. These data suggested that fasting stress during the early period of brain development could leave long term epigenetic modifications in neurons. These changes could be beneficial to the body, which keeps homeostasis of inner environment and prevent massive response to future same stress.

The EZH2 protein was knocked down and the H3K27 methylation status changes were monitored after applying the same treatment. We first confirmed that EZH2 antisense oligonucleotides (5.5 ug), but not EZH2 siRNA and artificial cerebrospinal fluid (ACSF), inhibit EZH2 protein by 86 % in the PVN. Then, on D3, chicks were subjected to a 24 hour fasting stress (D3-fasting) post either EZH2 antisense or ACSF injection. The EZH2 antisense blocked the surge of both EZH2 mRNA and H3K27 methylation after D3-fasting. At the same time, BDNF exhibited elevated expression levels and less methylated H3K27 deposition along the *Bdnf* gene. In addition, we were also interested in the changes of "epigenetic memory" post EZH2 antisense injection. We found that after EZH2 antisense injection, chicks' PVN no longer exhibited any "epigenetic memory" to repetitive fasting stress. While EZH2 mRNA was constantly inhibited, SUZ, EED and H3K27me2/3 levels were unpredictable. These findings suggested that neurons in the PVN utilized PRC2 as a major H3K27 methylation tool. Knockdown of EZH2 in the PRC2 impaired the proper response in PVN to fasting stress and PVN's ability to acclimate to repetitive fasting stresses. Thus, EZH2 is an important H3K27 methyltransferase inside chicken hypothalamus to maintain homeostasis.

In conclusion, fasting stress during the early life period could leave epigenetic markers on chromosomes of neurons in the feeding regulation center. These epigenetic markers will be left on chromosomes for a long period of time and have a beneficial role in keeping homeostasis when individuals face future fasting stress again. H3K27 methylation is one of these epigenetic markers and inhibits expression of various genes inside neurons. EZH2 is so far the only detected methyltransferases for H3K27 that form the PRC2. Thus EZH2 plays a key function in the body's response to fasting.

Keywords: Neuroscience, Fasting, PVN, EZH2, PRC2, BDNF

ACKNOWLEDGEMENTS

Time travels by fast. Now, it is the sixth years of my life in USA. I have been working very hard and praying for this very day to come. And now, it comes. I am officially a PhD in Neuroscience. All the tears and sufferings during the past mean less today and I am very proud of myself, who could survive in this toughest period of my life till today.

Well, without all these kinds of guidance, encouragement and support from many individuals, I do not think I could achieve this honor by myself. It is only because of you that my PhD has more fun and reward.

First, I would like to thank my major professor, Dr. Michael Denbow. He kindly accepted me into his lab on 2010 after I obtained my master degree. He provided me lots of teaching opportunities that allow me to improve myself in teaching and presentation skill. Dr. Denbow led my research back on the "right" track again and again during my difficult times. I was also allowed to explore some of my own research interests in his lab. Additionally, he spent countless hours proofreading my manuscript. I feel very blessed to have a major professor like him.

I would also like to express my gratitude to Dr. Cynthia Denbow for her generous support. I was able to use equipments in her lab and finish this dissertation. She corrected many mistakes in my researches and kept me in right direction. She spent countless hours proofreading my manuscript. And her big smile always keeps me warm.

I would like to extend my sincere appreciation to Dr. Paul Siegel for his guidance and humor. He brought a lot of laugh into the lab and fun into the researches. And thank you for providing me the chance to go to Poultry Science meeting in 2012.

I am indebted to Dr. Mark Cline for his guidance, support and advice. I learned many research techniques from him. His knowledge brought many things into my research.

Barbara Self is another wonderful lady I want to thank. Without her perfect organization, management and tutoring, it is impossible for me to finish this study. And I enjoy the conversation with her in the lab.

I am also grateful to Dr Elizabeth Gilbert. She is both a mentor and friend to me. Her big smile always bring fresh air to me. Thank you for allowing me to use your lab equipments. I will miss you.

I would like to thank Dr. Pingwen Xu, who introduced me lots of things when I started the lab.

More thanks go to the entire Animal and Poultry Sciences Department for the supporting environment.

Gratitude also goes to my friends: Lidan Zhao, Guohao Xie, Yafei Zhang, Xiaofei Cong, Dan Jia, Haibo Zhu, Xiaomei Ge, Shengcheng Su, Shuai Zhang, Wei Zhang and Ting Lu.

My gratitude also goes to Shanghai, the great city that raises me up.

Finally, thanks to my fantastic family. My Dad (Shouning Jiang), my Mom (Ying Zhao) and my lovely wife (Chi-fang Tsao) give me numerous supports and keep me working hard till today. I miss my beloved grandma (Xiuyun Zhang) from my mother's side, who passed away when I was in USA pursuing degree. You will always be in my heart. Much thanks to grandpa

from my mother's side, who passed away years ago as well. Thanks to my beloved grandma, grandpa and grand-grandma from my father's side. Without you, my father will not able to accomplish this much and I will never be able to stand on my father's shoulder, accomplishing this much. I would never have been able to make any accomplishment without them. I love you all.

TABLE OF CONTENTS

LISTS OF TABLES

LIST OF FIGURES

CHAPTER 1: Literature review

1.1. Introduction of food intake and feeding regulation

1.1.1. Brief introduction to the history of identifying hypothalamus as feeding regulating center

1.1.1.1. Pituitary instead of hypothalamus was identified as feeding regulating center at early time

Food intake is regulated by the brain [16]. However, there was a time when extreme intake was thought of as a psychological rather than a physiological problem. It was not until 1840 that this idea was first challenged. In 1840, Mohr reported about an obese woman who became extremely overweight and died one year later [17]. An autopsy found that a brain tumor was sitting on the sella turcica of the sphenoid bone, which extended from the base of the frontal lobe to the pons, which compressed the base of the brain including the optic nerve, optic chiasma, hypothalamus and crus cerebri. Later, after reviewing a series of similar cases [17], scientists started to attribute this pathological body weight increase to the destruction/interruption of the base region of the brain [18] and Fröhlich became the first one to summarize that the obesity was directly related to the malfunction of pituitary gland [17,19]. However, in 1904, Erdheim suggested opinion that rather than the pituitary gland, the base region of the brain was the reason for the obesity [20]. His argument was based on his finding that: 1) there were clinical cases where obese patients did not have the pituitary gland affected, 2) obesity and acromegaly could occur together, and 3) the pituitary tumor would not always cause obesity. Subsequent studies seemed to support Erdheim's hypothesis. For instance, some studies showed that pituitary gland resection did not affect food intake and body weight [21,22]. In addition, hypothalamic destruction would result in obesity no matter the status of the pituitary gland [21]. In 1921, Bailey et al. [23] accidently found their diabetes insipidus animals, which were induced by basomedial hypothalamus destruction, showed not only polyuria, but also hyperphagia and increased body weight. From that time, researchers started to focus on the hypothalamus as a potential target for feeding regulation.

1.1.1.2. The competition inside hypothalamus: the "Satiety Center" and the "Hunger Center"

The Horsley–Clarke apparatus was a monumental invention for neuroscience. As introduced in the early 1900s by Dr. Horsley [24], the Horsley–Clarke apparatus was used as a stereotactic device which ensured access to a specific area of the brain without interruption of other adjacent brain regions [25]. Hetherington was one of the first to use this apparatus in the study on feeding regulation. In 1941, Hetherington et al. [26] placed electrodes into specific brain regions guided by the Horsley–Clarke apparatus and induced destruction in different brain regions with and without damaging the pituitary gland. He showed that in rats, obesity could not be induced by simple pituitary gland damage. In addition, he and his colleagues later reported that obesity could be only induced by destroying the ventromedial hypothalamus but not the anterior and dorsal hypothalamus [27]. This finding was later confirmed by other scientists who conducted the same procedures on cats [28] and monkies [29].

After this finding, more and more focus was placed on the hypothalamic area and many researchers investigated different parts of the hypothalamus to find the relationship between sub-hypothalamic nuclei, feeding, and energy homeostasis. Finally, after the finding of satiety center [30] and hunger center [28], the model of two-center theory was introduced in the 1950s. In 1950, Kenndy reported his findings that rats showed apparent hyperphagia after destroying either the lateral part of the tuberal region or the region lying ventral-lateral to ventral-medial nuclei within the hypothalamus, [30]. He believed that there was a satiety mechanism in these areas of the hypothalamus which inhibited food-intake behavior in animals. After damage, or with the increasing age, the satiety mechanism became disrupted or weakened and animals started to show increased appetite, resulting in adipose deposition and obesity. Thus, he proposed the existence of the satiety center in the hypothalamus. This hypothesis was supported by many subsequent studies. For example, Brobeck et al. [17] showed that bilaterally damaging the ventromedial hypothalamus induced hyperphagia in rats. Later, Wyrwicka et al. [31] conducted an experiment by putting electrodes into the ventromedial hypothalamus of sheep, which greatly inhibited food intake of hungry sheep.

Only one year after Kenndy's "satiety center" hypothesis, in 1951, Anand and Brobeck purposed the "hunger center" hypothesis, which was located at the lateral side of the lateral hypothalamus. They reported that after bilateral, but not unilateral, destruction of the "hunger center", animals would stop eating completely (aphagia) and showed body weight loss [28]. Additionally, the "hunger center" could completely overrule the effect of bilateral "satiety center" destruction, which caused operation induced obese animal to be aphagia and weight loss. This hypothesis was later studied in sheep [31] and cats [32]. All of them reported the same aphagia in these operated animals.

1.1.1.3 Establishing the function of hypothalamus in energy balance and obesity

Based on the two center theory, researchers were trying to find the mechanisms within the hypothalamus involved with feeding and energy regulation. A lot of hypotheses were proposed. For example, some papers suggested that obesity was induced by long-term hyperphagia which resulted in adipose deposition [17]. Some papers attributed this to significantly reduced activity and reluctant running in animals that received either whole or ventromedial hypothalamus destruction [26,33].

The most promising hypothesis believed that there existed a certain connection between the central nerve system (hypothalamus) and peripheral digestive organs. As the information integration center, the hypothalamus mixed the signals from the peripheral digestive organs and made a final decision to eat or stop eating. Thus, there must be a signal loop where signals were sent back and forth between peripheral sites and the hypothalamus to balance body energy homeostasis. So what is the signal? Between 1940s to 1950s, this question was discussed intensely and three hypotheses were adopted, which postulated that body temperature [34], blood sugar level [35] and lipid amount [36] were the satiety signals which served as the messenger to let the hypothalamus control food intake.

In 1948, Brobeck first hypothesized that food intake was regulated by body temperature [34]. He proposed that at a high environmental temperature, animals would stop eating. He believed that at a high environmental temperature, it would be very difficult for animals to reduce their body temperature. Food intake would cause a thermal effect, which lead to further increasing in body temperature and harmful stress. In contrast, at low environmental temperatures, food intake would help to raise body temperature, thus preventing hypothermia and cold stress. Brobeck showed that at 65 to 76 ℉, adult male rats had increased food intake. However, at >92 ℉ adult male rats appeared hypophagia/aphagia, pyrexial and lost body weight [34]. Thus he believed that food intake was a potential mechanism of temperature regulation to avoid harmful stress. In the early 1940s, the thermotaxic center was also found in the hypothalamus [37]. Thus the integrated hypothesis was that the environmental temperature was a feeding signal, which was sent and processed in the hypothalamus and then directed alterations in food intake. However, this hypothesis ws discredited by later research findings [36,38]. Kennedy showed that the rats in Brobeck's study had lost more than 30g in body weight overnight after heat treatment, which was more than double than normal food starvation could cause [36]. As these rats were raised in high environmental temperatures, Kennedy showed that dehydration was the major reason for body weight loss. Increased body tissue catabolism under hyperthermia also played an important role. Once the rats were acclimated to the high environmental temperature, hypothalamic damaged rats gain weight and became obese, just like their counterparts at normal room temperature. Mayer also mentioned that after administration of thermal regulation agents (thyroxine as hyperthermal and thyrodectomy and thiouracil for hypothermal), results were contradictory to Brobeck's hypothesis [38].

The glucostasic-food regulation hypothesis was proposed in 1953 by Mayer [38]. In this hypothesis, blood glucose level was believed to have a key influence on food intake. The hypothalamic feeding center (including both hunger and satiety center) was believed to have glucoreceptors, which could monitor real-time blood glucose levels in the body. If the blood glucose was in the normal range, animals would not feed. If there was a drop of the blood glucose level, an afferent signal would activate the hypothalamus and the hunger center would be stimulated, which initiated the feeding process. To support this hypothesis, Mayer et al. showed that glucose or fructose administration, which made rats hyperglycemic, inhibited feed intake significantly [39]. In addition, the administration of small amounts of insulin induced hypoglycemia (the glucose level remained in the physiological range but relatively lower than the normal), which resulted in increased feeding. Furthermore, Mayer et al. [39] also used a special strain of rats with alloxan induced diabetes. Alloxan is a classical type I diabetes inducer [40]. It is known as an analogue of glucose, which is selectively stored in the beta cell in the rat pancreas *via* the GLUT2 transporter on its membrane [41,42]. The accumulation of alloxan causes necrosis of beta-cells in the pancreas and thus induced hyperglycemia, which is similar to the insulin-dependent type I diabetes mellitus [43]. Mayer and Bates [39] showed that after injection of glucose, the alloxan-diabetic rats remained hyperglycemic for a long time and reduced their food intake. The glucostasic-food

regulation hypothesis gave a good foundation for short-term food intake regulation. It helps explain the how the body regulates food intake in each meal. However, it cannot explain long-term body weight regulation.

The third hypothesis was introduced by Kennedy, who believed that the lipids controlled feeding status [36]. He found that young animals regulated food intake to keep their body fat in an almost fixed percentage [30,36]. In certain situations, when animals were put in hot or cold environments, or during lactation, the animals maintained a relatively fixed body weight as well [36]. In addition, even those animals with a damaged hypothalamus would maintained the body weight at a certain level [35]. Kennedy proposed the idea that the adipose deposit in the animal's body would regulate the food intake [36]. By sending out an inhibitory signal from the adipose tissue, the animal was able to regulate feeding and thus kept their body weight relatively stable. During starvation, the inhibitory signal gets weaker, which motivates the animal to eat. However, Kennedy was not able to determine the exact signal hormone that was used in this loop.

Kennedy's idea was later supported by the finding of Hervey. In 1959, Hervey did a parabiosis experiment, which he surgically paired two rats together [44]. This surgical fusion of the two rats allowed a 1% change in plasma per minute. Then he damaged the ventromedial hypothalamus of one of the pair. It would be expected that the two animals would grow obese together because the hyperphagia from the operated rat would transfer the excessive amount of nutrition to the normal rat. On the contrary, while the operated rat was obese as expected, the un-operated animal showed apparently decreased appetite, weight loss, a smaller liver, less food in the GI tract (found during autopsy) and eventually starved to death. Only an identical destruction of the hypothalamus of the normal rat could change the appetite of the normal rat and make both animals obese. He even proposed that some signals from the operated rats were sent to the hypothalamic food intake controlling center of the normal rats, which affect the normal feeding regulation in the normal rat. Compared to the glucostatic regulation, which focused more on a temporary food intake regulation, the lipostasis hypothesis explained how the hypothalamus could regulate the body weight for a long-term.

1.1.2. Sub-Hypothalamic nucleus

The hypothalamus is a crucial structure in the brain, which is involved in the many physiological roles of regulation, including feeding. Based on regional destruction and injection studies, five sub-hypothalamic nuclei have been shown to play pivotal roles in feeding regulation. They are the arcuate nucleus (ARC), ventromedial nucleus (VMN), dorsomedial nucleus (DMN), paraventricular nucleus (PVN), and lateral hypothalamus (LH).

1.1.2.1. Arcuate Nucleus (ARC)

The ARC is located at the bottom of the hypothalamus and is adjacent to the median eminence. The first study involving ARC function in feeding was conducted in 1969, when Olney injected monosodium glutamate (MSG) subcutaneously into

neonatal mice [45]. The result showed that MSG administration induced apparent neuronal degeneration in several parts of the brain, but specifically in the ARC of the hypothalamus. The treated animals showed marked obesity but not hyperphagia. Later experiments proved these results and also showed that the effect of MSG was species distinctive [46,47].

As mentioned above, there are certain regions of the brain that lack the blood brain barrier (BBB), which allow free access of large substances to pass freely into the CSF. The ARC receives hormonal signals directly from the peripheral circulating serum [48,49]. There are two major groups of neurons in the ARC, the Neuropeptide Y (NPY) -Agouti-related peptide (AgRP) and Amphetamine-Regulated Transcript (CART) -Proopiomelanocortin (POMC) [50,51]. These two neuron populations express orexigenic and anorexigenic signals, respectively, which regulate energy balance in the body. Instead of working separately, they are connected by γ-aminobutyric acid (GABA) containing fibers from the NPY-AgRP neurons [52]. GABA is an inhibitory neurotransmitter and causes CART-POMC neuron inhibition upon NPY-AgRP neuron activation [53] and results in an increased feeding behavior. In addition, both NPY-AgRP [54] and CART-POMC neuron [55] populations had leptin receptors on the membrane [56], which indicates their inter-connection with the leptin system. Thus, ARC is thought to be the most important nucleus involved in energy balance regulation.

1.1.2.2. Ventromedial nucleus (VMN)

VMN has long been recognized as an important nucleus involved in feeding and energy homeostasis regulation. Early studies that destroyed the VMN all reported hyperphagia and obesity [17,57,58] and VMN electric activation resulted in feeding suppression [31,59]. Many injection studies also confirmed the effectiveness of many anorexigenic factors after VMN micro-injection, including histamine [60], serotonin [61], urocortin [62], GABA antagonist [63], cholecystokinin (CCK) [64], leptin [65] and insulin antibody [66]. On the other hand, thyroid hormone [67], GABA [63], norepinephrine [68] and NPY [69,70] exhibited an opposite effect when microinjected into the VMN.

The communication between VMN and other nuclei in the hypothalamus confirmed its role in feeding and energy homeostasis regulation. For example, studies using retrograde tracer found small amounts of afferent fibers to VMN from LHA [71,72], DMN and PVN [73]. VMN also projected to the LHA [73] and PVN [74] in the hypothalamus and the nucleus tractus solitarii (NTS) in the brain stem [74]. Brain-derived neurotrophic factor **(**BDNF) is highly expressed in the VMN. The topography of the BDNF receptor, TrkB, demonstrated a highly expressed level not only in VMN, but also in other hypothalamic nuclei, which, however, did not include orexin and MCH neurons in the LHA nor CART and NPY neurons in the ARC [75]. This suggested an absence of innervations of BDNF(+) projection from VMN to the LHA and ARC. Contrarily, immunohistochemical studies revealed the boutons of γ-melanocyte-stimulating hormones (γ-MSH) and AgRP fibers from the ARC innervated the BDNF expression neurons in the VMN [75,76]. These results suggested unidirectional innervation to the VMN BDNF(+) neurons from the hypothalamic ARC. However, it was not until recently that one group using a laser scanning

photo-stimulation method, reported that the VMN did project to ARC [77]. Surprisingly, only CART/POMC neurons received strong excitatory innervations from VMN while the NPY/AgRP neurons did not. Instead, NPY/AgRP received weak inhibitory fibers within the ARC. This excitatory signal to CART/POMC neurons from VMN could be diminished when the animal was fasted [77].

Compared to other regions of the hypothalamus, the VMN contains a much higher level of BDNF, a member of neurotrophin family [75,78,79], and cholecystokinin (CCK) [80]. Because of the important role of VMN in feeding and energy homeostasis regulation, the high amount of BDNF and CCK were suspected to be the major satiety signals of VMN and carried out an inhibitory role in feeding.

1.1.2.3. Dorsomedial nucleus (DMN)

The first ever paper demonstrating the function of the DMN was in 1943, when a group put a pair of electrodes into the DMN of cats and stimulated the neurons in this area. The stimulation of the DMN in cats resulted in hyperphagia [81]. This study was repeated in other animals and yielded consistent results [82,83]. While some studies activated the DMN area, others were trying to see the results of DMN lesion (DMNL). Electrolytic lesions [84], ibotenic acid injection [85] and surgical cutting [86] at the DMN generated DMNL rats, who exhibited inhibited feeding and slower growth as well. Interestingly, unlike other animal with injured hypothalamic nuclei, the DMNL animals exhibited normal body fat composition and plasma fatty acid levels [87]. More surprisingly, there was no interruption in the animals' anabolic and growth-promoting hormone levels (insulin, thyroxine, triiodothyronine (T3), growth hormone (GH), and somatomedin (SM)) [87,88]. However, these DMNL animals had decreased body weight and disrupted plasma corticosterone [89] and prolactin [90] levels, which did not affect food intake [81]. The decreased body weight seemed to be appropriated to their decreased feeding behavior [87]. Based on these findings, the function of the DMN seemed to be a bit confusing compared to the direct effect from other regions of hypothalamus. However, cholecystokinin (CCK) is an active player in DMN, which regulates the feeding and energy homeostasis.

Cholecystokinin (CCK) was first discovered in the duodenum in 1930 [91] and was recognized by its stimulatory involvement in the secretion of pancreatic enzymes in gall bladder contraction and inhibition GI tract emptying [92]. Now, CCK is recognized as an important neuropeptide in short-term feeding and energy homeostasis both in central and peripheral tissues. In peripheral tissue, the CCK precursor was secreted in GI increasingly after fat or protein but not carbohydrate ingestion, suggesting its function in energy homeostasis [93,94]. In the CNS, CCK had been classified as the most abundant “brain-gut” neuropeptide [95] and detected in several mammalian brains, such as rat [96] and human [97]. The extremely high amount of CCK in areas, such as hippocampus, olfactory bulb, septum, amygdala, hypothalamus, etc, suggested that CCK was involved in various roles in CNS function. The relatively high amount of CCK in the hypothalamus, together with its role in peripheral

digesting tissues, indicated that CCK may play a pivotal role in feeding and energy homeostasis regulation at both the CNS and peripheral levels.

Different papers had reported CCK's concentration in different areas of the hypothalamus, which was almost consistent. The only discrepancy remained was which nucleus/areas contained the highest CCK concentration. One paper set the order from high to low as VMN, DMN, PVN and ARC [80] while the other reported the highest amount of CCK expressing neurons was gathering in the DMN [98]. Later, by using radioactive ^{125}I-CCK-8, the CCK receptors inside the hypothalamus were pinpointed, including VMN with the highest density, followed by the DMN [99]. Both results based on the topography of CCK and the CCK receptor suggested the similar importance of the VMN and DMN in the CCK signaling pathway. In another study, the researchers microinjected CCK-8 into different nuclei in the brain, including six regions in the hypothalamus and seven regions out of the hypothalamus [64]. While almost all areas in the hypothalamus affected feeding after CCK microinjection, the NTS was the only outer hypothalamic area that responded to microinjection. Among those areas, the DMN exhibited the most prominent feeding inhibition [64]. This implied that although the concentrations of CCK in the VMN and DMN were similar, the DMN could be the effective center of the CCK signal pathway. Subsequent groups studied the distribution of the CCK receptor by using CCK-A receptor specific radioactive agonist. CCK-A receptor was known as the major conductor of CCK for its feeding regulation (referring to the following paragraph). They found that the CCK-A receptor had the highest concentration in the DMN in the hypothalamus and NTS in the hinder brain [100]. On the contrary, the PVN contained a much lower amount of CCK-A receptor and there was none in the VMN [100]. In addition, VMN lesions did not abolished the feeding inhibition induced by CCK IP injection in rat [101]. Combining the result of CCK concentration, CCK-A receptor distribution, the CCK-8 microinjection's effect and lesion study, the DMN was believed to be the effective center for CCK in the CNS.

1.1.2.4. Lateral hypothalamic area (LHA)

The LHA was first related to feeding and energy homeostasis regulation in 1951 [28]. As previously mentioned, after bilateral, but not unilateral, destruction of LHA, animals would become aphagic, adipsic and demonstrated significant body weight loss [28]. Surprisingly, even VMN destruction could not reverse this effect. More than 35 different types of neurons have been identified in the LHA, indicating its role in both satiety and hunger signal integration [102]. This idea is also supported by the matrix of afferent/efferent fibers connected to the LHA. The LHA neurons project into the VMN, DMN and ARC in the hypothalamus and many other regions of the brain and also received the innervation fibers from the limbic system and brain stem [103].

Three kinds of neuropeptides have been detected in the LHA, melanin-concentrating hormone (MCH), orexin, and excitatory amino acid (EAA) glutamate. Unlike NPY- AgRP and CART-POMC neurons that co-express two neuropeptides in the ARC, MCH and orexin were distinct from each other [104].

1.1.2.5. Paraventricular nucleus (PVN)

Histology studies showed that the PVN receives innervation fibers from almost all areas of the hypothalamus [105], which implies its pivotal role in physiological function regulation. Nearly all known orexigenic factors increased feeding when micro-injected into the PVN [50]. These orexigenic factors included NPY [106], AgRP [107], $GABA_A$ receptor agonist (GABA and muscimol) [108], galanin [109,110], and orexin [111]. Feeding behavior was inhibited when the PVN was locally microinjected with anorexigenic factors, including Neuropeptide S (NPS) [112], α-MSH [107], nicotine [113], and corticotropin-releasing factor (CRF) -2 receptor agonist (CRF and urocortin-1) [114,115]. This information implies that feeding and energy homeostasis regulation must be one of the most important physiological roles that PVN is involved in.

Based on the nucleus size, the neurons in the PVN are divided into two groups, magnocellular and parvocellular neurons [116]. Although numerous neuropeptides have been detected in the PVN, three of them were suggested as signals involved in feeding and energy homeostasis regulation: oxytocin, corticotropin-releasing factor (CRF) and thyrotropin-releasing hormone (TRH) [56]. In general, the magnocellular neurons express oxytocin, but not vasopressin, inside the cell body and transport it through their axons to the posterior part of the pituitary gland [117]. On the other hand, the parvocellular neurons encode a high level of TRH [118,119] and CRF [120]. However, certain levels of oxytocin (OT) are also expressed in the parvocellular neurons, which have different projections compared to the OT-expressing magnocellular neurons [121,122]. The axon of these parvocellular neurons project to the median eminence and release TRH, CRH and OT into the systemic circulation through the pituitary gland [119,123,124].

1.1.3. Brain derived neurotrophic factor (BDNF) in feeding regulation

Before introducing the role of BDNF in feeding regulation, a general introduction of neurotrophins is presented. Neurotrophins are a family of neuron growth factors, which are capable of mediating many physiological functions, such as neuron proliferation, differentiation, growth and interaction [125]. Members of this family include nerve growth factor (NGF) [126], brain-derived neurotrophic factor (BDNF) [127], neurotrophin-3 (NT-3) [128], neurotrophin-4 and -5 (NT-4/5) [129], neurotrophin-6 [130] and neurotrophin-7 [131,132]. Most of these neurotrophic factors were initially discovered only in the brain which suggested limited physiological functions such as neuron survival [133]. However, more recent studies revealed other functions of the neurotrophin family, such as feeding and energy homeostasis regulation [134]. In this dissertation, the discussion would be focused on BDNF.

1.1.3.1. Brief introduction of BDNF protein discovery, function and distribution

The discovery of BDNF was first reported in 1982 [127]. In the study, the authors reported a small protein (12.3 KDa), which was extracted and purified from the pig brain. Then this protein was tested in an *in vitro* neuron culture assay and the results showed that it increased neuron survival as much as NGF. The authors named the protein BDNF. Subsequent studies confirmed BDNF's effect on neuron survival both *in vitro* [135] and *in vivo* [136]. Both the gene and the amino acid sequence of BDNF were reported in 1989 by the same group of scientists who discovered it [133]. The sequence alignment indicated a similarity of amino acid sequence between BDNF and NGF. In addition, they also located BDNF mRNA expression by Northern blot and showed that BDNF was exclusively expressed in neurons but not other peripheral tissues. However, later studies using a more advanced PCR method found BDNF expression in peripheral tissues, such as placenta [137], heart, muscle [138], liver and spleen [78].

1.1.3.2. Brief introduction of BDNF receptors

As a neuropeptide, the physiological effect of BDNF was conducted via its specific neurotrophin receptors. In 1988, a paper reported that labeled ^{125}I-BDNF was able to bind to cell membrane in an *in vitro* neural culture [139], suggesting the existence of a BDNF cell membrane receptor. Based on the dissociation constant detected from a kinetic assay, the receptors could be sub-divided into two groups, high-affinity receptors (dissociation rate (K_d) = 1.7 x 10^{-11} M) and low-affinity receptors (K_d = 1.3 x 10^{-9} M) [139,140,141]. Based on their structure, high and low affinity neurotrophin receptors were defined as members of either the tropomyosin-related kinases (Trk) receptor family or the tumor necrosis factor (TNF) receptor family, respectively [140]. The low affinity neurotrophin receptor, named P75, was an unspecific neurotrophin receptor and capable of interacting with all neurotrophins [142] and tumor necrosis factor (TNF) [143]. The Trk subtype, high affinity neurotrophin receptors, showed high selectivity to their specific neurotrophins [142]. According to pharmacological studies, the Trk receptor was further classed into TrkA, TrkB and TrkC, which were defined as the specific receptors for NGF (and NT-6 and NT-7), BDNF (and NT-4/5) and NT-3, respectively [140,141]. But this did not mean that there was no interaction between non-specific Trk receptors and neurotrophins. Instead, different neurotrophins could still bind to their non-specific Trk receptor but the dissociation rate (K_d value) was much higher than the specific neurotrophin [144]. For example, in order to decrease the binding rate of BDNF to TrkB by 50%, NGF needed to increase by 1000-fold concentration, which was enough to inhibit the binding between BDNF and the P75 receptor [145].

P75 and Trk receptors are both cell membrane surface receptors and, in most cases, are expressed on the same cell membrane [146]. Interestingly, the P75 and Trk receptors exhibit opposite biological effects, which regulate the status of certain cells [140,147,148]. While the Trk receptor is the gate of the neurotrophic effect, the P75 receptor shared the "death domains" of the tumor necrosis factor receptor family [149] and was more involved in cell death [150]. This suggests the different intracellular signaling pathways these two receptors utilize. This idea was supported by many studies and, to date, three signaling

pathways were discovered for Trk [140] and two signaling pathways for P75 receptor [151,152], respectively. Trk conducts its biological effect through Rat sarcoma (RAS), Phosphatidylinositide 3-kinases (PI-3K) and Phosphoinositide phospholipase C (PLC)-γ1 pathways [140]. On the other hand, P75 activation causes ceramide production, c-Jun N-terminal kinases (JNK) level increasing and nuclear factor kappa-light-chain-enhancer of activated B cells (NF-κB) activation in the cell [153]. Interestingly, the P75 signaling pathway could change the affinity of different Trk receptors to its cognate ligand, BDNF [146,154], suggesting P75 could also be a regulator in BDNF's signal pathway.

1.1.3.3. BNDF has important role in feeding regulation in hypothalamus

In the brain, BDNF is widely expressed in various regions and the highest concentration was detected in the hippocampus and hypothalamus [78,155]. As the importance of the hypothalamus in feeding and energy homeostasis regulation was uncovered, the involvement of BDNF in this capacity was hypothesized. The involvement of BDNF in feeding regulation was not unveiled until 1992 when Lapchak and Hefti accidently discovered the relationship between BDNF and body weight in neuron regeneration related research [156]. Initially, they were trying to rescue the hippocampal cholinergic dysfunction after a partial fimbrial transaction by chronic BDNF ICV administration. The BDNF failed to save neurons, but the BDNF administrated mice all showed decreased body weight [156]. Simultaneously, other members of the neurotrophin family, such as NGF, were suggested as feeding regulators by showing decreased food intake and weight loss after application [157,158]. Thus, more researchers started to look into the role of BDNF in feeding and energy homeostasis regulation.

In the hypothalamus, the highest BDNF concentration is detected in the VMN [75,79], which anatomically supports the role of BDNF as an important factor involved in feeding and energy homeostasis regulation. Almost all studies supported the idea that BDNF was an anorexigenic factor. For example, after 48 hours fasting, BDNF levels in the VMN [75] and dorsal vagal complex (DVC) of the hinder brain (where NTS located) [159] was significantly lowered, suggesting an increased feeding after fasting. When animals were re-fed, the BDNF level went back to normal. Acute microinjection of BDNF in the VMN [160], DVC [159] and PVN [161] inhibited the feeding and increased energy expenditure in test animals. Following chronic ICV injection of BDNF, rats showed dose-dependent food intake suppression and body weight loss [162]. However, when pre-treating animals with TrkB-Fc fusion proteins, an antagonist of TrkB, the BDNF ICV administration no longer inhibited feeding [160]. This suggested that BDNF used the TrkB receptor pathway to perform its anorexignic effect. In humans, a recent study also supports the idea of BNDF as an anorexigenic factor. In female with either bulimia nervosa or anorexia nervosa, serum BDNF levels were significantly lowered [163], with the anorexia nervosa patients having the lowest [163].

Just like other studies of orexigenic and anorexigenic factors, these utilizing knockout mutation rodent strains offered the most direct insight into BDNF's effect. However, as an important peptide involved in neural development, BDNF double KO ($BDNF^{-/-}$) animals were not able to be obtained for relatively long-term obesity studies because of their early postnatal mortality

[164]. In 2000, BDNF heterozygous mice (with only one functional BDNF allele) were created with significantly lowered BDNF protein levels in the hypothalamus, including PVN, LHA, VMN, ARC and DMN, when compared to the wild type (WT) [79]. Based on body weight, two phenotypes of BDNF heterozygous mice were subdivided into fat (FBH) or non-fat (NBH). Interestingly, the FBH strain showed late-onset body weight gain, which was significantly higher than both the WT and NBH, while there was no body weight difference between WT and NBH. In addition, FBH strain also had more adipose tissue and had endocrine abnormalities, including hyperleptinemia and hyperinsulinemia, but normal serum glucose and corticosterone level. Additionally, BDNF or NT4/5 application into the third ventricle could transiently but noticeably inhibit feeding and lower body weight. The study also reported that both leptin receptors and other feeding related neuropeptides, such as NPY and CART, remained at a normal level in the hypothalamus, which suggested a unique pathway of BDNF in feeding and energy homeostasis regulation. Part of the results from BDNF heterozygous mice was confirmed by a human case. In 2006, one case report describe an 8-year-old girl who exhibited severe hyperphagia and obesity [165]. The genotyping showed a chromosomal inversion at 46,XX,inv(11)(p13p15.3), which was the area coding the BDNF gene, and resulted in BDNF heterozygous human model. A more recent study also reported the selective deletion of BDNF in the VMN and DMN together in adult mice exhibited hyperphagia and obesity starting at week 5 and 7, respectively [166].

The role of TrkB in feeding and energy homeostasis was confirmed in later studies by showing that TrkB malfunction mimics the effect of BDNF knock down. The TrkB double KO ($TrkB^{-/-}$) was as fatal as that of BDNF KO. Thus, by using a transgenic method, one group created a mouse strain that exhibited mutant TrkB receptor (functional KO). These mice exhibited distinctively elevated food intake and longer feeding behavior starting at week 5 [75]. They also had apparent obesity at the maturity period and increased linear length [75]. As another BDNF pathway conductor, the P75 receptor also plays a role in feeding and energy homeostasis regulation. In the "New Zealand obese" mice strain, there was an increased P75 receptor mRNA level in the hypothalamus [167]. Additionally, compared to the mortality of TrkB double KO ($TrkB^{-/-}$), the P75 double KO ($P75^{-/-}$) mice were able to survive, but exhibited lower body weight starting at week 4 [168]. The food deprivation of these animals caused significantly decreased serum insulin and leptin. Another study using $P75^{-/-}$ mice confirmed the abnormally increased latency to feed after being moved to a new environment [169]. However in obese rodents, such as the *ob/ob* strain, the tumor necrosis factors (TNF) level was also increased [170]. This suggested the interaction between P75 with TNF rather than BDNF, which caused feeding inhibition and body weight loss.

The BDNF role in feeding and energy homeostasis regulation was also connected to other signaling pathway, such as leptin, insulin, POMC, NPY, and AgRP [134]. The receptors of leptin [171], insulin [172], orexin [173] and MCH [174] are presented in the VMN. In normal mice, acute intravenous leptin administration induced up-regulated expression of BDNF in the VMN [175]. In addition, one group found that in an *in vitro* real-time imaging experiment, leptin administration activated the PI-3K pathway in the CART/POMC neurons in the ARC while leptin removal activated the same pathway in NPY/AgRP neurons

[176]. Interestingly, another adipose signal, insulin, elicited the same result as leptin on CART/POMC neurons but opposite results on NPY/AgRP neurons [176]. Because PI-3K was one of the three major signaling pathways of the BDNF receptor, TrkB, PI-3K could be a common pathway for leptin, insulin and BDNF. In two leptin resistant mice strains, BDNF administration corrected not only the hyperphagia and obesity, but also glucose homeostasis [177]. Blood tests revealed that BDNF application noticeably decreased serum insulin and leptin level [177].

An immunohistochemistry study revealed the boutons of γ-MSH and AgRP fibers from the ARC innervated the BDNF expression neurons in the VMN [75]. Both pro-opiomelanocortin (POMC) and melanocortin receptor 4 (MC4R) double KO and agouti over expression mice exhibited decreased BDNF mRNA levels in the VMN [75]. In addition, as mentioned above, food deprivation could significantly decrease the BDNF level in the VMH. This phenomenon was partially relieved by ICV MC4 receptor agonist (melanotan II) ICV application [75]. NPY micro-injection into the VMN increased feeding, which was also able to be reversed by BDNF co-application [160]. Microinjection of BDNF in inhibited NPY mRNA in the ARC and PVN [161]. Additionally, ICV infusion of BDNF increased CRH and urocortin levels in the PVN and promoted feeding [178]. However, CRH and urocortin receptor antagonist application abolished the hyperphagia.

1.1.3.4. BDNF gene construction

Presently, the human BDNF gene is encrypted and covers a ~70 kb regions on chromosome 11, which contains eleven exons and nine of its promoters are tissue-specific [179]. The BDNF precursor (pro-BDNF) used trans-splicing method to splice different 5' non-coding exons with the 3' exon, which encoded the pro-BDNF mRNA. Based on different tissue locations or regulation requirements, different combinations of mRNA from the 5' non-coding exons were fused to the pro-BDNF mRNA, which generated at least 17 transcripts [179]. For example, I, II and III 5' non-coding exons were abundant in the brain while IV was highly expressed in the lung and heart [180]. After a kainic acid-induced seizure, the mRNA of the I, II and III 5' non-coding exons increased significantly while there was no change in the level of IV's level [180]. The 3' exon product of the BDNF gene, the pro-BDNF (~32 KDa), was alternatively spliced into either mature BDNF mRNA (14 KDa) or a minor truncated form (28 KDa) [134,181]. After translation and protease cleavage [134], the BDNF protein was stored in the vesicles in the somatodentritic domain of the neurons and released upon neuron excitation [181]. For rodents, both mice and rats had a similar BDNF gene arrangement to that of human. Their pro-BDNF was coded by one protein coding 3′ exon and eight regulatory 5′ exons [182]. Initially, in the avian animal, the *Bdnf* gene was believed to be formed with no 5' non-coding exons but only one 3'exon, whose transcription was regulated by the methylation status of the stand-alone C-phosphate-G (CpG) island upstream of its promoter [183]. One recent study reported three 5' non-coding exons in the *Bdnf* gene in chicken [184]. These three 5' non-coding exons encoded three mRNA transcripts (BDNF1, BDNF2 and BDNF3), which were spliced to the pro-BDNF mRNA coded by the BDNF 3′ exon. BDNF1 and BDNF2 were found specifically in brain (among eight tissues tested by the authors).

In the CNS, BDNF1 and BDNF2 were detected in the hypothalamus while BDNF3 was not [184]. This new finding revealed that the chicken BDNF gene structure was similar to mammalian animals.

1.2. Introduction to epigenetics

1.2.1. What is epigenetics?

The word "epigenetics" was first coined by Conrad H. Waddington (1905-1975). He defined epigenetics as "the branch of biology which studies the causal interactions between genes and their products, which bring the phenotype into being" (Waddington, 1942). The prefix "epi-" means above and "genesis" indicates the unit of heredity or gene, which in a broad sense is like a bridge connecting an organism's genotype and phenotype thus changing the final phenotypic outcome without changing the actual DNA sequence. In other words, epigenetics is a term used to describe the events that cannot be explained by genes alone (Goldberg et a., 2007). In 1957, Waddington described what he called the "epigenetic landscape", in which he portrayed a fertilized embryo as a "ball" sitting on the slope of a valley. The "ball" during its development can at various points take specific trajectories down the slope, which ultimately could lead to different phenotypic outcomes. It was a good visual representation to illustrate that cellular differentiation can be governed by the cell's physical environment in addition to its genetic predisposition.

A more modern definition of epigenetics is the study of the stable and ideally heritable changes that are not related to changes in the actual gene sequence, but that result in a particular cellular phenotype [185]. Gene expression in eukaryotic organisms is regulated by several epigenetic mechanisms including DNA methylation and histone modifications. In this proposal, a brief discussion of these underlying mechanisms beginning with some background on gene structure will be addressed.

1.2.2. Chromatin Structure

The human genome contains about 6 billion base pairs (bp) of DNA, which, if stretched out, would be close to 2 meters long [186]. So how is the 2-meters long DNA packaged into the nucleus of a cell that is only several micrometers in diameter? In cells, the DNA and its associated proteins bind together and are known as chromatin, which, after nuclease treatment, demonstrated the "bead-on-a string" as seen under the electron microscope (Olins et al., 1975; Oudet et al., 1975). This "string" is double-stranded DNA and approximately 2 nm in diameter. The beads are the fundamental units of chromatin, called "nucleosomes", which are 10 nm in diameter. The nucleosome is the combination of both DNA and the nucleosome core particle (NCP). The NCP is approximately 206 K in molecular weight, 6.5 nm in diameter and consists of disk-shaped protein polymers, which is wrapped 1.65 times by 146 bp of tight-superhelical DNA in a left-handed mode [187,188,189]. Inside the NCP, four types of core canonical histones have been identified, which are H_{2A}, H_{2B}, H_3 and H_4. At physiological condition, $(H_3\text{-}H_4)2$ tetramer locates in the middle while one $H_{2A}\text{-}H_{2B}$ dimer stays on each side [190]. The nucleosomes are then connected by the linker DNA at different lengths with linker histones. This allows the chromatin fibers to form a higher-order structure,

which increases packing efficiency and only unpacks chromatin partially during gene transcription. The characters presented above are from the human α-satellite DNA in the nucleosome with canonical histone octamer. Different organisms may contain different lengths of DNA in a nucleosome, varying from 100 to 170 bp [191]. One recent review paper mentioned the discovery of a saturated nucleosome form, which could accommodate DNA up to 173 bp [191].

In each nucleosome, there exists two kinds of bonds between the NCP and wrapping DNA, including direct binding and water-bridge interaction, which give approximately similar contributions to the nucleosome stability [188]. There are 14 direct-binding sites in one nucleosome between the minor groove of the DNA double helix and NCP [187,188]. Some researchers reported the discovery of NCP preferred sequences, which explained the situation of uneven NCP distribution on the DNA and nucleosome depletion at the gene promoter and tail sites where transcription factors are bound [192]. Additionally, a total of 3120 water molecules exist in one nucleosome, among which, 121 forms the hydrogen bond between NCP and DNA [188]. This nucleosome model offers the foundation to explain the chromatin remodeling process, which allow cells to control their gene expression.

Based on the density of the chromatin structure, two chromatin forms have been proposed, which are the euchromatin and heterochromatin [193]. The euchromatin is the chromatin in a "loose" form and appears during the interphase of the cell cycle. It contains most of the coding genes in the cell, and thus allows recognition and binding of transcription machinery. On the contrary, the heterochromatin is constantly in a condensed pattern throughout all cell cycles, which is inaccessible and impossible for transcription. Thus, the transformation between these two forms of chromatin dramatically changes gene expression and DNA replication in the cell. The nucleosome, which is a key in chromatin transformation packing, has been shown to be the most important method for euchromatin/heterochromatin transformation both *in vitro* [194] and *in vivo* [195] for nearly two decades. The NCP, which is an important component of the nucleosome, plays a key role in this process.

1.2.3. Histone post-translational modification (PTM)

All histone proteins in the NCP contain two motif domains, which are the N-terminal tail domain and the fold domain [196]. In addition, the H_{2A} also has a C-terminal tail domain [196]. The histone fold domain is highly responsible for NCP formation and nucleosome stability maintenance. The N-terminal tail domain, on the other hand, extends out from the nucleosome core.

1.2.3.1. The function of histone N-terminal tails

So what is the biological function of the histone N-terminal tail domain? Early studies showed that the NCP remained intact even though the N-terminal tail domain was removed by trypsin treatment [197]. Thus, the histone N-terminal tail is not involved in the NCP stability. Biochemical studies identified the constituents of the N-terminal tail domain as containing mainly

four different amino acid residues, including lysine, serine, threonine and arginines [198]. On the tail, all these amino acids can be post-translationally modified by histone modification enzymes, which either changes the binding affinity between DNA and the NCP or recruits the chromatin remodeling complex. Furthermore, unlike the co-translational N-terminal modification of many other proteins, the histone N-terminal PTM is more reversible [199]. Thus, due to different histone N-terminal tail PTMs, chromatin structure becomes switchable between tightly packed heterochromatin and loosely packed euchromatin. If properly performed, cells can decide when and where to make certain genes accessible/resistible to DNA binding proteins and the transcriptional machinery, which indirectly affects physiological processes (e.g. gene transcription, DNA replication and DNA repair). It is worth mentioning that some types of histone N-terminal tail PTMs are more stable than others. For instance, acetylation and phosphorylation tend to be less stable than methylation, which suggests a more sustained effect from methylation to control the gene [200,201]. This is because the deacetylation only requires a hydrolysis of a single amide bond while the demethylation needs more energy to breakdown the C-N bond [202].

After the very first report of core histone N-terminal tail acetylation promoting gene expression *in vitro* in 1964 [203], gene epigenetic regulation through histone N-terminal tail PTM received more attention. So far, many types of histone N-terminal tail PTMs have been identified, including acetylation, methylation, phosphorylation, ADP ribosylation, proline isomerization, deimination, glycosylation, ubiquitylation/ubiquitination, carbonylation and sumoylation [12,198]. Each type of modification will be balanced with another type and overall they result in a concerted combinatorial effect on gene transcription [204]. The two most important histone N-terminal tail PTMs are acetylation and methylation. In the following paragraphs, a brief discussion will be addressed about these two PTMs.

1.2.3.2. Histone methylation

By providing proper spatiotemporal inhibition on different genes, organisms establish and maintain the identity of different types of cell. Epigenetically speaking, the function of histone methylation is one of the most important regulation mechanisms in the organism to provide this process. Examples of this type of regulation involve X chromosome inactivation, heterochromatin formation and transcriptional inhibition/activation [205]. Malfunction of histone methylation has long been related to increases in the rate of cell transformation, thus increasing the chance of oncogenesis [206]. However, recent studies also showed that histone methylation can activate genes, which suggests it has a dual effect in cells [205]. The methylation could happen on different amino acid residues, including both lysine and arginine residues [207]. At the same amino acid residue, the methylation could happen to different degrees, including mono-, di-, or trimethylation [208,209]. For example, the lysine methylation could obtain up to three methyl groups while arginine could only do one [210].

Numerous studies so far, focused on the function of the lysine (K) residue, especially on the H_3 N-terminal tail. This is because each lysine methylation on the H_3 N-terminal tail induces a unique effect on chromatin structure and gene transcription

[211]. Compared to H_4, which has only one lysine methylation site (H_4K_{20}), there are more than 20 methylation sites on the H_3 N-terminal tail that have been identified and five lysine residues are thought to be the most functionally important [202]. These sites are K_4, K_9, K_{27}, K_{36} [201] and K_{79} [212]. Table 1 lists the biological effect of methylation at different lysine sites on the H_3 N-terminal tail. Many studies have established a close relationship between the H_3 N-terminal tail methylation and normal development/neoplasm genesis [213]. Among them, K_{27} is the most important methylation site, which inhibits gene transcription [214].

1.2.3.2.1. H_3K_{27} Methylation induced gene transcription inhibition

H_3K_{27} methylation exists in three forms, which are mono-, di- and tri-methylated [215]. In mammalian cells, the distribution percentage for H_3K_{27} Me_0, $H_3K_{27}Me_1$, $H_3K_{27}Me_2$ and $H_3K_{27}Me_3$ is 15%, 25%, 50% and 10% [216]. In Drosophila and mammalian cells, all H_3K_{27} is conducted by EZ and EZH1/2 proteins (their properties will be discussed later in this thesis). The mechanism of histone N-terminal tail induced gene repression will be discussed in later paragraphs.

Compared to $H_3K_{27}Me_2$ and $H_3K_{27}Me_3$, $H_3K_{27}Me_1$ function and regulation remains poorly known. While the plants use specific mono-HMTs to conduct H_3K_{27} Me_0 to $H_3K_{27}Me_1$ [217], EZH1, EZH2 and EED together are the responsible for both Me_0 to Me_1 and Me_2 to Me_3 [218,219]. In Drosophila, chromatin scanning revealed the distribution of $H_3K_{27}Me_1$ is prevalent at both heterochromatin (e.g. pericentromeric region) and euchromatin (but selectively depleted around transcription start sites of active genes) [14,220]. This suggests that $H_3K_{27}Me_1$ might be involved in heterochromatin structure maintenance and a reservoir for inhibitory DNA binding proteins at active gene loci. Additionally, $H_3K_{27}Me_1$ could also prevent the acetylation of H_3K_{27} and other PTMs. One most current review paper suggested the existence of a $H_3K_{27}Me_1$ binding protein, which could either directly induce chromatin structure change or recruit other proteins [217]. A potential candidate for such a protein is the Decrease in DNA Methylation 1 (DDM1) protein identified in the plant, Arabidopsis [221,222].

Although no experiment so far has directly shown a correlation between $H_3K_{27}Me_2$ and gene expression level, some studies have indirectly suggested it as an inhibitory biomarker. For example, in Drosophila, $H_3K_{27}Me_2$ coincides with $H_3K_{27}Me_1$ at chromocenter regions [14], which are highly packed area and have no access to polymerase. Similar results were obtained in Arabidopsis [223]. Similar to $H_3K_{27}Me_3$, the $H_3K_{27}Me_2$ is methylated from $H_3K_{27}Me_1$ by EZH2 in the PRC2 complex in Drosophila [224], and indicated by the knock-down of EZH2 which decreased the levels of both $H_3K_{27}Me_2$ and $H_3K_{27}Me_3$ [215]. Recently, $H_3K_{27}Me_2$ is suggested as an intermediate status [215], which prevents gene activation through both supplying $H_3K_{27}Me_3$ raw material and preventing H_3K_{27} acetylation [213].

The $H_3K_{27}Me_3$ is the only methylated H_3K_{27} that is clearly demonstrated as a biomarker for gene repression. In Drosophila cells, although also detected at limited euchromatin loci, $H_3K_{27}Me_3$ locates constantly at pericentric heterochromatin at high concentrations [14]. Similar condensed distribution of $H_3K_{27}Me_3$ is also observed in inactivated X chromosomes in

mammalian cells [13]. In Arabidopsis defective in $H_3K_{27}Me_3$ and $H_3K_{27}Me_3$, specific demethylases (JMJ12) caused hundreds of genes to fail to be silenced and extensively silenced, respectively [225]. EZH2 knock-down [215] and knock–out [218] caused significant decreases, but not a total loss of $H_3K_{27}Me_3$. The explanation is the existence of EZH1, which is a homolog of EZH2 and replaces EZH2 and keeps minimal necessary $H_3K_{27}Me_3$ for embryo development. Additionally, noticeable increases of $H_3K_{27}Me_3$ were recently reported after a novel point mutation in the SET domain of EZ protein, which resulted in substantially lowered *Abd-B* gene expression in Drosophila [226].

Table 1. lists all lysine residues on H_3 N-terminal tail, which so far has been found as potential methylation sites. Their function was indexed with some relevant references.

Histone	**Methylated Lysine Residue**	**Level of Methylation**	**Effect on gene transcription**	**Reference**
H_3	Lys_4	Me_1	activate	[227,228]
		Me_2		
		Me_3		[208,229]
	Lys_9	Me_1	found within silent domains of euchromatin [230], maybe related to activation	[231,232]
		Me_2	found enriched within silent domains of euchromatin, function unclear.	[230]
		Me_3	inhibit	[14,216,226,230,231,233]
	Lys_{27}	Me_1	Function unknown. Majority of papers tend to suggest it as an inhibitory marker. But one suggests it as marker for active gene [214].	[14,216,220,230]
		Me_2	Function unknown. One paper suggested it as an intermediate state between Me_1 and Me_3 [215].	[14,215]
		Me_3	inhibit	[13,234]
	Lys_{36}	Me_1	inhibit	[235,236]
		Me_2	activate	
		Me_3		

Table 1. Potential methylation lysine residues on the H_3N-terminal tail and their effect on gene expression

1.2.3.2.2. Introduction to the PRC2

Histone N-terminal tail methylation is carried out by the histone methyltransferases (HMTs), whose key characteristic is the SET domain. The SET domain is short for the Su(var)3-9; E(z); Trithorax, which is defined as the conserved protein domain that has methyltransferase capacity [237]. So far, many proteins containing the SET domain have been found to be members of the HMTs family, including the polycomb repressive complex (PRC).

The PRC is highly conserved from Drosophila to human and two subtypes of the PRC have been identified, which are PRC1 [238] and PRC2 [239]. These two subtypes consist of different components and methylate histone N-terminal tails. It remains elusive as to which protein serves as the HMT in PRC1 [240,241]. On the other hand, PRC2 has so far the only specific HMT for H_3K_{27} di- and tri-methylation. In humans, its HMT function is conducted via the key component in the functional core, called EZH [213]. Additionally, three more proteins are identified in the PRC2 functional core as well, which are EED, SUZ12 and RbAp46/48 (or called RBBP7/4) [213,242,243]. In Drosophila, PRC2 is also known as the ESC-EZ complex. The ESC/ESCL, histone H4 binding protein p55 and EZ of the ESC-EZ complex are the ortholog of EED, RbAp46/48 and EZH protein in humans, respectively.

All the protein in the PRC2 and PRC1 functional cores belong to the Polycomb group (PcG) family [244]. In early Drosophila studies, the PcG family served as an important repressor to the *Hox* gene and controlled Drosophila body-segmental development. Now, the PcG family is proven to be required during physiological processes including embryonic development and cell pluripotency [245]. Selective knocking-out of one of the PcG proteins in the PRC2 and PRC1 functional cores leads to embryonic lethality and developmental abnormalities, respectively [246]. The following paragraphs will shortly address the known knowledge of these four PcG proteins in the PRC2 functional core.

1.2.3.2.2.1. Components in the functional core of the PRC2

In a 2002 study, the structure of the SET domain in the EZH2/EZ protein was determined [247] In this study, the EZH2/EZ was determined as the catalytic site of the PRC2, which conducted methylation on H_3K_{27} and H_3K_9 residues [213,247]. Although subsequent studies reported different findings for which EZ had no effect on H_3K_9 residue [242,248]. It is with no doubt that its methylation on H_3K_{27} is specific since the mono-methylation process on H_3K_{27} gradually accumulates methyl groups from Me_0 to Me_1, Me_1 to Me_2, Me_2 to Me_3 [249].

Many studies have bridged the reverse relationship between EZH2 and gene transcription via H_3K_{27} methylation on genes. After overexpression of EZH2 in cancer cells an increased $H_3K_{27}Me_3$ and histone deacetylases (HDAC) were observed at the promoter site of Runt-related (*RUNX*) family genes [250]. On the other hand, the EZH2 knockdown exhibited both a decreased $H_3K_{27}Me_3$ and HDAC at the promoter site of the *RUNX* gene, which allowed the recovery of *RUNX* gene expression [250]. In the EZ knockout, Drosophila larva methylated at H_3K_{27} were barely detectable [14]. If the SET domain inside the

EZH2/EZ is disrupted, its HMT function is abolished as well. For example, by replacing a conserved histidine residue (H689) with an alanine (H689A) inside the SET domain of EZ, the HMT activity of PRC2 was decreased *in vivo* [247]. Similarly, switching the cysteine-545 (C545Y) to tyrosine within the SET domain not only decreased the HMT activity, but also inhibited the binding between the PRC2 and special DNA regions called PcG response elements (PREs), thus inhibiting the histone methylation as well [247].

However, even with the existence of normal EZH2/EZ, the PRC2 still has no HMT function at all if EZH2/EZ lacks cooperation from the other three proteins inside the PRC2 functional core. The explanation for this phenomenon is that EZH2/EZ requires DNA binding before it performs the HMT function. Because EZH2/EZ itself does not have a DNA binding domain, it needs help from other proteins to locate the position, anchor to the chromosome and potentiate the methylation. So far, EZ had been shown to have a direct connection with the ESC in Drosophila [251] and SUZ12 [252], or maybe RbAp46/48 as well [253]. These three proteins inside the functional core, together with other accessory proteins, complete the well regulated methylation process.

The EED is a conserved protein found in the PRC2 complex and is essential for the PRC2 silencing function. In Drosophila, the EED has two homologues, which are the ESC and ESCL [254], and both are coded by the *Esc* gene [255]. The function of EED is believed to be a connecter inside the PRC2, which bridges the histone with the HMTs inside the PRC2. For example, in both Drosophila [256] and mice [257], the *Esc* gene knock-out in the embryo inhibits the homeotic genes, just as other PcG proteins in the PRC2. Subsequent *Esc* gene knock-in could rescue the embryo, if only the supplement was given in the first several hours of development [256]. This suggests the unique time-sensitive biological effect of the EED protein, which is different from other PcG proteins [258]. The PcG protein subunits inside the PRC could recognize the polycomb response elements (PREs). RNA interference specifically knocking down the ESC led to obviously decreased levels of the EZ-PRG binding, which inhibited the methylation and subsequent regulatory protein binding [242]. Subsequent studies showed that this was partially due to the failure of the bridge effect of EED/ESC and proper EED/ESC association. Biochemical studies showed that EED/ESC had a C-terminal with seven WD regions, which could directly bind to both the N-terminal of EZH2/EZ [251] and H_3 [255]. After proper bridging by EED/ESC, the EZH2/EZ then performed its methyltransferase effect and conducted the global H_3K_{27} methylation [259]. Interruption of the EED/ESC protein bridging resulted in global H_3K_{27} methylation failure, which caused embryo development failure in both Drosophila.[259] and mammals [260]. Only in the presence of EED/ESC, H_3K_{27} methylation was properly conducted [259]. Additionally, the EED showed a connection to the HDAC in the PRC2 as well [261,262]. Histone deacetylation is a critical step in gene repression. One study reported the finding of a highly specific interaction between HDAC1/2 proteins and EED [262].

The SUZ12 protein is a relatively new component found in the PRC2 complex. Gene alignment demonstrated that it was a highly conserved protein from plants to mammals [263]. Although its detailed function remained unclear, the loss of the

Suz12 gene resulted in the total absence of the $H_3K_{27}Me_3$ in Drosophila [264]. Biochemical analysis identified two regions inside the SUZ12 protein, the zinc finger motif domain and the VEFS (VRN2-EMF2-FIS2-Suz12) domain [252]. The function of zinc finger motif is unknown, and one paper reported that this region did not have DNA binding ability [263]. On the other hand, the VEFS had direct physical contact with EZH2 and heterochromatin protein 1α (HP1α) both *in vitro* and *in vivo* [252], which was confirmed by an immunohistochemistry study [264]. VEFS domain malfunction induced by a *Suz12* gene missense mutation caused the PRC2 to lose its methyltransferase ability while still maintaining a proper PRC2 complex structure [259].

RbAp46 and 48 are two proteins discovered inside the PRC2 core in humans [242,247] and their homolog is called p55 in nucleosome remodeling factor NURF (NURF55) in Drosophila and p55 in fly [265]. Both RbAp46/48 [266,267] and NURF55 could directly bind to H_4 and H_{2A} [253,268]. Biochemical analysis reported the structure of RbAp46/48 contained a seven WD repeat motif, which was similar to that of EED [253]. Previous studies reported that the RbAp46/48 was directly associated with SUZ12 [269] and HDAC1 [253]. These data suggested that RbAp46/48 functions as a bridge to connect its binding histone to other catalytic units in the PRC2. The exact function of RbAp46/48 in PRC2 remained unclear due to conflicting studies. Two recent studies found p55 was either essential [270] or not essential at all for PRC2 functioning [271]. However, its function in Drosophila chromatin assembly factor 1 (dCAF-1) might give a clue about how it works. A previous study showed that p55 was also detected in dCAF-1, in which p55 had direct contact with RPD3, a HDAC [253]. The deletion of p55 in dCAF totally abolished the function of dCAF-1 [272]. This indicated that p55 might conduct its function through setting up a bridge between the histone protein and functional unit inside the dCAF-1, including RPD3. Thus, some papers proposed the same model for p55 in the PRC2 based on the following experiment results: 1) the HDAC1/2 proteins were identified in the PRC2 [262]; 2) p55 had direct contact with HDAC1/2 in PRC2 [253]; and 3) p55 mutant Drosophila strain had reduced levels of both PRC2 and its product, $H_3K_{27}me_3$ [270].

1.2.3.2.2.2. Proteins out of the functional core of PRC2

There are also some other proteins, which are not in the functional core, that help in PRC2 functioning. So far, several sequence-specific DNA-binding proteins had been identified. For example, in both PRC1 and 2, PREs recognition proteins were identified [273], which were the pleiohomeotic (PHO) in Drosophila and its mammalian orthologue, Yin Yang (YY) 1 [274]. One study showed that the YY1 and PHO were crucial for recognizing the PREs region, thus allowing the PRC complex to conduct methylation at well defined areas [273]. Additionally, the Zeste protein co-localized with both PRC1and PRC2 on the chromatin at many sites, suggesting the association of Zeste with the PRC [275]. Because the Zeste protein could recognize and bind to a specific DNA sequence (T/CGAGT/CG), it is believed that Zeste also helps the PRC to locate sites [276]. Other proteins include GAGA factor (GAF), pipsqueak (Psq), dorsal switch protein (Dsp1), grainy head (Grh) and SP1/KLF [277]. Nevertheless, how all these proteins help the PRC to locate the position is still not clear.

1.2.3.3. Histone Acetylation

Although the core histone and certain C-terminal tails are subjected to acetylation modification as well, they seem to be much less common compared to that of the N-terminal tail acetylation [12]. Histone acetylation is overall related to increased gene expression [193,278,279]. For example, in chicken embryo erythrocytes, the alpha-D-globin gene is an actively transcribed gene, which contains 15- to 30-fold more acetylated histone compared to those genes that are not actively transcribed [280]. After deleting H_4 N-terminal tail, H_4 tail could no long be acetylated, which resulted in genes transcription inhibition [281].

Among all canonical histones, H_3 is the most popular post translationally modified protein in epigenetic research regulation. Increased levels of acetylated H_3 were found at the gene promoter area, which is highly correlated with gene transcription activation [282]. The H_3 N-terminal tail has the most varieties and sites of PTM compared to its counterpart as well [12]. The lysine residue is the major site for enzymatic PTM [201]. Although in eukaryotic cells, there remained some differences among sample sources (e.g., human organ cellc *vs* yeast) most of the time, the lysine sites on the H_3 N-terminal tail are either methylated or acetylated [201]. So far, in eukaryotic cells, five lysine sites on the H_3 N-terminal tail have been identified to be acetylation modifiable, which are the Lys (K) 9, K14, K18, K23 and K27 [201]. The H_3K_{27} acetylation (Ac) has been reported in yeast [283], human, and mouse [201]. Using CHIP-Seq techniques, $H_3K_{27}Ac$ was confirmed to be positively correlated with gene expression and located around transcription start sites [15]. It is a biomarker to distinguish active enhancers and a poised enhancer, which are enriched and absent in $H_3K_{27}Ac$, respectively [284,285]. Additionally, $H_3K_{27}Ac$ has a complimentary effect with methylated H_3K_{27}, and can replace or be replaced by $H_3K_{27}Me_2$ and $H_3K_{27}Me_3$ [15,284,286,287], thus switch the gene transcription status.

Histone N-terminal tail acetylation is conducted by acetyltransferase (HATs) first reported in yeast [288] and, now, many HATs have been identified in various animals [198]. In Drosophila, the most well known HAT-bearing complex is trithorax acetylation complex (TAC), whose functional core has trithorax protein (TRX) and CREB binding protein (CBP) [289]. TRX belongs to one sub-family of *trithorax* group (*TrxG*) gene, which is capable of recognizing a specific DNA domain called TrxG response elements (TREs) [290]. Additionally, TRX also bears a HMTs' SET domain and methylates H3K4 specifically as an excitatory gene biomarker [291]. TREs serve the exact same function as that of PREs for the PcG complex. This allows the TrxG complex bearing TRX to be able to recognize a specific gene locus. On the other hand, CBP is the true HAT, which directly and selectively conducts acetyl group transfer to H_3K_{27} and H_3K_{18} [287,292].

The function of the TrxG family protein is involved in multiple cell developmental/aging processes [293]. Although it remains controversial, the current hypothesis is that the TrxG protein counteracts the effect of the PcG [294,295]. For example, in Drosophila, the TrxG and PcG regulates the on and off status of the *Hox* gene, which affects Drosophila body segment development [294]. The TREs usually cluster or even coincide with the PREs [295,296]. With the help of some shared

components inside the TrxG and PcG (e.g. PRC2), these two complexes could be recruited to the same DNA regions [293], bind simultaneously [297] and compete for the same residue, H_3K_{27} [255]. Without affecting CBP level, decreased TRX protein was correlated with reduced H_3K_{27}Ac levels and vise versa [255]. T*rx* gene or TRX protein mutation gave the same results [289].

CBP has long been identified as a HAT [298], which is as essential as HMTs during early life development. For example, CBP knock-out caused developmental arrest in Drosophila embryoes [299]. On the contrary, regional overexpression of CBP in Drosophila caused body developmental abnormality and global histone acetylation, while ubiquitous overexpression induced mortality [300]. Recently, H_3K_{27} was reported as specific acetylation site for CBP [255]. In the study, the authors found that partial CBP knock-out allowed Drosophila to develop but with significant decreased H_3K_{27}Ac, increased $H_3K_{27}Me_3$, and no changes in $H_3K_{27}Me_2$. Conversely, moderately overexpressed CBP levels exhibited increased H_3K_{27}Ac and moderately reduced $H_3K_{27}Me_3$ in Drosophila. Lately, the same group reported the physical association of CBP with H_3K_{27}-specific demethylase UTX and chromatin-remodeling factor BRM [301]. This suggests further support for the counteractive effects between acetylation and methylation on H_3K_{27} and chromatin structure change after H_3K_{27}Ac.

1.2.4. Chromatin Remodeling

As mentioned above, although the presence of nucleosomes helps the 2 m DNA to be well folded into the eukaryotic cell, it sterically occludes the accessibility of DNA to the DNA binding molecules from small proteins (DNase I) and to huge transcriptional machiner. Thus gene transcription would be inhibited if there is no way to release the nucleosomes on the chromatin [302,303]. The biological system is smart enough to incorporate several mechanisms , such as chromatin structure remodeling, to allow access of polymerase to DNA. But, in a 6 million bp DNA pool, how is the cell able to know the exact site and time to remodel chromatin structure? The histone N-terminal tail PTM is one of the most important biomarkers that cells utilize to accurately remodel chromatin structure.

1.2.4.1. Brief introduction of chromatin structure remodeling and remodeling complex

The chromatin structure remodeling is a process that cells utilize to regulate gene expression without changing their DNA sequence. So far, five types of chromatin dynamic changes have been demonstrated, including histone switching, histone ejection and recruitment, histone replacement and histone sliding. The overall biological roles of these changes make chromatin switchable between heterochromatin and euchromatin. These remodeling processes are conducted by the chromatin remodeling complex.

Chromatin remodeling complex is a protein polymer, which use ATP to manipulate nucleosomes on the chromatin [304]. This complex usually consists of motor proteins and accessory proteins [305]. The accessory proteins are mainly involved in nucleosome binding, recognizing histone covalent modification, interacting with transcriptional factors or other

regulatory proteins and regulating the motor protein. On the other hand, the motor protein contains the real ATP hydrolysis domain, which utilizes the ATP to break down the interaction between NCP and DNA, and cause chromatin remodeling. So far, inside the chromatin remodeling complex, four families of SF2 have been identified, which are SWI/SNF family, imitation SWI (ISWI) family, chromodomain, helicase, DNA binding (CHD) family and inositol requiring 80 (INO80) family [305].

1.2.4.2. Histone acetylation induced chromatin remodeling

Histone acetylation activates gene transcription by changing chromatin structure into a less packed status.

1.2.4.2.1. Two mechanisms for histone acetylation induced chromatin structure change

Firstly, histone acetylation has been shown to weaken/decrease the contacts in the nucleosome between DNA and NCP [198,306]. The histone tail acetylation can neutralize histones' positive charge, and thus decrease their affinity for DNA. The reduced affinity or even direct binding between DNA and NCP lead to unfolded chromatin and out-looped or even naked DNA strands, which facilitate the binding between DNA and the transcription machinary [198,204]. Opposite to the acetylation, histone deacetylation is believed to restore the positive charge on the nucleosome, which strengthens the binding and results in gene inhibition. Although this model is the most popular hypothesis and supported by many studies, it is challenged by a later study, which reported that histone acetylation did not weaken the DNA-histone binding [307]. Additionally, histone acetylation changes the binding affinity between chromatin and transcription-related proteins. In *S. cerevisiae*, several silencing related transcription factors (TFs), such as type 3 and 4 of silent information regulators (Sir) [308] and Tup1p [309], decreased their affinity to acetylated H_3 and H_4, which resulted in reduced gene-inhibition. The H_4 deacetylation, on the other hand, will recruit the Sir3 [310].

Secondly, histone acetylation could recruit chromatin-remodeling factor, which facilitates the heterochromatin-to-euchromatin transformation [198]. An early study observed that histone acetylation disrupted the higher-order of chromatin and activated gene expression [311]. However, the decreased binding between DNA and NCP alone is not supposed to allow such a change. Later, more and more researchers realized that histone acetylation is also able to recruit chromatin-remodeling factors, such as SWI/SNF [312,313,314], to help them facilitate chromatin remodeling.

1.2.4.2.2. Two models of histone acetylation induced gene activation

Combining all these mechanisms together, two models have been proposed to explain the overall gene activation effect induced by histone acetylation [315,316].

The first model believes that gene activation is based on the ability of the chromatin-remodeling factor/TF to recognize locus-specific acetylation/deacetylation [316]. There remains a *cis*-element at the up-stream of gene promoter. After binding of sequence-specific DNA-binding proteins to this region, a protein-recruiting cascade occurs. Taking the repressing-process as an

example, during this cascade, HADCs reach this region, followed by chromatin-remodeling complex. The chromatin-remodeling complex facilitates the histone moving to the vicinity of the promoter core after the HADCs deacetylate the promoter. In this case, the transcriptional machinery could no longer gain access to the promoter area of the down-stream gene, which is how transcription gets inhibited [198,317]. If the repressing DNA-binding protein does not bind to the *cis*-element, the HADCs will not be recruited, which is followed by no chromatin-remodeling protein. Thus, if the nucleosome histones are acetylated, the chromatin remodeling complex will be attracted to this locus by its subunit called bromodomains [318]. After a series of nucleosome dynamic changes, the chromatin structure at the promoter region is wide enough for transcriptional machinery to start transcription.

The second model presents a more non-specific and global effect as compared to that of the first pathway. Instead of just promoter vicinity regions, the whole genome is getting acetylated by HAC [198,315,316]. The chromatin remolding complex will then be attracted to the acetylated chromatin areas. In this case, the whole genome becomes looser, which offers more accessibility to the transcriptional machinery. This sounds like that histone acetylation will cause unspecific gene activation. Well, different genes locate at different chromosome regions, where chromatin structure, nucleosome numbers and protein accessibility are different. These properties makes the acetylation to be at different level and time period which indirectly makes it gene specific. Additionally, HADCs is constantly in company with the HAC, which balance the transcription of different genes [319]. This makes the gene transcription regulation even more precise.

1.2.4.3. Histone methylation induced chromatin remodeling

As mentioned above, the histone-acetylation neutralizes the positive charge of the histone. However, for methylation, no change in electrical charge has been detected [205]. Specifically, for H_3K_{27}, no evidence so far suggest that its methylation is directly related to changes in the chromatin structure [320]. Thus, histone methylation must use other mechanisms to conduct its inhibitory effect. So far, two models have been proposed.

The first model hypothesizes that the histone tail methylation is to recruit or offer a docking place for some chromatin remodeling factors, which manipulate the downstream chromatin structure [205]. One example is the observation that methylated H_3K_{27} recruits the PRC1 [247,321,322]. The PRC1 has a protein constituent called Polycomb, which bears a chromodomain [321,322]. Because chromodomain specifically recognizes $H_3K_{27}Me_3$, it is reasonable to suspect that the PRC1 is recruited to this locus. To support this hypothesis, one study showed after H_3K_{27} de-methylase UTX knock-down, both methylated H_3K_{27} and PRC1 significantly increased binding to chromatin [323]. Another biochemical study revealed that PRC1 obtained an extended recognition groove which specifically recognized H_3K_{27} methylation [322]. However, opposite results were also published later by showing PRC2 independent recruitment of PRC1 [324]. Thus, this hypothesis remains inconclusive.

Recent studies also suggest that $H_3K_{27}Me_3$ can stop nearby transcriptional machinery passing locally. In human embryonic stem (ES) cells, some genes are enriched with binary modifications (two coexisting PTMs on the same histone N-terminal tail). For example, both gene-activating $H_3K_4Me_3$ and gene-inhibiting $H_3K_{27}Me_3$ have been detected at several genes promoters [325,326,327]. These genes are called bivalent genes. Although the function of these remains unclear, the prevailing idea is that these genes remain in a "poised" state, which is ready for rapid transcriptional activation at the presence of specific signals [328]. One study found that at the promoters of these bivalent genes, a high level of transcriptional machinery was detected, but with low transcription levels [329]. A following study repeated and agreed with their results [330]. Thus, it suggested that $H_3K_{27}Me_3$, put together with $H_3K_4Me_3$ at promoter areas, is able to prevent transcriptional machinery from passing, and thus inhibit gene transcription. Additionally, one paper demonstrated that the binary modification on H_3 tail (di-methylation and phosphorylation) also allows chromatin to fold into a specific conformation [331], which might prohibit the association of chromatin-remodeling factor from obtaining a chromodomain and preserve its heterochromatin structure.

Additionally, a newer novel model was introduced for HMT induced gene repression. This study reported that histone tail methylation by HMTs prevented unliganded nuclear receptors from binding to their target gene, which prohibited gene conformational changes and kept them inactivated [332]. However, detailed information remains unclear.

CHAPTER 2: Changes of Polycomb Repressive Complex 2 (PRC2) caused by neonatal fasting stress protect chickens from future fasting stress

Ying Jiang, Cynthia J. Denbow, Michael D. Denbow

Abstract

Unfavorable nutritional conditions during the neonatal critical-period can cause both acute metabolic syndromes and severe diseases in later life. It is due to epigenetic changes on different genes controlling feeding regulatory factors. Early studies reported that 24 hr fasting at 3 day-of-age (D3) caused changes in inhibitory epigenetic marks on neurons in the hypothalamic paraventricular nucleus (PVN), an area associated with energy homeostasis. In the current study, we further investigated the effects of fasting at D3 on epigenetic changes in the brain of chickens. Methylation of histone 3 at lysine 27 (H3K27) and H3K27 methyltransferase (HMTs) were increased after fasting in PVN neurons, and this effect was also evident at 10 (D10) and 40 days-of-age (D40). By comparing to the significantly elevated methylated H2K27 and HMTs caused by single late day fasting (D10 or D40), a pre-treated D3-fasting were able to prevent these surges and bring these parameters back or close to control. Changes in brain-derived neurotrophic factor, which is an important protein for neuron survival and energy homeostasis, further supported these data. These findings show that neurons in the PVN are capable of acclimating to repetitive fasting stresses due to the early exposure to fasting. It suggests that the epigenetic changes can induce "molecular memory" to protect individuals against future similar stresses.

2.1. Introduction

The developing brain is sensitive to environmental influences such as unfavorable nutrition during the neonatal period that may result in acute metabolic disorders [1,2,3] and severe diseases in later life [4,5]. These early life experiences occurring during heightened periods of brain plasticity help determine the lifelong structural and functional aspects of brain and behavior. In humans, for example, weight gain during the first week of life after birth increased the propensity for developing obesity several decades later [5]. This may be due to extreme susceptibility of the developing brain, whose function is easily disrupted and conditioned by nutritional stress [3,333,334]. Long-term consequences of adverse conditions in early life may be a reflection of transcriptional changes for genes within the central nervous system (CNS) that occur as a result of epigenetic modifications [335,336,337].

Epigenetics refers to genome expression regulation that is not due to DNA sequence changes [338]. Chemical modifications made to histone proteins on the chromatin is one of the most important options to perform epigenetics [338]. Although it has been shown that acute nutritional stress changed inhibitory modifications on histones at a genome-wide level [6] and altered the CpG methylation status of specific genes [8], the longevity of these epigenetic marks induced by nutritional conditioning during brain development period remain unknown. Neither the function nor purposes of these changed epigenetic marks is known.

N-terminal tail post-translational modification (PTM) of histone proteins is one of the most important epigenetic changes utilized in all cells to regulate gene expression. Thus far, various types of PTMs have been identified on various histones [12]. Among them, the methylation and acetylation on lysine residue (K) 27 on histone 3 (H3) has been linked to gene repression [13,14] and activation [15], respectively. H3K27 methylation is carried out by histone methyltransferases (HMTs) in a multi-protein complex, called polycomb repressive complex 2 (PRC2) [339]. Three polycomb group (PcG) proteins make up the PRC2 functional core [213], including embryonic ectoderm development (EED) protein, enhancer of zeste 2 (EZH2) and suppressor of zeste (SUZ) [213,242,340]. While EED and SUZ recognize a specific histone site on chromatin and bridge it with the PRC2 [242,259], EZH2 is the only HMT within the PRC2 that produces di- (H3K27Me2) and tri-methylated H3K27 (H3K27Me3) [259]. No experiment to date has studied the dynamic changes in these subunits of PRC2 during normal development and under nutritional stress in chickens.

Brain-derived neurotrophic factor (BDNF) is an important hormone involved in neuron survival and brain development, and is highly expressed in the hypothalamus [78]. As an anorexigenic factor, BDNF induces feeding suppression after acute application [161,341] and weight loss during long-term application in animals [162]. On the other hand, fasting inhibited BDNF mRNA level in several areas of the hypothalamus [75]. The paraventricular nucleus (PVN) is a key integrating nucleus for various metabolic signals and maintains normal energy homeostasis by coordinating other hypothalamic nuclei [342]. It contains a high level of BDNF [79] and responds to local BDNF microinjection by instantly inhibiting appetite and feeding behavior [161].

The BDNF gene has been the focus of many developmental studies aimed at understanding the relationship between early-life stress, brain responses, and behavioral outcomes. Data demonstrate that early-life events influence the *Bdnf* gene and behavioral outcome [343,344]. A previous study reported the genome-wide changes of inhibitory epigenetic marks (H3K27me2, H3K27me3 and EZH2) after fasting in neonatal chicks [6]. However, no study has correlated these changes at the *Bdnf* locus to gene expression.

In our prior study fasting induced changes in methylated H3K27 levels in neonatal chickens [6]. In the current study, we monitored genome-wide changes in the di- and tri-methylation status of H3K27 and expression of key components of HMTs (EED, SUZ and EZH2) in PVN neurons following a 24 hr fast in both neonatal and mature chickens. We also investigated the effects of preconditioning chicks at an early age by fasting and looking at the changes in methylation status of H3K27 following a subsequent fast. The di- and trimethylation levels of H3K27 along the *bdnf* gene during fasting of 3-day-old chicks and during subsequent fast after the critical period of feed-intake control establishment were evaluated by chromatin immunoprecipitation assays.

2.2. Materials and methods

Animals

The day of hatching was considered postnatal day 0. One days-of-age (D1) male white Plymouth Rock chickens were obtained from the Cobb-Vantress Hatchery in Wadesboro, NC, USA. They were transported to VT and initially housed in Petersime batteries in groups of ten prior to twenty-one days-of-age (D21) and in groups of four afterwards. The room temperature was 30 ± 2 ℃ and 50 ± 5% relative humidity. Water and food were available *ad libitum*. All experimental procedures were performed in accordance with the Virginia Tech Animal Care and Use Committee.

Chemicals

Antibodies were purchased from Cell Signaling Technology (Danvers, MA, USA) and included Histone 3 (H3), tri-Methylated Histone H3 at Lysine 27 (H3K27Me3), di-Methylated Histone H3 at Lysine 27 (H3K27me3) H3K27Me2, β-actin antibodies and chromatin immunoprecipitation assay kits. BDNF antibody was purchased from Abcam Inc. (Cambridge, MA, USA). Anti-rabbit IgG horseradish peroxidase-conjugated antibody was from Santa Cruz Biotechnology (Santa Cruz, CA, USA). SYBR Green was from Life Technologies Corp (Carlsbad, CA, USA). All additional chemicals were purchased from Sigma-Aldrich (St. Louis, MD, USA).

Protein isolation and western blotting

Nuclear protein extractions were conducted as described previously [6]. Before western blots, the protein concentration was quantified by BCA protein assay, according to the manufacturer's instruction (Thermo Fisher Scientific, Rockford, IL, USA). All samples were then adjusted to the same concentration. Before loading, samples were mixed with Laemmli loading buffer [345] at 1:1 volume and heated for 10 min at 99 ℃. Protein extracts were separated on 12% SDS-PAGE pre-cast gels (Lonza, Walkersville, MD, USA) and transferred to nitrocellulose membranes (12 V for 1 h, 24 V for 1 h). The membranes were then blocked in 5% bovine serum albumin (BSA) overnight at 4 ℃ with shaking. On second day, the membranes were washed by 1% BSA 5min * 3 times. Primary antibodies (Ezh2 at 1:500, H3K27Me2 at 1:1000, H3K27Me3 at 1:1000, H3 at 1:1000, β-actin at 1:1000 and BDNF at 1:1000) were incubated with the membranes overnight at 4 ℃ with shaking. On the second day, membranes were washed and incubated with anti-rabbit IgG horseradish peroxidase-conjugated antibody at room temperature for 1 h with shaking. A chemiluminescent signal was detected following incubation with SuperSignal West Pico substrate (Pierce, Rockford, IL, USA) using a Gel Doc XR System (Bio-Rad, Hercules, CA, USA). The Quantity One (Bio-Rad, Hercules, CA, USA) image analysis software was used for band density analysis. The final ratio value of each protein was equal to the ratio of the target protein to the density value of β-actin protein.

Real-time polymerase chain reaction (qPCR) assay design

The total RNA was isolated and followed by reverse transcription as described previously [6]. Real-time PCR was performed in a 7500 Sequence Detection System (Life Technologies Corp., Carlsbad, CA, USA) with 2 μl sample and a SYBR Green PCR Master Mix (1 μl DEPC H_2O, 2 ul primers at 2 μM and 5 μl SYBR Green). Primers are listed in Table 2. The product specificity of every reaction was confirmed by melting curve test. The ΔΔCt method was used for all qPCR results.

Chromatin immunoprecipitation assays (ChIP)

SimpleChIP® Enzymatic Chromatin IP Kit (Cell Signaling, Danvers, MA, USA) was used for ChIP assays. Manufacturer's protocol was followed with some modifications. Nuclear proteins in PVN were first cross-linked with 1% formaldehyde for 10 min and quenched by glycine solution. Chromatin was sheared by sonication, using Vibracell Sonix (maximal power 750 watts; Sonics & Materials Inc, Newtown, CT, USA) at 32% power for 9 rounds of 10 sec sonication with 350 ul SDS lysis buffer (SDS, 1%; EDTA, 10 mM; and Tris, pH 8.1, 50 mM). Then, 50 ul sheared chromatin were incubated with H3 (4 ul), H3K27Me2 (8 ul), H3K27Me3 (8ul), Ezh2 antibody (5 ul) and anti-IgG (4 ul as a mock background immunoprecipitation) overnight. Then, the antibodies were retrieved by using Protein G Agrose Beads and target proteins were eluted at 65 ℃ overnight. On the next day, Protein G Agrose Beads were centrifuged down at 6,000 rpm and incubated at 65 ℃ overnight with Proteinase K. After purification as provided in the kit, all samples were subjected to real-time PCR using primers targeting on different regions of the BDNF gene. Primer design was listed in Table 1. The data were normalized to an input control that consisted of qPCRs from 1% crosslinked chromatin before immunoprecipitation and final results were reported by ΔΔCt methods.

Statistical analysis

JMP 9.0 (SAS Institute Inc, Cary, NC, USA) was used for all data analysis. Data presented were means ± SEM. For experiment 1, comparisons between control and treatment group used unpaired t-test for each single time point. For experiment 2, control, treatment 1 and treatment 2 comparison used analysis of variance (ANOVA), which used the general linear modeling procedure (GLM, SAS Institute Inc.). Significant differences were considered as $P < 0.05$ unless otherwise stated.

2.3. Experimental design

Experiment 1: single fasting on three days-of-age (D3)

Thirty-six one-day-old chicks were used to test the effect of a single fasting on early postnatal days. They were randomly assigned into two groups, which had eighteen chicks per group and marked as treatment and control. All chicks have access to food and water *ad libitum*. On D3, food was withdrawn from all 3 groups for 24 hr in treatment group (called D3-fasting for short in following paragraph). On D4, six chicks were sacrificed by decapitation in each group while the rest were given *ad*

libitum access to food. On D11 and D41, six chicks was sacrificed from each group, respectively. PVN and forebrain (FB) were collected.

Experiment 2: double fasting on both D3 and ten days-of-age (D10)

For D3 and D10 double fasting (called D3/10-fasting in the following paragraph) group, eighteen chicks were randomly picked and divided into three groups (six per group). All of them were applied with food and water available *ad libitum*. One group was randomly picked as control group, which would never been fasted. For the other two groups, on D3, food was withdrawn from them for 24 hr. On D4, food was back to normal supply for both of the fasted groups. On D10, one group of previous fasted chicks were fasted again for 24hr. All three groups of chicks were sacrificed on D11 and PVN and FB samples were collected .

2.4. Results

Elevation of global methylation at H3K27 in the PVN but not in the FB was detected 24 hours following fasting stress.

Previous research reported that chicken BDNF gene has four exons, which generated three variants with the same coding area, Exon IV [346]. In our study, we first aligned BDNF gene sequence (GenBank, accession number NM_001031616) in the entire chicken genomic sequence (2006, UCSC), which verified the testing region in this study was Exon IV. For easy of wording, we use BDNF gene instead of BDNF gene, Exon IV for short in rest of the paper.

We first measured the body weight changes at different time point between naive group and D3-fasting group. We found that 24 hour fasting on day 3 posthatch resulted in a significant decrease in body weight on D4 and D11, but not D41 (Table 1).

Then, we were interested in evaluating the role of covalent histone modifications occurring at an early critical age in which the hypothalamic control of feed intake is thought to be established. It is known that changes in chromatin structure contribute to the regulation of neuronal plasticity [347]. In this study, we concentrated on the methylation of lysine 27 on histone 3 (H3K27). Using western blot analyses with specific antibodies against H3K27me2, H3K27me3, and histone H3, we found that 24 hour fasting on day 3 posthatch, resulted in a significant increase in total histone H3 levels (Fig 1A), H3K27me2 (Fig 1B), and H3K27me3 (Fig 1C) in the PVN on D4. Total H3 levels were significantly increased on D11, but reduced by Day41 after the 24 hour fast on D3. However, no significant changes were observed on D11 or D41 for H3K27me2 or HeK27me3. H3K27 modifications were also evaluated in an additional brain area: the forebrain (FB). Total H3 levels (Fig 1D) were significantly increased in the D3 fasted chicks on D4, D11, and D41. However, no significant differences in H3K27me2 (Fig 1E) or H3K27me3 (Fig 1F) were observed, as a result of fasting on D3.

Since PRC2 is specific methyltransferases for covalent modification at H3K27, we next tested the mRNA level of key gradients of this complex. As shown in Fig 2, in PVN, the expression of the histone methyltransferases – SUZ (Fig 2A), EZh2 (Fig 2B), and EED (Fig 2C) were significantly increased by D4. While all these factors became insignificant in D3-fasted group on D11, SUZ and EZh2 expression levels were significantly decreased at D41 post fasting. The mRNA expression level of these factors agreed with the changes of H3K27Me2 and H3K27Me3 in PVN as shown in Fig 1. Compared to the notable changes of PRC2 and TRX in PVN, FB remain "quite" to the fasting stress. In FB, no significant differences was detected between D3-fasting and naive group in SUZ (Fig 2D), EZH2 (Fig 2E), and EED (Fig. 2F). It agreed with the changes of H3K27Me2 and H3K27Me3 as shown in Fig 1.

BDNF protein and mRNA expression agreed with the increased global methylation at H3K27 in the PVN following 24 hrs fasting stress

The global changes of methylation at H3K27 could affect multiple genes' expression. As mentioned early, BDNF is an anorexigenic factor and inhibits food intake. In the current study, we were interested in evaluating the expression level of BDNF in PVN. Using western blot analyses with specific antibodies against BDNF protein, we found that a significant decrease in BDNF protein in the PVN in D4 chicks following the 24 hr fast as compared to naïve chicks (Fig 3A). This follows the pattern of mRNA expression which was significantly decreased in that group (Fig 3B). Although no significant decrease in BDNF mRNA by D11 or D41, there was a significant decrease at D11 of the BDNF protein but no changes at D41. Compared to PVN, in the FB, there was a also significant decrease in the BDNF protein on D4 following the fast (Fig 3C), while BDNF mRNA expression was significantly increased at D4 (Fig 3D). ON D11, BDNF protein went back to control level but BDNF mRNA remained significantly decreased on D11 in the fasted chicks. No significant difference was detected for both BDNF protein and mRNA on D41.

The inhibited BDNF expression level was controlled by the distribution of H3K27me2 and H3K27me3 on *Bdnf* gene

Although the global methylation at H3K27 had apparently affect the BDNF mRNA expression, we had no idea about the detailed changes of H3K27 methylation status at *Bdnf* gene on chromosome. Thus, we used CHIP assay to detect the dimethylation and trimethylation levels of H3K27 along the *Bdnf* gene in both PVN and FB following D3-fasting on D4, D11, and D41. Three different regions along the gene were evaluated: the *Bdnf* promoter area (-869 to -801 bp upstream of the coding region); the *Bdnf* transcription start region (+91 to +190 bp); and the *Bdnf* 3' untranslated region (+1623 to +1698 bp).

In the PVN, H3K27me2 was significantly increased on D4 at the transcription start site but not transcription start region and 3'-UTR (Fig 4B, E& H). By D11, however, the H3K27me2 level became significantly increased at all areas along the *Bdnf* on D11 post fast. This pattern of H3K27me2 remained on D41. On the other hand, the patterns of H3K27me3 varied from that

of the H3K27me2 along the *Bdnf*. After D3-fasting, H3K27me3 had already increased noticeably at all areas along the *Bdnf* on D4 (Fig 4C, F & I). By D11, along the *Bdnf*, H3K27me3 level became insignificant in D3-fasted chicks when compared to the naïve chicks. On D41, H3K27me3 again apparently elevated at *Bdnf* promoter and transcription start region but not 3'-UTR. The significance of total H3 spared in PVN, which is only shown on D4 at *Bdnf* promoter and 3'-UTR and D41 at *Bdnf* transcription start region.

As a H3K27 specific methylation catalyzer, EZH2 has been shown to be involved in the methylation of H3K27 in chicks [7]. We hypothesized that EZH2 distribution along *Bdnf* should be compatible to methylation status at H3K27 site. By using CHIP assay, we first found that the dynamic change patterns of EZH2 remained constant along *Bdnf* in PVN: increased on D4, dropped on D11 but elevated again on D41 (Fig 6A, B & C). This was compatible to overall similar to changing pattern in H3K27 methylation as detected. As shown in Fig 6A, B & C, deposition of EZh2 in the PVN along the *Bdnf* followed the same pattern as H3K27me3 on D4 and D41. However, the EZH2 level showed a significant drop on D11 while H3K27me3 was insignificant between treated and naive groups. On the other hand, the H3K27me2 showed a constant compatible pattern to EZH2 on D41 along Bdnf. However, only at *Bdnf* promoter region that H3K27me2 and EZH2 exhibited increased level. On D11, H3K27me2 exhibited a constant increased level in D3-fasting group while EZH2 exhibited the reversal.

In FB, H3K27me2 remain unchanged along *Bdnf* after D3-fasting (Fig 5B, E& H). It was until D41 that H3K27me2 showed decreased level at *Bdnf* promoter and transcription start region but not 3'-UTR. On the other hand, the patterns of H3K27me3 varied from that of H3K27me2. After D3-fasting, H3K27me3 exhibited an instant elevation along *Bdnf* gene on D4 and last till D11 (Fig 5C, F & I). On D41, H3K27me3 became indifferent between D3-fasted and naive groups. Total H3 exhibited very similar pattern as that of methylated H3K27 except total H3 was significantly inhibited on D41 along *Bdnf* in D3-fasted group. Next, we also compared EZH2 distribution along *Bdnf* to methylation status on H3K27 in FB. Similar to the PVN, EZH2 overall exhibited very similar distribution patterns along *Bdnf* gene in FB: increased on D4 and D11, but went back to control level on D41 (except D4 at *Bdnf* promoter area and D11 at *Bdnf* 3'-UTR) (Fig 6D, E & F). Again, similar to the PVN, EZH2 in FB exhibited perfect match to H3K27me3.

Preconditioned chicks by early fasting reduced homeostasis disturbance in PVN caused by late fasting

Preconditioned animals/tissues tends to have stress tolerance towards future same type stress [7,348]. As PVN exhibited significant and long-lasting changes of epigenetic markers after 24 hr on D3, we suspected that these changes serve as a protective mechanism towards potential future fasting stress. Thus, we were interested in seeing if preconditioned chicks that received an early fasting challenge at D3 would have reduced homeostasis disturbance effects when subsequently challenged again on day 10.

First, we measured changes in body weight of chicks following D10-fasting or D3/10-fasting. We found that compared to naïve group, non-pre-conditioned chicks showed higher body weight level while pre-conditioned chicks showed lower body weight on D11 (Table 2).

Single fasting on D10 resulted in significantly elevated global H3, H3K27me2, and H3K27me3 levels in the PVN compared to naïve birds (Fig 7A). The SUZ, EED, and EZH2 mRNA expression were also significantly elevated after a 24 hr fasting on D10 when compared to naïve birds (Fig 7B). However, the chicks previously fasted on D3 and then challenged again on D10, showed varied results. Previously conditioned chicks showed further elevated H3 (Fig 7A) and EZH2 (Fig 7B) compared to the chicks receiving only one fasting challenge at D10. However, levels of H3K27me2, H3K27me3, SUZ and EED became insignificantly different compared to that of the naive group (Fig 7A & B). D10-fasting significantly reduced the level of BDNF protein and its mRNA in the PVN (Fig 7C & D), but previously conditioned chicks that were subsequently fasted again on D10 showed a return of BDNF protein and mRNA back to control levels (Fig 7C & D).

FB exhibited a very different story from that of the PVN. In the FB, after D10-fasting, only global H3 levels were significantly increased, which was similar to that seen in previously conditioned and re-fasted chicks (Fig 8A). Contrary to what was observed in the PVN, SUZ, EED, H3K27Me3 and EZH2 exhibited a significant increase after D3/10-fasting compared to that of D10-fasted chicks (Fig 8A & B). Although D3/10-fasting induced a significant inhibition of BDNF mRNA compared to the naive group, no BDNF protein change observed (Fig 8C & D).

The distribution of epigenetic markers on the *Bdnf* gene were significantly changed between previously conditioned chicks and those fasted only once on D10. The CHIP results for the PVN agreed with the above western-blot and qPCR results. Throughout three different tested *bdnf* loci, the pattern remained almost identical in the PVN (Fig 9 A, B & C). Total H3 levels at each site on the *Bdnf* gene after D3/10-fasting was more elevated from naive level compared to that of D10-fasting. H3K27me2 and H3K27me3 levels at all three sites remained at a similar level as naïve controls after D3/10-fasting while D10-fasting exhibited significantly increased levels compared to controls in the PVN (except H3K27me3 at *Bdnf* 3'-UTR). The distribution of EZH2 along *Bdnf* gene agreed with the change of H3K27me2 and H3K27me3 (Fig 10A).

All detected epigenetic markers on the *Bdnf* gene in the FB had almost the same distribution patterns. H3K27me2 was not affected by either D3-fasting or D3/10-fasting at all (Fig 9 D, E & F). However, after D10-fasting, H3 exhibited a significant decrease while D3/10-fasting significantly increased the H3 deposition on *Bdnf*. In addition, H3K27me3 levels were also elevated after D3/10-fasting but not D10-fasting compared to controls . Although EZH2 was not affected by D10-fasting, D3/10-fasting elicited significant increase compared to the naive group, which was consistent with that of H3K27Me3 (Fig 10 B).

2.5. Discussion

The studies described here showed that fasting early in life was able to: (1) elevated the gene expression of PRC2 key subunits and thus (2) increased the methylation modification on H3K27 in PVN; (3) Some of these changes would last for a long period of time; (4) both BDNF protein and mRNA level were inhibited post fasting treatment, which was tightly related to the H3K27me2/me3 deposition along *Bdnf* gene; (5) helps chicks to develop epigenetic memory towards future fasting stress. Together, all these results support the hypothesis that early-life fasting would have a long-term effect in re-setting neurochemistry set-point. This effect had a protective mechanism for the body to preserve endocrine homeostasis.

Feeding regulation is determined by the neural-networking in the five hypothalamic nuclei [51]. Among them, the PVN is considered one of the most important nuclei among them. A histology study showed that the PVN received innervating fibers from almost all areas of the hypothalamus [105], which implied a pivotal role in regulating physiological functions. In addition, nearly all known orexigenic [50,106,107,111] and anorexigenic factors [107,112,113,114] increased and decreased feeding, respectively when micro-injected into the PVN. In addition, multiple numerous neuro-peptides, including BDNF [79], was also detected in the PVN. Thus, in the current study, we chose the PVN for our main focus.

In previous study of our lab, we fasted the Cobb male chicks for either 6 hours or 24 hours on 3 day-of-age. We reported that reported that compared to the non-fasted chick, 6 hours-fasting increased, but not significantly, EZH2 protein level in PVN but not in FB [6]. If fasting stress was extended to 24 hours, the elevation of EZH2 protein became apparent ($P < 0.05$) while FB remained no changed. These changes were accompanied by an increased trend ($P > 0.05$) of H3K27me2/me3 in PVN but not in FB. These data suggested a potential upcoming surge of global methylation at H3K27 site. In current study, we further extended the previous study and obtained overall consistent result. We found that after a 24-hour fasting on D3, both the FB and PVN responded showing changed levels of different epigenetic markers globally. As expected, in the FB, fasting had a limited capacity to change global epigenetic marker expression levels. This agreed with the fact that the FB is not feeding regulatory center and not directly involved in feeding regulation. However, for the PVN, a single 24 hr fast on D3 induced significantly increased methylation modification on H3K27. Firstly, this finding suggest that histone modification is highly responsive rather than static towards nutritional stresses. Histones are now known to be highly dynamic and responsive towards environmental stress [10,11]. Through covalent modification of the histone tail, histones regulate the DNA scaffold and regulates gene expression [10,12]. So far, to the author's knowledge, only a limited number of publications reported the changes in histone [6,349] and nucleotide [350,351] modifications and their related modification enzymes [349] in the hypothalamus after unfavorable nutritional stress. Thus, our finding first provided evidences to establish the relationship between fasting stress and direct histone modification. Secondary, the massive inhibitory H3K27me2/me3 deposition on chromatin after fasting suggested a massive inhibitory change in neuropeptides production. This phenomenon could change neurochemistry set-point in the hypothalamus and feeding behavior. This hypothesis was supported by the finding of dropped BDNF protein and mRNA level inside PVN after fasting treatment. Furthermore, 24 hour fasting at D3 surprisingly resulted in long term decreasing of PRC2 key

subunits (SUZ and EZH2, but not EED) at least till 38 days post fasting. The drop of SUZ and EED potentially up-regulate gene transcription of multiple genes, which cause imbalance of neurpeptides production inside PVN. One early study showed separation of the pups from their mothers left a long term effect on neurochemistry in PVN [352], it is possible that fasting could have the same effect in PVN and reset the neurochemistry set-point in CNS for a long term.

Although we report lasting epigenetic modifications, it remains to be seen whether these changes are beneficial or harmful to the chicks. Previous studies in humans revealed that unfavorable nutritional conditioning during the neonatal critical-period can induce acute metabolic syndromes [1,2,3] as well as severe diseases in later life [4,5]. Other studies in animals suggested that it helps individuals to acclimate to the same environmental changes and maintain homeostasis by obtaining "molecular memory" [353,354]. In the current study, we challenged chicks with subsequent fasting on D10 in order to determine whether these changes might be beneficial or harmful. We found that early-life fasting induced a beneficial response: a "memory" had been developed inside PVN to the PRC2, but not FB, to kept body away from harmful response from fasting at later life period. Interestingly, this memory was only seen in certain factors in PRC2: while D10-fasting significantly increasing EED and SUZ mRNA expression, pre-fasted birds did not elevated EED and SUZ at all; on the other hand, EZH2 kept increasing in both D10- and D3/10-fasting situation. PRC2 is a huge H3K27 methylation machinery [213] and EZH2, SUZ and EED are all located in its functional core [213]. If we just monitor EZH2 mRNA expression, it would suggest a constant increasing of H3K27 methylation in both fasting stress we applied . On the contrary, H3K27me2/me3 develop the similar "memory" pattern as well after repetitive fasting stress. Literature review suggested that EZH2 had barely no function if presented alone without other non-catalytic subunits in PRC2 [248]. This is because EZH2 does not have a DNA binding domain, which prevent EZH2 from histone binding [259,355]. However, EED can bind to histones [255,356] while SUZ connects proteins on chromosome, such as heterochromatin protein 1alpha [252]. And EZH2 was directly linked to EED [251,259,357] and SUZ [252,259,358] inside PRC2, which forms a triplet model that EZH2 sits in the middle [259]. These linkages insure the EZH2 to have full contact with histones and proceed methylation. Mutation or knocking-out SUZ [259,357,358] and EED [259,277,359] depleted the function of PRC2. These data suggest that both catalytic (EZH2) and non-catalytic subunits (EED and SUZ) are pivotal to PRC2. Thus, although body responds to the fasting stress through EZH2-methylating-H3K27, it is indeed via regulating of EED and SUZ. However, we are not clear how the body instills memory toward SUZ and EED and why EZH2 does not.

BDNF is initially known for its function in neuron proliferation, differentiation, growth and interaction [125]. Recently, it is also categorized as an anorexigenic factor [75,159]. Both acute injection [159,160] (including at PVN [161]) or long term intracerebroventricular injection [162] of BDNF inhibited feeding and increased energy expenditure in tested animals. While fasting inhibited BDNF level inside in the ventromedial hypothalamus [75] and dorsal vagal complex of hinder brain [159], re-fed led recovered BDNF [159]. In human, female with either bulimia nervosa (BN) or anorexia nervosa (AN) had significantly

lowered serum BDNF level [163]. In addition, it was also reported to regulate other neuropeptide levels in the PVN [360] and to change the body's metabolic rate [161]. All these data suggested the pivotal role of BDNF in feeding regulation. In the current study, we identify an instant drop in both BDNF protein and mRNA level after fasting stress. This finding agreed with the finding from previous studies. But more importantly, we were able to comply BDNF mRNA changes with the H3K27me2/me3 distribution along *Bdnf* gene. It is widely accepted that H3K27 methylation compact nucleosomes and thus block transcriptional elongation on gene templates [361,362]. Thus, tremendously increased H3K27me2/me3 after fasting indicated massive gene transcription inhibition in PVN. However, it remained out of clue that when and where of H3K27me2/me3 deposition will lead to induce specific gene inhibition. We picked three areas on *Bdnf* gene, which are promoter (-869 to -801 bp), coding starting region (+91 to +190 bp) and 3'-UTR side (+1623 to +1698 bp). Same as the global changes in PVN, instant increased level of H3K27 me2/me3 was deposited along *Bdnf* gene. EZH2, on the other hand, was also significantly changes and comply that that of H3K27 methylation level. This indicates that fasting could inhibit *Bdnf* transcription via deposition of PRC2 along *Bdnf* gene. Once PRC2 methylates H3K27, local chromatin structure become much more compacted, which inhibited gene transcription. However, we do not understand how PRC2 could recognize these specific sites. Neither do we know about other modification on other residues of other histones.

In summary, the present study showed that fasting in chickens at different life stages could all elicit acute neurochemical changes due to epigenetic imprinting changes. For the neonatal period of chickens, fasting can also chronically cause genome-wide epigenetic imprinting changes. These changes provide evidences to support the finding from human epidemiological study. In addition, this epigenetic imprinting serves as "molecular memory" in the neurons, which protects cells from massive interruption of genes' transcription and keeps individuals in homeostasis after same type of fasting stress in later life. BDNF, which is a key anorexigenic and brain-developmental factor, verified this conclusion.

Primer Name	**Gene accession number**	**Sequence**	PCR products (bp)
BDNF	NM_001031616	F: 5'-ACTGGCGGACACTTTTGAAC-3'	312
		R: 5'-GTTGCACCAGACATGTCCAC-3'	
BDNF promoter site	NM_001031616	F: 5'-TGGTTTTCATGAGGAGCCCT-3'	69
		R: 5'-TTTCCCAGAGCCCCATATCA-3'	
BDNF transcription start site	NM_001031616	F: 5'-GCTTGGCTTACCCAGGTCTTC-3'	100
		R: 5'-TCAAAAGTGTCCGCCAGTG-3'	
BDNF 3'-untranslated region	NM_001031616	F: 5'-GTCCCCTCCCCTTTCCTCTC-3'	76
		R: 5'-CAAGCTCCAGTTGTATGCTGAGTG-3'	
β-actin	NM_205518	F: 5′-CCGCAAATGCTTCTAAACCG-3′	101
		R: 5′-AAAGCCATGCCAATCTCGTC-3′	
CBP	XM_414964	F: 5'-GATCCTGAGCCGTTTGTTGACT-3'	139
		R: 5'-TTTTCCTTCCGTGTTCTACCAGTT-3'	
EED	NM_001031376	F: 5'-ATACCCCAACGAACACTCCTAATG-3'	138
		R: 5'GGACTCCAAACAAAGGCTGACC-3'	
EZH2	XM_418879	F: 5'-GCCCTGACTGCTGAGCGTAT-3'	168
		R: 5'-GTTTTCTCCTCCAGTTTCTGTTCC-3'	
SUZ	XM_415658	F: 5'-TTTATCATCCGAAAGGTGCTAGG-3'	127
		R: 5'-TTGACTGGTCCATTGCGACTG-3'	

Table 2. The primer design for different genes.

	D4		D11		D41	
D3-fasting	-	+	-	+	-	+
Body weight	85.28	71.13 *	265.9	240.5 *	2218	2158
±SEM	0.89	1.263	3.934	3.592	24.56	27.03

Table 3. Changes in chick body weight following D3-fasting. At three day-of-age, birds were fasted for 24 hours (D3-fasted) or fed *ad libitum* (naïve). Naïve controls and fasted chicks were sacrificed on day 4 (D4), day 11 (D11), and day 41 (D41). Body weight was measured before sacrifice. Each value is the mean ± standard error of the mean of 22 to 24 individual chicks. ****$P < 0.0001$ indicated a significant difference relative to D4, D11, and D41 naïve chicks. There was an overall significant decrease of body weight between naïve and D3-fasted chicks on 24 hrs and 8 days post fast, but no difference at 38 days post fasting.

	D11		
D3-fasting	-	-	+
D10-fasting	-	+	+
Body weight	265.9 [a]	310.5 [b]	208.3 [c]
±SEM	4.08	5.01	4.26

Table 4. Changes in body weight of chicks following D10-fasting or D3/10-fasting. Chicks were divided into three groups. Naive groups were fed *ad libitum* and never fasted . D3/10-fasted birds were pre-conditioned with a fasting for 24 hours on 3 days-of-age in addition to a 24 hours fasting on 10 days-of-age. The non-pre-conditioned birds were fasted for 24 hours only on 10 days-of-age (D10-fasting). All groups were sacrificed on day 11 (D11). Body weight were measured before sacrifices. Each value is the mean ± standard error of the mean of 22 to 24 individual chicks. Data bared different letters indicate significant different. There was an overall significant increase in the levels of body weight between naïve and non-pre-conditioned chicks on D11. However, body weight became significantly decreased in preconditioned birds compared to non-pre-conditioned birds and naïve birds.

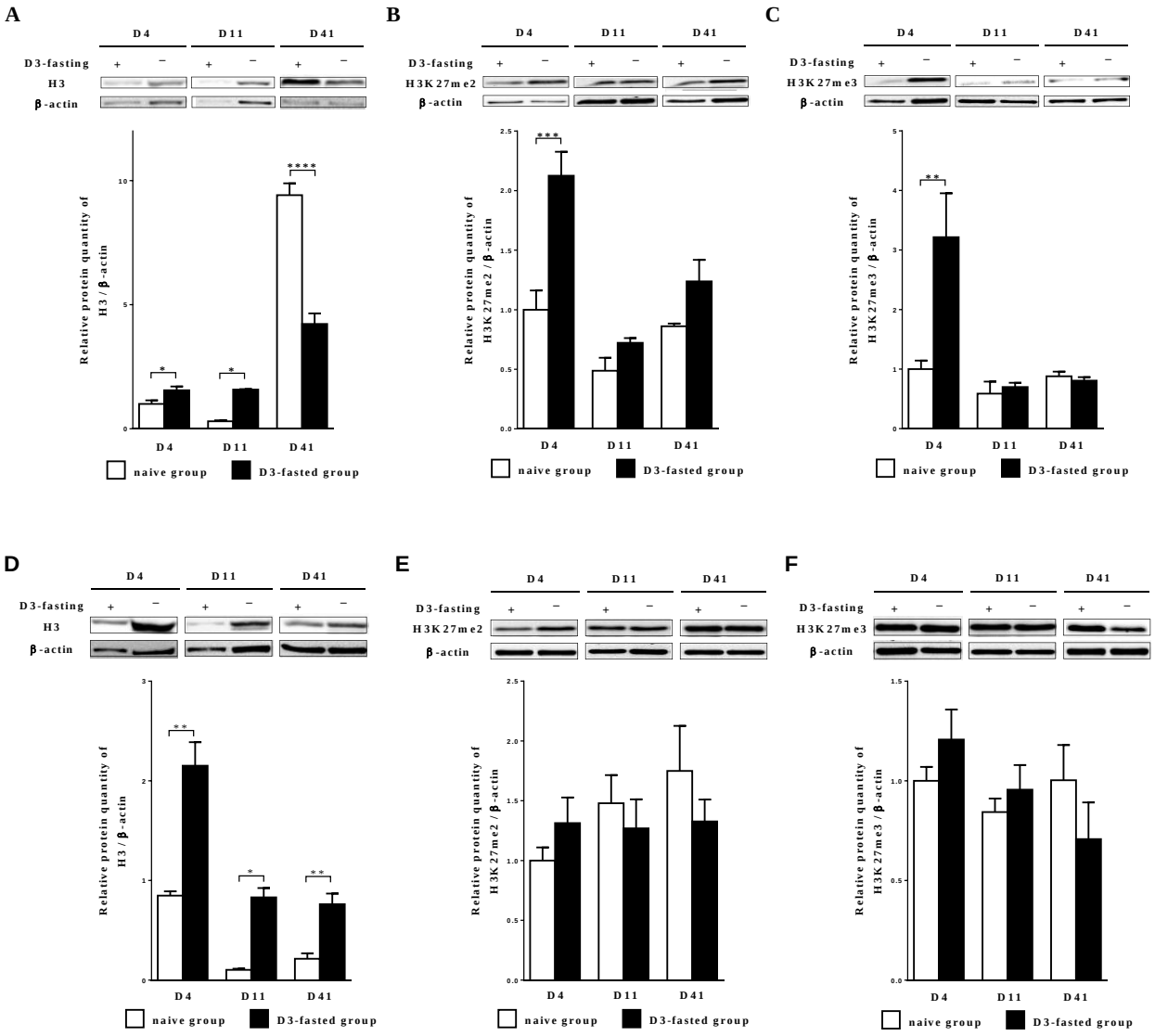
A
D4
D11
D41
D3-fasting
H3
β-actin
Relative protein quantity of H3 / β-actin
naive group
D3-fasted group
B
H3K27me2
Relative protein quantity of H3K27me2 / β-actin
C
H3K27me3
Relative protein quantity of H3K27me3 / β-actin
D
E
F

Figure 1. Changes in protein levels of H3, H3K27me2 and H3K27me3 in the chick paraventricular nucleus (PVN) (A, B & C) and the forebrain (FB) (D, E & F) following fasting. At three days of age, birds were fasted for 24 hours (D3-fasted) or fed *ad libitum* (naïve). Naïve controls and fasted chicks were sacrificed on day 4 (D4), day 11 (D11), and day 41 (D41). Total protein was isolated and evaluated by Western blot using the antibody against H3, H3K27me2 and H3K27me3. Blot density were compared with β-actin. Each value is the mean ± standard error of the mean of 6 to 12 individual chicks. *P < 0.05, **P < 0.01, **P < 0.001 and ****P < 0.0001 indicated a significant difference relative to D4, D11, and D41 naïve chicks. (A, B & C) There was an overall significant increase in the levels of global H3 between naïve and D3-fasted chicks on 24 hrs and 8 days post fast, but with a reversal at 38 days post fasting. Global di- and tri-methylated lysine 27 levels on H3 were significantly increased at 24 hours post fast, but by D11 and D41 no significant differences were found. (D, E & F) The global histone 3 levels in the FB were significantly increased at D4, D11, D41 post fast. However, there was no significant differences between the global di- and tri-methylated lysine 27 levels on H3 levels in D4, D11, or D41 post fast.

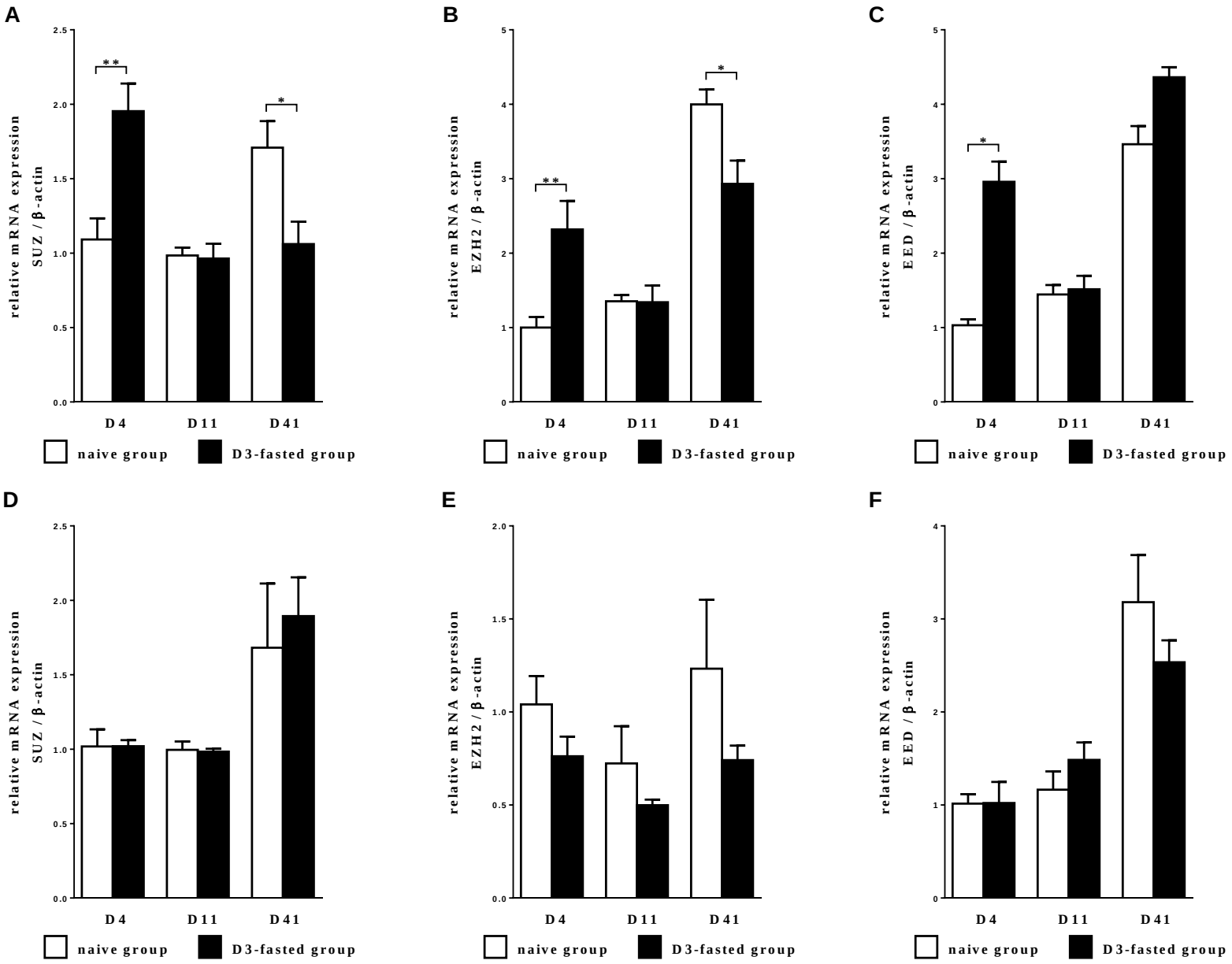
A
B
C
D
E
F
relative mRNA expression
SUZ / β-actin
EZH2 / β-actin
EED / β-actin
D4
D11
D41
naive group
D3-fasted group
**
*

Figure 2. Changes in mRNA levels of histone methyltransferases (HMTs) of the Polycomb repressive complex 2 (PRC2) and a histone acetyltransferase (HAT) in the chick paraventricular nucleus (PVN) (A, B & C) and the forebrain (FB) following fasting (D, E & F). At 3 days of age, chicks were fasted for 24 hours (D3-fasted) or fed *ad libitum* (naïve). Naïve controls and fasted chicks were sacrificed on day 4 (D4), day 11 (D11), and day 41 (D41). Total mRNA was isolated and evaluated by real-time polymerase chain reaction (PCR) using the Sybr green method with *SUZ*, *EZh2* and *EED* gene-specific primers (see Table 1). Gene expression levels were compared with β-actin. Each value is the mean ± standard error of the mean of 6 to 12 individual chicks. *P < 0.05, **P < 0.01, **P < 0.001 and ****P < 0.0001 indicate a significant difference relative to D4, D11, and D41 naïve chicks. Abbreviations: *SUZ* (suppressor of zeste), *EZh2* (enhancer of zeste 2); *EED* (embryonic ectoderm development). (A , B & C) In PVN, there was an overall significant increase in the expression of SUZ, EZH2 and EED mRNA in D3-fasted chicks compared to naïve group on 24 hrs post fast. On 8 days post fast, no significant differences were found. However, a reversal at 38 days post fasting was found. (D, E & F) FB did not respond to the D3-fasting by showing no changes in global SUZ, EZH2 and EED mRNA level till 38 days post fast.

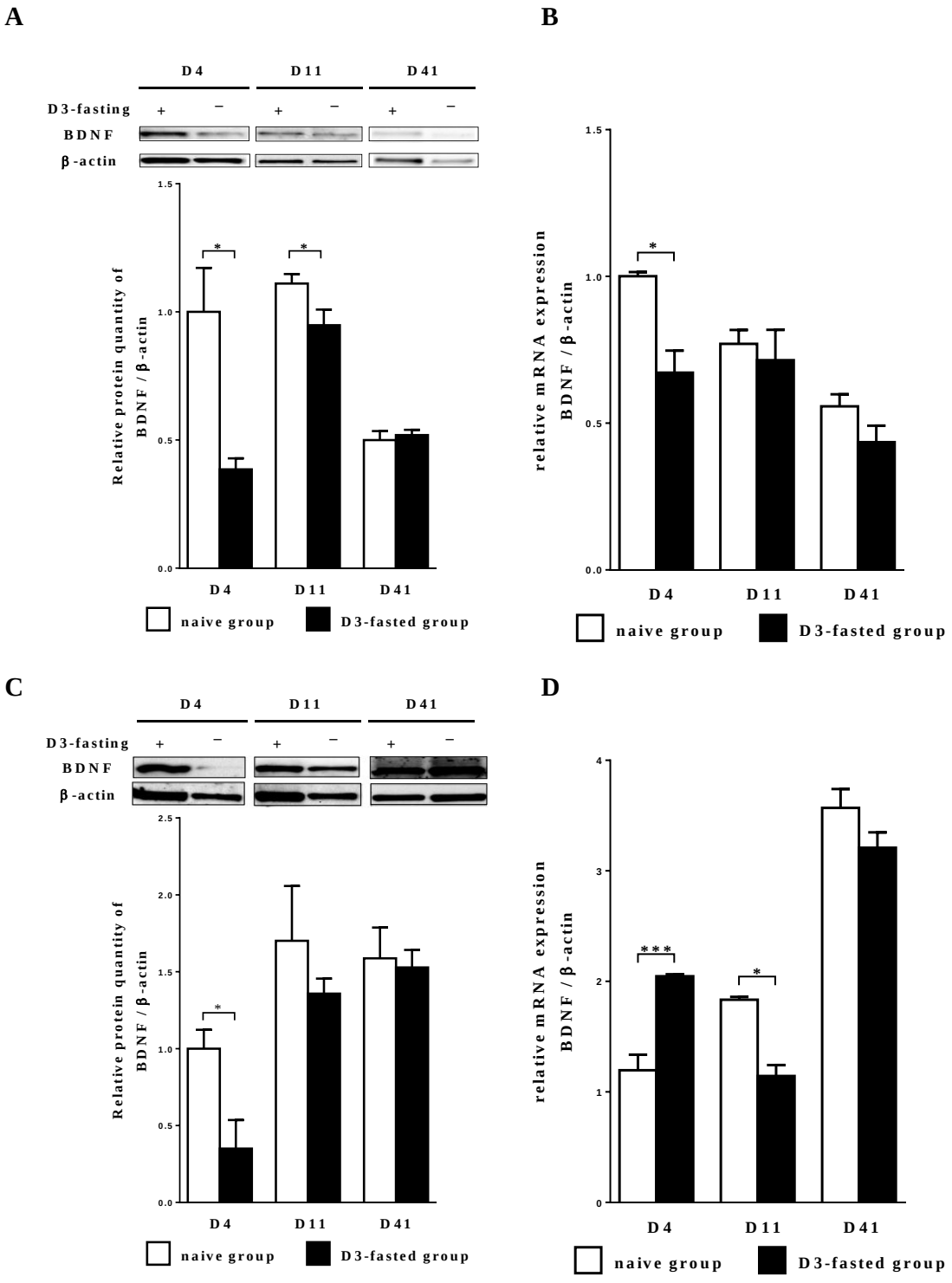
A
B
C
D
D4
D11
D41
D3-fasting
+
−
BDNF
β-actin
Relative protein quantity of BDNF / β-actin
relative mRNA expression BDNF / β-actin
naive group
D3-fasted group
*
***

Figure 3. Changes in protein and mRNA levels of BDNF in the chick paraventricular nucleus (PVN) (A & B) and the forebrain (FB) (C & D) following fasting. At three days of age, birds were fasted for 24 hours (D3-fasted) or fed *ad libitum* (naïve). Naïve controls and fasted chicks were sacrificed on day 4 (D4), day 11 (D11), and day 41 (D41). Total protein was isolated and evaluated by Western blot using the antibody against BDNF. Blot density were compared with β-actin. Total mRNA was isolated and evaluated by real-time polymerase chain reaction (PCR) using the Sybr green method with *Bdnf* gene-specific primer (see Table 1). Gene expression levels were compared with β-actin. Each value is the mean ± standard error of the mean of 6 to 12 individual chicks. *$P < 0.05$ and ***$P < 0.001$ indicated a significant difference relative to D4, D11, and D41 naïve chicks. (A & B) In PVN, there was an overall significant decrease in the levels of BDNF protein and mRNA in D3-fasted chicks compared to naïve group on 24 hrs post fast. While BNDF protein remained decreased in D3-fasted chicks on 8 days post fast, BDNF mRNA in D3-fasted chicks became indifferent compared to naïve group. On D41, no significant differences were found in both BDNF protein and mRNA. (C & D) In FB, there was an overall significant decrease and increase in the levels of BDNF protein and mRNA in D3-fasted chicks, respectively, compared to naïve group on 24 hrs post fast. While no difference was found in BNDF protein on 8 days post fast, BDNF mRNA in D3-fasted chicks became significantly decreased in D3-fasted chicks compared to naïve group. On D41, no significant differences were found in both BDNF protein and mRNA.

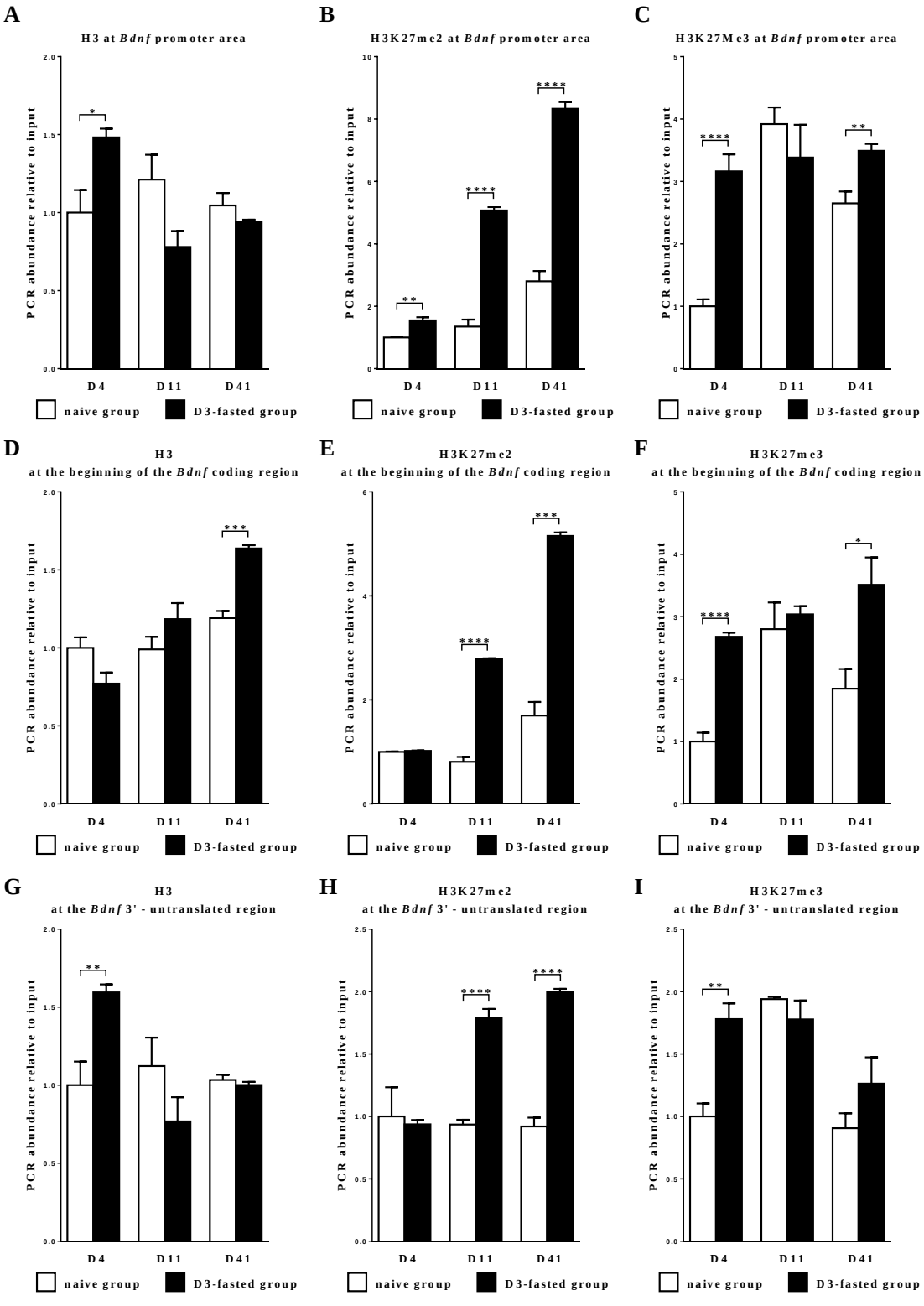
A
H3 at Bdnf promoter area
B
H3K27me2 at Bdnf promoter area
C
H3K27Me3 at Bdnf promoter area
D
H3
at the beginning of the Bdnf coding region
E
H3K27me2
at the beginning of the Bdnf coding region
F
H3K27me3
at the beginning of the Bdnf coding region
G
H3
at the Bdnf 3' - untranslated region
H
H3K27me2
at the Bdnf 3' - untranslated region
I
H3K27me3
at the Bdnf 3' - untranslated region
PCR abundance relative to input
D4
D11
D41
naive group
D3-fasted group

Figure 4. Alterations in dimethylation and trimethylation levels of histone H3 lysine 27 (H3K27) along the *Bdnf* gene in the paraventricular nucleus (PVN) following a 24 hour fast on day 3. To assess the histone modifications present at the *Bdnf* gene, chromatin immunoprecipitation (ChIP) assays were performed. PVN samples of chicks fasted on day 3 or naïve controls were taken from 4 day old, 11 day old and 41 day old chicks and were immunoprecipitated with antibodies against H3, dimethyl H3K27 (H3K27me2), trimethyl H3K27 (H3K27me3) and IgG (as negative control). (A, B & C). PCR results with *Bdnf*-specific primers (see Table 1) aligning at the promoter region and producing amplicon -869 to -801 bp upstream of the coding region. (D, E & F). PCR results with *Bdnf*-specific primers aligning at the transcription start site and producing amplicon +91 to +190 bp. (G, H and I). PCR results with *Bdnf*-specific primers aligning at the 3'-untranslated region (3'-UTR) and producing amplicon +1623 to +1698 bp. Each value (PCR abundance relative to input) is the mean ± standard error of the mean of 6 individual chicks deduct the background signal (IgG) and then normalized to that of age comparable control naïve chicks. *P < 0.05, ** P< 0.01, and *** P<0.001 indicated a significant difference relative to naïve chicks of the same age.

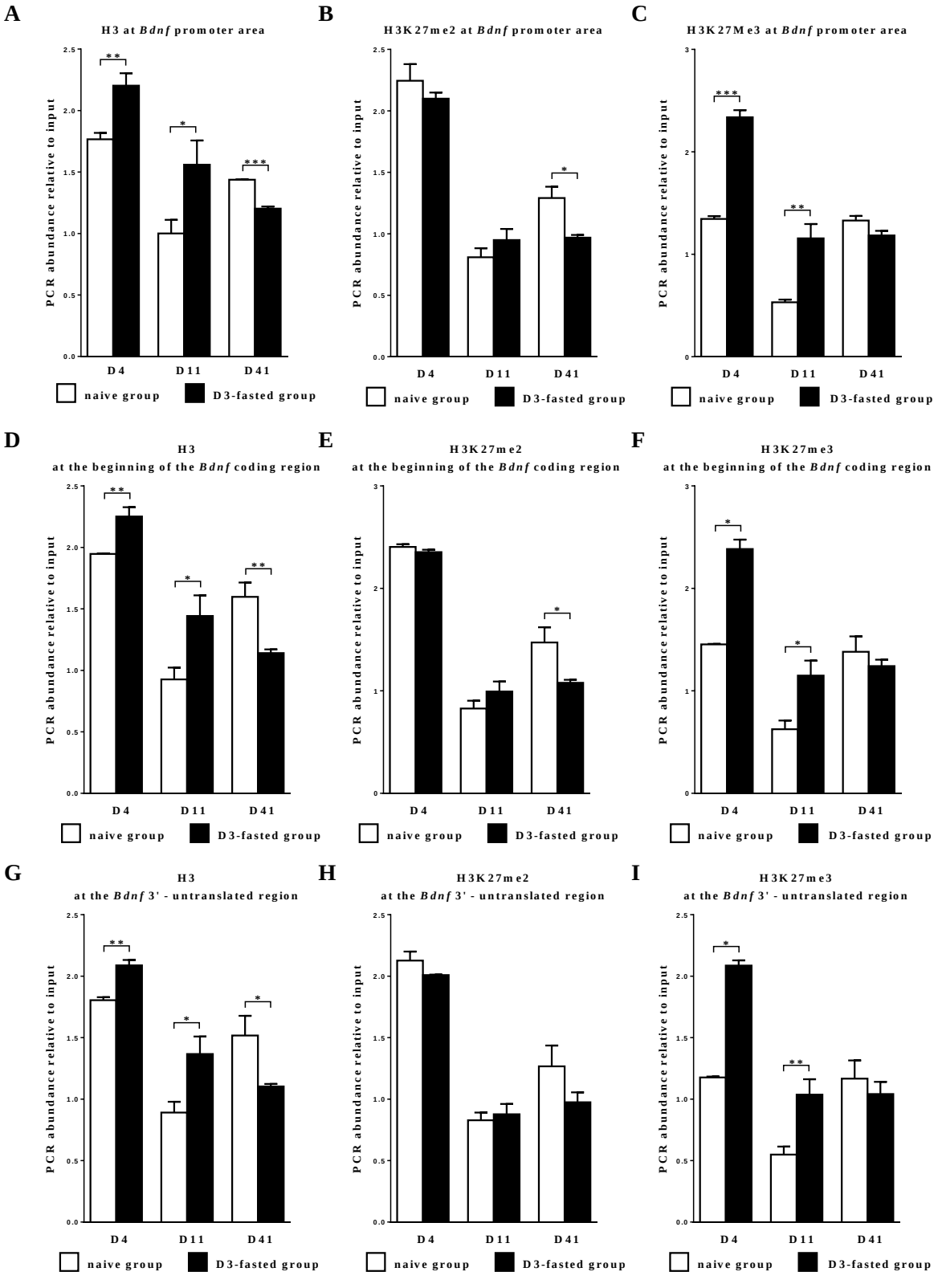
A
H3 at Bdnf promoter area
B
H3K27me2 at Bdnf promoter area
C
H3K27Me3 at Bdnf promoter area
D
H3
at the beginning of the Bdnf coding region
E
H3K27me2
at the beginning of the Bdnf coding region
F
H3K27me3
at the beginning of the Bdnf coding region
G
H3
at the Bdnf 3' - untranslated region
H
H3K27me2
at the Bdnf 3' - untranslated region
I
H3K27me3
at the Bdnf 3' - untranslated region
PCR abundance relative to input
D4
D11
D41
naive group
D3-fasted group

Figure 5. Alterations in dimethylation and trimethylation levels of histone H3 lysine 27 (H3K27) along the *Bdnf* gene in the forebrain (FB) following a 24 hour fast on day 3. To assess the histone modifications present at the *Bdnf* gene, chromatin immunoprecipitation (ChIP) assays were performed. FB samples of chicks fasted on day 3 or naïve controls were taken from 4 day old, 11 day old and 41 day old chicks and were immunoprecipitated with antibodies against H3, dimethyl H3K27 (H3K27me2), trimethyl H3K27 (H3K27me3) and IgG (as negative control). (A, B & C). PCR results with *Bdnf*-specific primers (see Table 1) aligning at the promoter region and producing amplicon -869 to -801 bp upstream of the coding region. (D, E & F). PCR results with *Bdnf*-specific primers aligning at the transcription start site and producing amplicon +91 to +190 bp. (G, H and I). PCR results with *Bdnf*-specific primers aligning at the 3'-untranslated region (3'-UTR) and producing amplicon +1623 to +1698 bp. Each value (PCR abundance relative to input) is the mean ± standard error of the mean of 6 individual chicks deduct the background signal (IgG) and then normalized to that of age comparable control naïve chicks. *$P < 0.05$, ** $P< 0.01$, and *** $P<0.001$ indicated a significant difference relative to naïve chicks of the same age.

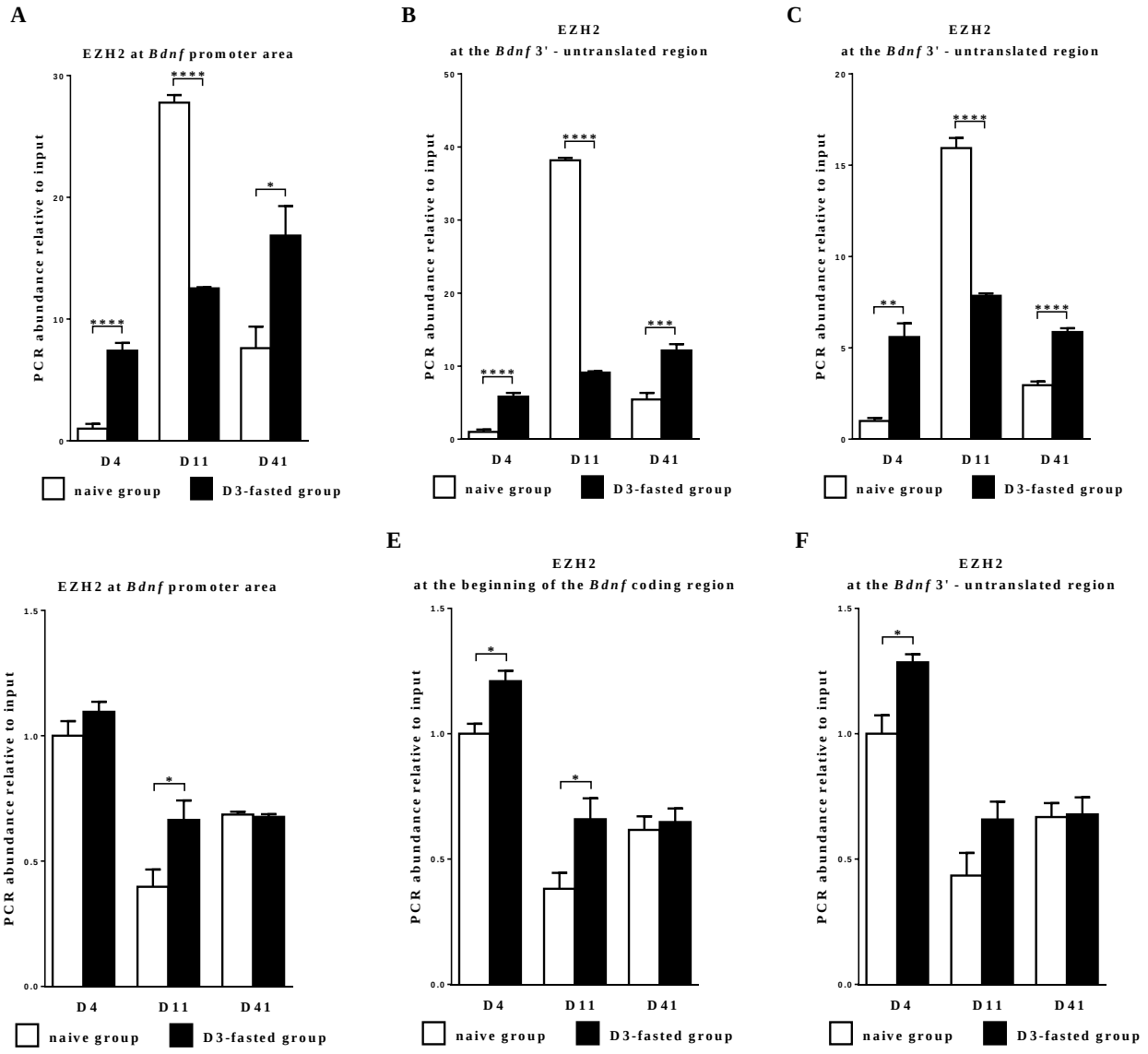
A
EZH2 at Bdnf promoter area
PCR abundance relative to input
D4
D11
D41
naive group
D3-fasted group
B
EZH2
at the Bdnf 3' - untranslated region
C
EZH2
at the Bdnf 3' - untranslated region
D
EZH2 at Bdnf promoter area
E
EZH2
at the beginning of the Bdnf coding region
F
EZH2
at the Bdnf 3' - untranslated region

Figure 6. Alterations in EZH2 along the *Bdnf* gene in the PVN and FB following a 24 hour fast on day 3. To assess the histone modifications present at the *Bdnf* gene, chromatin immunoprecipitation (ChIP) assays were performed. PVN (A, B & C) and FB (E, E & F) samples of chicks fasted on day 3 or naïve controls were taken from 4 day old, 11 day old and 41 day old chicks and were immunoprecipitated with antibodies against EZH2 and IgG (as negative control). PCR results with *Bdnf*-specific primers (see Table 1) aligning at the promoter region and producing amplicon -869 to -801 bp upstream of the coding region bp in PVN (A) and FB (E) samples.. PCR results with *Bdnf*-specific primers aligning at the transcription start site and producing amplicon +91 to +190 bp in PVN (B) and FB (F) samples. PCR results with *Bdnf*-specific primers aligning at the 3'-untranslated region (3'-UTR) and producing amplicon +1623 to +1698 bp in PVN (C) and FB (G) samples.. Each value (PCR abundance relative to input) is the mean ± standard error of the mean of 6 individual chicks deduct the background signal (IgG) and then normalized to that of age comparable control naïve chicks. *P < 0.05, ** P< 0.01, and **** P<0.0001 indicated a significant difference relative to naïve chicks of the same age.

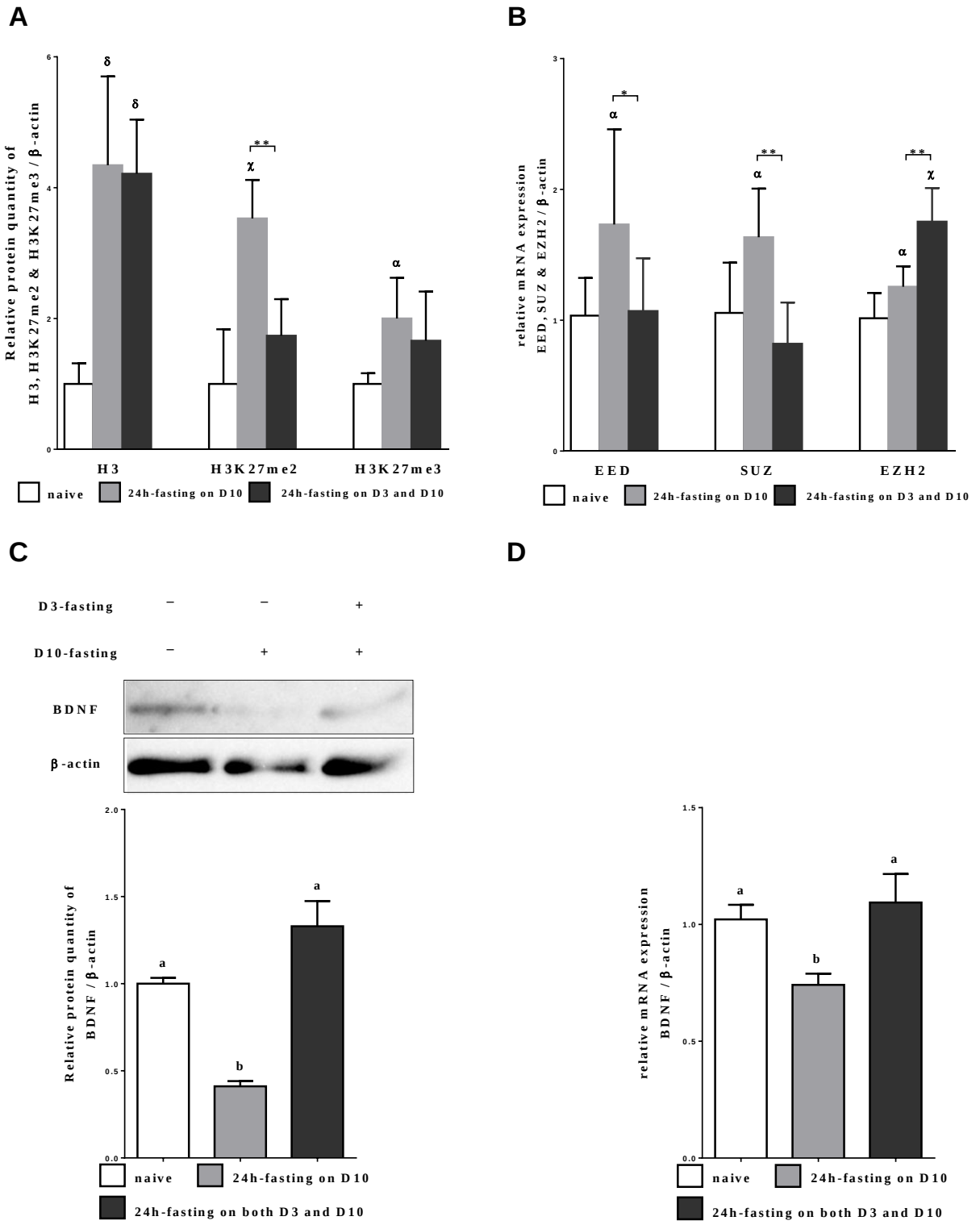
A
Relative protein quantity of
H3, H3K27me2 & H3K27me3 / β-actin
δ
δ
**
χ
α
H3
H3K27me2
H3K27me3
naive
24h-fasting on D10
24h-fasting on D3 and D10
B
relative mRNA expression
EED, SUZ & EZH2 / β-actin
*
α
**
α
**
χ
α
EED
SUZ
EZH2
naive
24h-fasting on D10
24h-fasting on D3 and D10
C
D3-fasting
D10-fasting
BDNF
β-actin
Relative protein quantity of
BDNF / β-actin
a
b
a
naive
24h-fasting on D10
24h-fasting on both D3 and D10
D
relative mRNA expression
BDNF / β-actin
a
b
a
naive
24h-fasting on D10
24h-fasting on both D3 and D10

Figure 7. Changes in protein levels of H3, H3K27me2, H3K27me3 (A) and BDNF (C) and mRNA level EZH2, EED, SUZ, CBP (B) and BDNF (D) in the chick paraventricular nucleus (PVN) following D3/10-fasting. Chicks were divided into three groups. Naive groups were fed *ad libitum* and never fasted . D3/10-fasted birds were pre-conditioned with a fasting for 24 hours on 3 days-of-age in addition to a 24 hours fasting on 10 days-of-age. The non-pre-conditioned birds were fasted for 24 hours only on 10 days-of-age (D10-fasting). All groups were sacrificed on day 11 (D11). Total protein was isolated and evaluated by Western blot using the antibody against H3, H3K27me2, H3K27me3 and BDNF. Blot density were compared with β-actin. Each value is the mean ± standard error of the mean of 6 to 12 individual chicks. Total mRNA was isolated and evaluated by real-time polymerase chain reaction (PCR) using the Sybr green method with *SUZ*, *EZh2*, *EED*, and *CBP* gene-specific primers (see Table 1). Gene expression levels were compared with β-actin. Each value is the mean ± standard error of the mean of 6 to 12 individual chicks. Abbreviations: *SUZ* (suppressor of zeste), *EZh2* (enhancer of zeste 2); *EED* (embryonic ectoderm development); *CBP* (CREB [cAMP response element binding] protein). α: $P < 0.05$, β: $P < 0.01$, χ: $P < 0.001$ and δ: $P < 0.0001$, indicated a significant difference between naive and treated group. *$P < 0.05$, **$P < 0.01$, **$P < 0.001$, ***$P < 0.0001$ and ****$P < 0.00001$ indicated a significant difference between D10-fasting and D3/10-fasting group. Column bared different letters indicate significant different. (A) There was an overall significant increase in the levels of global H3, H3K27me2 and H3K27me3 between naïve and non-pre-conditioned chicks on D11. Similarly, significant increase of global H3 also existed between naïve and D3/10-fasted chicks on D11. However, global H3K27me2 and H3K27me3 became significantly decreased preconditioned birds compared to non-pre-conditioned birds and exhibit no difference compared to naïve birds. (B) There was an overall significant increase in the expression of EED, CBP and EZH2 mRNA between naïve and non-pre-conditioned birds. Similarly, pre-conditioned birds also showed increase of EZH2 mRNA compared to naive and was even higher than non-pre-conditioned birds on D11. However, EED and SUZ became significantly decreased in preconditioned birds compared to non-pre-conditioned birds and exhibit no difference compared to naïve birds. (C & D) In PVN, there was a significant decrease in the levels of both BDNF protein ($P < 0.0001$) and mRNA ($P < 0.05$) in D10-fasted chicks compared to naïve group on 24 hrs post fast. However, if pre-conditioned chicks with an additional 24 hours fasting on 3 days-of-age, both BDNF protein and mRNA became significant increased compared to D10-fasted chicks and no different compared to control.

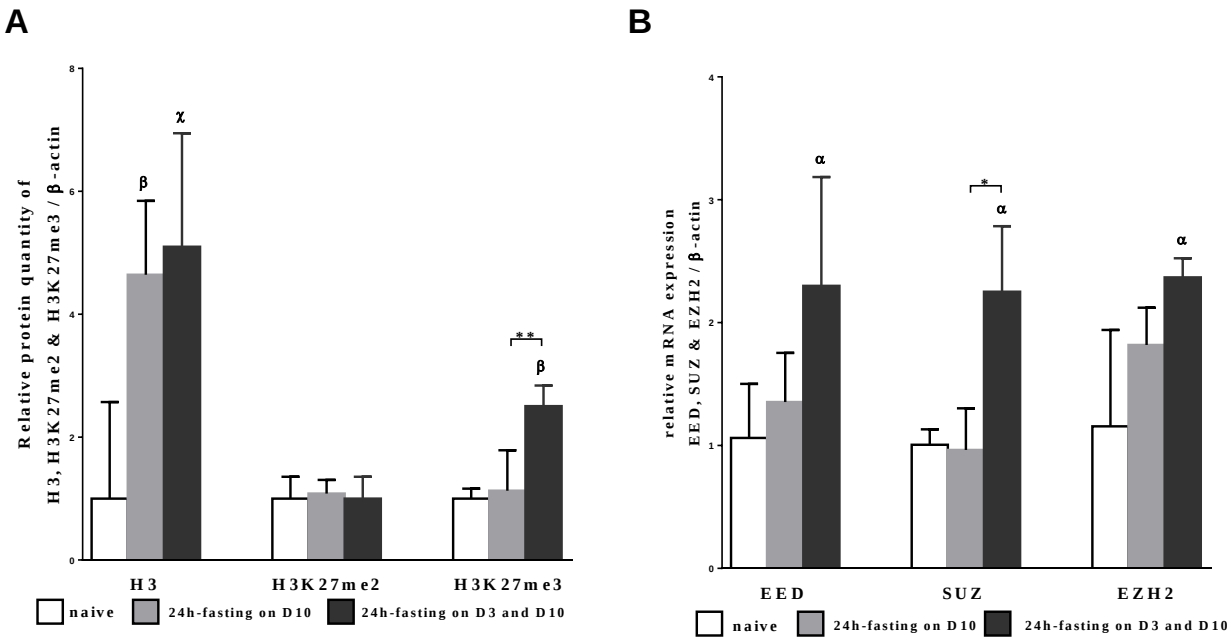
A
Relative protein quantity of
H3, H3K27me2 & H3K27me3 / β-actin
χ
β
**
β
H3
H3K27me2
H3K27me3
naive
24h-fasting on D10
24h-fasting on D3 and D10
B
relative mRNA expression
EED, SUZ & EZH2 / β-actin
α
*
α
α
EED
SUZ
EZH2
naive
24h-fasting on D10
24h-fasting on D3 and D10

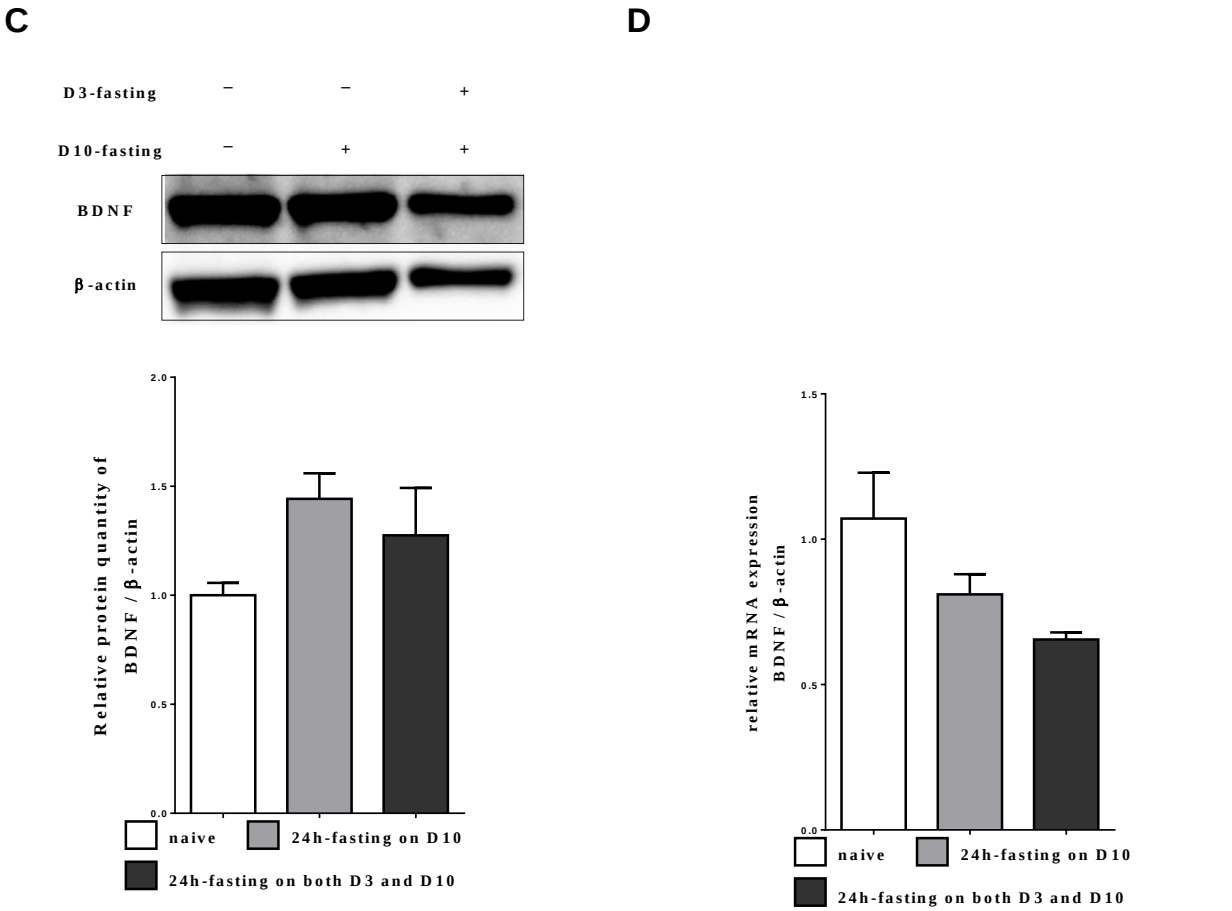
C
D3-fasting
D10-fasting
BDNF
β-actin
Relative protein quantity of
BDNF / β-actin
naive
24h-fasting on D10
24h-fasting on both D3 and D10
D
relative mRNA expression
BDNF / β-actin
naive
24h-fasting on D10
24h-fasting on both D3 and D10

Figure 8. Changes in protein levels of H3, H3K27me2, H3K27me3 (A) and BDNF (C) and mRNA level EZH2, EED, SUZ, CBP (B) and BDNF (D) in the chick forebrain (FB) following D10-fasting or D3/10-fasting. Chicks were divided into three groups. Naive groups were fed *ad libitum* and never fasted . D3/10-fasted birds were pre-conditioned with a fasting for 24 hours on 3 days-of-age in addition to a 24 hours fasting on 10 days-of-age. The non-pre-conditioned birds were fasted for 24 hours only on 10 days-of-age (D10-fasting). All groups were sacrificed on day 11 (D11). Total protein was isolated and evaluated by Western blot using the antibody against H3, H3K27me2, H3K27me3 and BDNF. Blot density were compared with β-actin. Each value is the mean ± standard error of the mean of 6 to 12 individual chicks. Total mRNA was isolated and evaluated by real-time polymerase chain reaction (PCR) using the Sybr green method with *SUZ*, *EZh2*, *EED*, and *CBP* gene-specific primers (see Table 1). Gene expression levels were compared with β-actin. Each value is the mean ± standard error of the mean of 6 to 12 individual chicks. Abbreviations: *SUZ* (suppressor of zeste), *EZh2* (enhancer of zeste 2); *EED* (embryonic ectoderm development); *CBP* (CREB [cAMP response element binding] protein). α: $P < 0.05$, β: $P < 0.01$ and χ: $P < 0.001$, indicated a significant difference between naive and treated group. *$P < 0.05$, **$P < 0.01$, **$P < 0.001$, ***$P < 0.0001$ and ****$P < 0.00001$ indicated a significant difference between D10-fasting and D3/10-fasting group. Column bared different letters indicate significant different. (A) There was an overall significant increase in the levels of global H3, but not H3K27me2 and H3K27me3 between naïve and non-pre-conditioned chicks on D11. Significant increase of global H3 also existed between naïve and D3/10-fasted chicks on D11. While, global H3K27me2 was not changed by D3/10-fasting, H3K27me3 became significantly increased in preconditioned birds compared to non-pre-conditioned birds and naïve birds. (B) There was overall no difference in the expression of EED, CBP and EZH2 mRNA between naïve and non-pre-conditioned birds. However, pre-conditioned birds increased EZH2, EED and SUZ mRNA compared to naive. SUZ mRNA level was significant increased also in pre-conditioned birds compared to non-pre-conditioned birds. (C & D) In FB, there was no significant changes in the levels of either BDNF protein or mRNA among three groups.

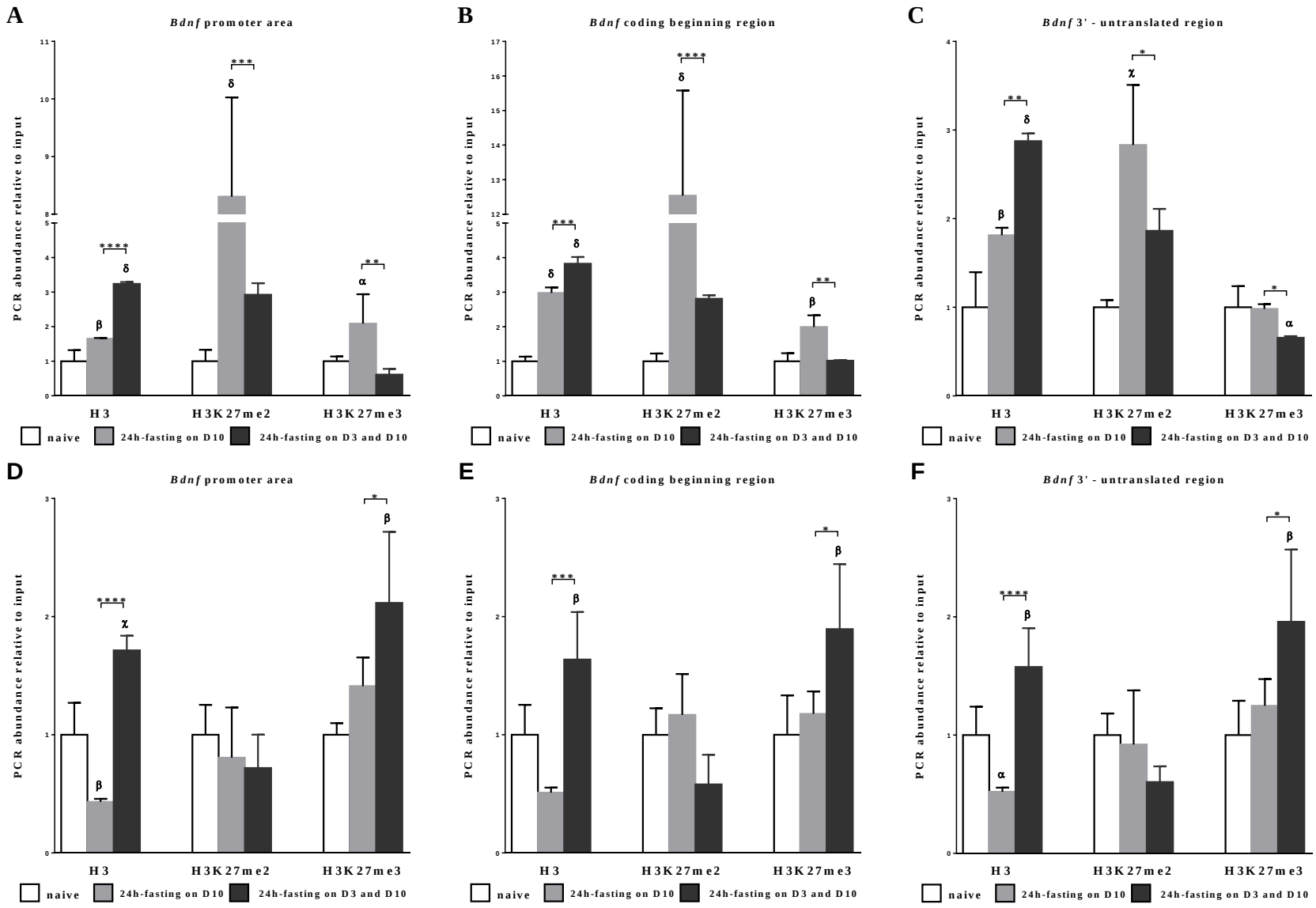
A
Bdnf promoter area
B
Bdnf coding beginning region
C
Bdnf 3' - untranslated region
D
Bdnf promoter area
E
Bdnf coding beginning region
F
Bdnf 3' - untranslated region
PCR abundance relative to input
H3
H3K27me2
H3K27me3
naive
24h-fasting on D10
24h-fasting on D3 and D10

Figure 9. Alterations in dimethylation and trimethylation levels of histone H3 lysine 27 (H3K27) along the *Bdnf* gene in the paraventricular nucleus (PVN) (A, B & C) and forebrain (FB) (D, E & F) following D10-fasting or D3/10-fasting. Chicks were divided into three groups. Naive groups were fed *ad libitum* and never fasted . D3/10-fasted birds were pre-conditioned with a fasting for 24 hours on 3 days-of-age in addition to a 24 hours fasting on 10 days-of-age. The non-pre-conditioned birds were fasted for 24 hours only on 10 days-of-age (D10-fasting). All groups were sacrificed on day 11 (D11). To assess the histone modifications present at the *Bdnf* gene, chromatin immunoprecipitation (ChIP) assays were performed. The PVN and FB samples of chicks all three groups were taken from 11 days-of-age chicks and were immunoprecipitated with antibodies against H3, dimethyl H3K27 (H3K27me2), trimethyl H3K27 (H3K27me3) and IgG (as negative control). (A & D). PCR results with *Bdnf*-specific primers (see Table 1) aligning at the promoter region and producing amplicon -869 to -801 bp upstream of the coding region. (B & E). PCR results with *Bdnf*-specific primers aligning at the transcription start site and producing amplicon +91 to +190 bp. (C & F). PCR results with *Bdnf*-specific primers aligning at the 3'-untranslated region (3'-UTR) and producing amplicon +1623 to +1698 bp. Each value (PCR abundance relative to input) is the mean ± standard error of the mean of 6 individual chicks deduct the background signal (IgG) and then normalized to that of age comparable control naïve chicks. α: $P < 0.05$, β: $P < 0.01$ and χ: $P < 0.001$, indicated a significant difference between naive and treated group. *$P < 0.05$, **$P < 0.01$, **$P < 0.001$, ***$P < 0.0001$ and ****$P < 0.00001$ indicated a significant difference between D10-fasting and D3/10-fasting group.

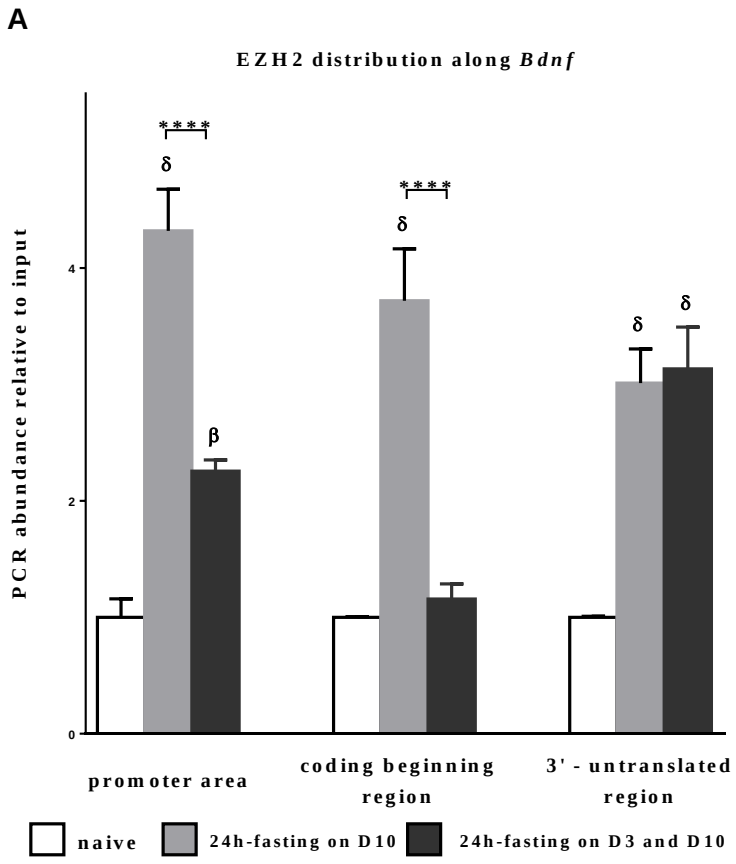
A
EZH2 distribution along Bdnf
PCR abundance relative to input
****
****
δ
δ
δ
δ
β
0
2
4
promoter area
coding beginning region
3' - untranslated region
naive
24h-fasting on D10
24h-fasting on D3 and D10

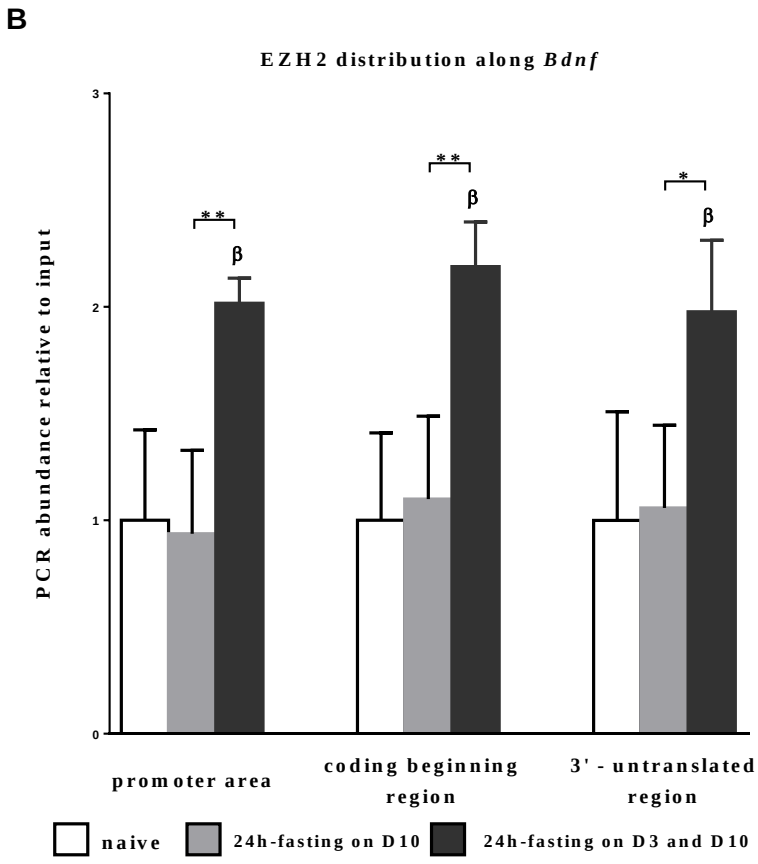
B
EZH2 distribution along Bdnf
PCR abundance relative to input
**
**
*
β
β
β
0
1
2
3
promoter area
coding beginning region
3' - untranslated region
naive
24h-fasting on D10
24h-fasting on D3 and D10

Figure 10. Alterations in EZH2 along the *Bdnf* gene in the paraventricular nucleus (PVN) (A) and forebrain (FB) (B) following D10-fasting or D3/10-fasting. Chicks were divided into three groups. Naive groups were fed *ad libitum* and never fasted . D3/10-fasted birds were pre-conditioned with a fasting for 24 hours on 3 days-of-age in addition to a 24 hours fasting on 10 days-of-age. The non-pre-conditioned birds were fasted for 24 hours only on 10 days-of-age (D10-fasting). All groups were sacrificed on day 11 (D11). To assess the histone modifications present at the *Bdnf* gene, chromatin immunoprecipitation (ChIP) assays were performed. The PVN and FB samples of chicks all three groups were taken from 11 days-of-age chicks and were immunoprecipitated with antibodies against EZH2 and IgG (as negative control). Promoter region represents PCR results with *Bdnf*-specific primers (see Table 1) aligning at the promoter region and producing amplicon -869 to -801 bp upstream of the coding region. Coding beginning region represents PCR results with *Bdnf*-specific primers aligning at the transcription start site and producing amplicon +91 to +190 bp. 3'-untranslated region (3'-UTR) represents PCR results with *Bdnf*-specific primers aligning at the 3'-UTR and producing amplicon +1623 to +1698 bp. Each value (PCR abundance relative to input) is the mean ± standard error of the mean of 6 individual chicks deduct the background signal (IgG) and then normalized to that of age comparable control naïve chicks. α: $P < 0.05$, β: $P < 0.01$ and χ: $P < 0.001$, indicated a significant difference between naive and treated group. *$P < 0.05$, **$P < 0.01$, **$P < 0.001$, ***$P < 0.0001$ and ****$P < 0.00001$ indicated a significant difference between D10-fasting and D3/10-fasting group.

CHAPTER 3: EZH2 antisense oligonucleotides inhibits EZH2 methyltransferase expression and blocks the fasting-tolerance acquisition

Ying Jiang, Cynthia J. Denbow, Michael D. Denbow

Abstract

Both acute metabolic syndromes and severe diseases in later life of human have been related to the unfavorable nutritional conditions during their neonatal critical-period. This observation has been tightly related to the epigenetic changes on various genes controlling feeding regulatory factors in the feeding regulation centers, such as the paraventricular nucleus (PVN). A previous studies showed that 24 hr fasting at 3 day-of-age (D3) caused a significant increase in methylation modification at the lysine 27 residue (K27) of the histone 3 tail (H3) in the PVN. This process is mainly catalyzed by enhancer of zeste 2 (EZH2) protein in polycomb repressive complex 2 (PRC2). In the current study, we investigated the importance of EZH2 in feed intake regulation by the knockdown of EZH2 expression. We found that 24 hours post lateral ventricle injection, EZH2 antisense oligonucleotides (1μg/μl injection concentration), but not siRNA, led to significant inhibition of EZH2 protein in both forebrain (45% inhibition) and PVN (86% inhibition) of 3 day-of-age (D3) chicks. Then, on D3, chicks were subjected to 24 hour fasting stress (D3-fasting) following either EZH2 antisense or artificial cerebrospinal fluid (ACSF) injection. EZH2 antisense blocked the surge of H3K27 methylation after D3-fasting. Brain-derived neurotrophic factor (BDNF), an anorexigenic factor, exhibited elevated expression and less methylated H3K27 deposition along the *Bdnf* gene. A previous studiesalso reported fasting-tolerance acquisition after repetitive fasting stress on both D3 and D10, which we called "epigenetic memory". However, after EZH2 antisense injection, chicks' PVN no longer exhibited "epigenetic memory" to repetitive fasting stress. These findings suggest that neurons in the PVN utilize PRC2 as a major H3K27 methylation tool. Knockdown of EZH2 in PRC2 impaired the response of the PVN to fasting stress and the ability to acclimate to repetitive fasting stresses. Thus, EZH2 is an important H3K27 methyltransferase to maintain homeostasis.

3.1. Introduction

The developing brain is highly sensitive to environmental influences. Unfavorable nutrition is one kind of stresses that can cause acute metabolic disorders during the neonatal period [1,2,3] and severe diseases in later life [4,5]. These early life experiences occur during heightened periods of brain plasticity and help determine the lifelong structural and functional aspects of brain and behavior. In humans, for example, weight gain during the first week of life after birth increased the propensity for developing obesity several decades later [5]. This susceptibility is, if not all, related to the dynamic reversible epigenetic imprints left on the histones [6,7,8], especially during the prenatal and postpartum period [9].

Histones are highly dynamic and responsive to environmental stress [10,11]. Through covalent modification of the histone tail, histones alter the DNA scaffold and regulate gene expression [10,12]. Various types of post translational modification have been identified on various histones tails [12]. Among them, the methylation and acetylation on lysine residue (K) 27 on histone 3 (H3) has been tightly linked to gene repression [13,14] and activation [15], respectively. The Polycomb group (PcG) proteins are groups of evolutionarily conserved proteins, which are essential for genes silencing via histone methylation [245]. SUZ (suppressor of zeste), EZh2 (enhancer of zeste 2) and EED (embryonic ectoderm development) all belong to this group. These three proteins form the functional core of polycomb repressive complex 2 (PRC2), which put di- and tri-methylation group onto H3K27 [242,243,247,248]. EZH2 obtained the SET (Su[var]3-9; E[z]; Trithorax) and perform as methyltransferases [237]. On the other hand, although lacking of catalytic ability, SUZ [259] and EED [256,257] play a key to help EZH2 to finish methylation reaction. On the other hand, the Trithorax group (TrxG) proteins counteract the function PcG group [294,363], which activate gene transcription. Similar to that of EZH2, the CBP (CREB [cAMP response element binding] protein) belongs to TrxG and is the catalytic subunit of TRX, which acetylates H3K27 [364].

Brain-derived neurotrophic factor (BDNF) is widely expressed in various regions of brain but has the highest concentration in the hypothalamus [78,155]. Although initially known for its pivotal role in brain development and plasticity [78], BDNF had also been identified as an anorexigenic factor [156]. Previous studies showed that animals exhibited feeding suppression [161,341] and weight loss [162] after BDNF acute and long term application, respectively. From another point of view, fasting also inhibited BDNF mRNA level in several areas of the hypothalamus [75]. Human suffered severe hyperphagia and obesity also had been reported to obtain mutant *Bdnf* gene [165]. Previous studies reported that early-life events affect the *Bdnf* gene expression and thus changed behavioral outcome of animals, including different propensity for social interaction [365,366] and levels for stress responsivity and anxiety [343,344]. This *Bdnf* gene expression had been tightly related to the epigenetic imprints on *Bdnf* gene, including dynamic deposition of modified histones [7,343,344]. However, no studies have shown any changes at the *Bdnf* locus after fasting stress.

The hypothalamus, a crucial structure in the brain, is involved in many physiological roles of regulation, including feeding. The hypothalamic paraventricular nucleus (PVN) is one of the most important feeding regulating nuclei [342]. The

micro-injection of orexigenic factors [50] into the PVN could instantly increase feeding and vice versa [107,112,113,114,115]. BDNF is also a pivotal feed regulator in the PVN. Not only the PVN had a high expression level of BDNF [79], but micro-injection of BDNF into the PVN inhibited feeding [161]. A previous study reported the genome-wide increasing of EZH2 in PVN after fasting in neonatal chicks [6]. However, little is known about the mechanism leading to changes in PRC2 and its products.

The oligodeoxyribonucleotides is a small piece of DNA molecule [367,368]. Compared to normal DNA oligonucleotides, the oligodeoxyribonucleotide had a nonbridging oxygen atom replaced by a sulfur atom at every single phosphorus site, which makes them highly resistant towards endonucleases [368]. The additional phosphorothioate modification on the oligodeoxyribonucleotides makes it more stable and resistant to endonucleases degradation [368]. In theory, after uptaken by cells, oligodeoxyribonucleotides hybridize to its specific complementary nucleotides inside cells. This hybridization could be used to inhibit target gene either by triggering the RNase H to hydrolyze mRNAs [369,370,371], blocking transcription initiator progression [372] or inhibiting mRNA splicing [368]. Because of the effectives of oligodeoxyribonucleotides, multiple clinical therapeutic trials have been conducted to test effectiveness of oligodeoxyribonucleotides in cancer treatment [373,374,375]

We previously demonstrated a role for epigenetic regulation involved in fasting stress. We showed that 24 hours fasting on 3 day-of-age chick significantly increased PRC2 subunits and its product, which last at least for 38 days. In addition, early fasting stress was able to induce "molecular memory" in certain subunit of PRC2 (SUZ and EED, but not EZH2) inside PVN neurons, which provided protection from fasting later in life. These data confirmed the importance of EZH2 in fasting related histone methylation regulation. In the present study, we investigated the importance of EZH2 by knocking down EZH2 proteins. Our data shown that EZH2 knockdown blocked the "normal" response towards early fasting stress in the PVN. In addition, the PVN lost "molecular memory" towards fasting stress.

3.2. Materials and methods

Animals

In the current study, postnatal day 0 was defined as the first day of hatching. Male White Plymouth Rock chickens were obtained on one day-of-age (D1) from the Cobb-Vantress Hatchery in Wadesboro, NC, USA. When transported to VT, chicks were first housed in Petersime batteries in groups of ten. The room temperature was set at 30 ± 2 ℃ and relative humidity at 50 ± 5%. Water and food were fed *ad libitum*. The Virginia Tech Animal Care and Use Committee had approved all experimental procedures.

Chemicals

Anti-Histone 3 (H3), anti-tri-Methylated Histone H3 at Lysine 27 (H3K27Me3), anti-di-Methylated Histone H3 at Lysine 27 (H3K27me3) H3K27Me2, anti-β-actin antibodies and chromatin immunoprecipitation assay kits were purchased from Cell Signaling Technology (Danvers, MA, USA). Antibody purchased from Abcam Inc. (Cambridge, MA, USA) included BDNF antibody. Antibody purchased from Santa Cruz Biotechnology (Santa Cruz, CA, USA) included anti-rabbit IgG horseradish peroxidase-conjugated antibody. SYBR Green and Invivofectamine® 2.0 were purchased from Life Technologies Corp (Carlsbad, CA, USA). The Silencer® Select GAPDH siRNA was purchased from Ambion® (Austin, T**X**, USA). Both EZH2 antisense and sense phosphorothioate oligodeoxyribonucleotides were purchased from Eurofins MWG Operon (Huntsville, AL, USA). All additional chemicals were purchased from Sigma-Aldrich (St. Louis, MD, USA).

Protein isolation and western blotting

Nuclear protein extractions were performed as previously described [6]. After the extraction, the protein concentration was quantified by BCA protein assay before western blot, according to the manufacturer's instruction (Thermo Fisher Scientific, Rockford, IL, USA). Then, the Laemmli loading buffer [345] was mixed with samples at 1:1 volume ratio and heated at 99 ℃ for 10 min. The mixes were loaded onto and separated by the 12% SDS-PAGE pre-cast gels (Lonza, Walkersville, MD, USA). Samples were transferred onto the nitrocellulose membranes at 12 Volts for 1 hour followed by 24 Volts for 1 hour. After transferring, nitrocellulose membranes were blocked in the 5% bovine serum albumin (BSA) overnight at 4 ℃ with shaking. On the second day, the membranes were transferred into 1% BSA for 3 times' 5 minutes wash followed by overnight incubation with primary antibodies at 4 ℃ with shaking. The dilution of these primary antibodies are: Ezh2 at 1:500, H3K27Me2 at 1:1000, H3K27Me3 at 1:1000, H3 at 1:1000, β-actin at 1:1000 and BDNF at 1:1000. On the next day, membranes were transferred into 1% BSA for 3 times' 5 minutes wash followed by incubation with anti-rabbit IgG horseradish peroxidase-conjugated antibody at room temperature for 1 h with shaking. The SuperSignal West Pico substrate (Pierce, Rockford, IL, USA), Gel Doc XR System (Bio-Rad, Hercules, CA, USA) and Quantity One (Bio-Rad, Hercules, CA, USA) image analysis software were used to detecte

the chemiluminescent signal. The final relative ratio value of each protein was equal to the ratio of the target protein to the density value of β-actin protein.

Real-time polymerase chain reaction (qPCR) assay design

The total RNA was isolated and followed by reverse transcription as previously stated [6]. The 7500 Sequence Detection System (Life Technologies Corp., Carlsbad, CA, USA) was used to perform the real-time PCR. Total loading in each well included 2 μl sample and one volume of SYBR Green PCR Master Mix (2 μl primers at 2 μM, 1 μl DEPC H_2O and 5 μl SYBR Green). Primers are listed in Table 1. A melting curve test was performed after every qPCR experiment to confirm the specificity of the final products. The ΔΔCt method was used for all qPCR results.

Chromatin immunoprecipitation assays (ChIP)

The CHIP assay procedure followed modified manufacturer's protocol of the SimpleChIP® Enzymatic Chromatin IP Kit (Cell Signaling, Danvers, MA, USA). First, samples were fixed by 1% formaldehyde for 10 min and transferred into 350 μl SDS lysis buffer (SDS, 1%; EDTA, 10 mM; and Tris, pH 8.1, 50 mM). The Vibracell Sonix (maximal power 750 watts; Sonics & Materials Inc, Newtown, CT, USA) were then used to shear fixed samples (32% power, 9 rounds of 10 sec sonication). Then the sheared chromatin were aliquoted into seven tubes with 50 μl each and incubated with H3 antibody (4 μl), H3K27me2 antibody (8 μl), H3K27me3 antibody (8 μl), Ezh2 antibody (5 μl) and anti-IgG antibody (4 μl, used for background) overnight at 4 ℃ with shaking. On the next day, Protein G Agarose Beads were used to retrieve antibodies-chromatin complex followed by elution at 65 ℃ overnight with shaking. On the third day, each aliquots were centrifuged at 6,000 rpm for 10min and the supernatant were transferred into Proteinase K tube for 65 ℃ overnight incubation. On the fourth day, chromatin were transferred into purification column tube as provided in the kit. All samples were then subjected to qPCR using *Bdnf* gene primer targeting promoter, translational start site and 3'-UTR (Table 1). The data were first deducted by background signal and then normalized to an input control that consisted of qPCRs from 1% crosslinked chromatin before immunoprecipitation and final results were reported by ΔΔCt methods.

Statistical analysis

JMP 9.0 (SAS Institute Inc, Cary, NC, USA) was used for all data analysis. For experiment 1, unpaired t-test were used to compare control and treatment group at each single time point. For experiment 2, control, analysis of variance (ANOVA) were used to compare the difference among naive, D10-fasting and D3/10-fasing, which used the general linear modeling procedure (GLM, SAS Institute Inc.). Significant differences were considered as $P < 0.05$ unless otherwise mentioned.

3.3. Experimental design

Experiment 1: test the feasibility of *in vivo* siRNA injection to knock down gene

Eighteen one-day-old chicks were used to test the effectiveness of a single injection of siRNA targeting GAPDH mRNA. They were randomly divided into three groups, which had six chicks per group and marked ACSF injection, siRNA negative control and siRNA targeting GAPDH. All chicks had access to food and water *ad libitum*. On experimental day, both negative and positive control siRNA targeting GAPDH were diluted into 208333 nM in Invivofectamine® 2.0 followed manufacturer's protocol. Briefly, first, 6 µl DEPC water was added into the siRNA aliquot following centrifuge at 12,000 rpm for 10 minutes. Then, 6 µl complexation buffer was added into the siRNA aliquot. After brief vortexing, 12 µl Invivofectamine® 2.0 was added into the siRNA aliquot and followed by another brief vortexing. After incubating at 50 ℃ for 30 minutes, siRNA was ready to be used when cooled down to 37 ℃. Then 6 µl of ACSF or siRNAs were injected into the lateral ventricle of D3 chicks. On D4, all chicks were sacrificed instantly by decapitation. The forebrain (FB) was collected.

Experiment 2: test the selectiveness and effectiveness of EZH2 anti-sense oligo

a. EZH2 antisense oligonucleotides preparation

The sequences of EZH2 antisense and sense phosphorothioate oligonucleotides were adopted from previous studies [7], which were 5'-ACATTCCCCGGACTCTCAA-3' and 5'-TTGAGAGTCCGGGGAATG-3', respectively. On arrival, they were diluted into artificial Cerebrospinal fluid (ACSF) (124 mM NaCl, 2.5 mM KCl, 2.0 mM $MgSO_4$, 1.25 mM $KH2PO_4$, 26 mM $NaHCO_3$, 2.5 mM $CaCl_2$, 10 mM Glucose and 4 mM sucrose) solution at final concentration of 1 µg/µl or 0.5 µg/µl and kept at 4 ℃. On the day of injection, they were slowly warmed up to 37 ℃.

b. test the effectiveness of EZH2 anti-sense

Eighteen one-day-old chicks were used to test the effectiveness of a single EZH2 anti-sense injection. They were randomly divided into three groups, which had six chicks per group and marked ACSF, EZH2 anti-sense (0.5 µg/µl) and EZH2-anti-sense (1 µg/µl). All chicks had access to food and water *ad libitum*. On D2, EZH2 anti-sense were diluted to 0.5 µg/µl and 1 µg/µl in ACSF and kept at 4 ℃. On D3, all injection solutions were slowly warmed up to 37 ℃. Then 5.5 µl of ACSF and EZH2 anti-sense (at both 0.5 µg/µl and 1 µg/µl) were injected into the lateral ventricle. On D4, all chicks were sacrificed instantly by decapitation. The hypothalamus and forebrain (FB) were collected.

c. test the selectiveness of EZH2 anti-sense

Eighteen one-day-old chicks were used to test the effectiveness of a single EZH2 anti-sense injection. They were randomly divided into three groups, which had six chicks per group and marked ACSF, EZH2 sense (1 µg/µl) and EZH2-anti-

sense (1 μg/μl). All chicks have access to food and water *ad libitum*. Then 5.5 μl of ACSF, EZH2 sense and EZH2 anti-sense were injected into the lateral ventricle. On D4, all chicks were sacrificed instantly by decapitation. The hypothalamus and FB were collected.

Experiment 3: single fasting at three day-of-age (D3) after EZH2 anti-sense injection

Sixty-six one-day-old chicks were randomly picked and evenly divided into three groups (eighteen for naive, twenty for control and twenty for the treatment group). All of them were supplied with food and water available *ad libitum*. The naive group received a 5.5 ul ACSF on D3 into the lateral ventricle. They were never restrained from food or water. On D4 and D11, nine chicks were randomly picked from naive group and sacrificed instantly by decapitation. In the mean time, on D3, 5.5 ul of ACSF and EZH2 anti-sense (1 ug/ul) were injected into the lateral ventricle of the control and treatment groups, respectively. Right after injection, food was withdrawn from both for 24 hr. Twelve chicks from each group were randomly picked and sacrificed instantly by decapitation on D4. For the other twelve in each group, food was supplied *ad libitum*. On D11, all chicks left in each group were sacrificed by decapitation. PVN and forebrain (FB) were collected from all chicks.

Experiment 4: double fasting on both D3 and ten days-of-age (D10) after EZH2 anti-sense injection

Thirty-six chicks were randomly picked and divided into two groups (eighteen per group). All of them were supplied with food and water available *ad libitum*. On D3, one group received ACSF 5.5ul injection into the lateral ventricle while the other group received EZH2 anti-sense (1 ug/ul) instead. After injection, in ACSF injected group, eighteen chicks were randomly divided into control, D10-fasted and D3-and-D10 repetitive fasted (D3/10-fasted) group. For the control group, chicks were never fasted. For D10-fasted group, chicks were fasted only on D10 for 24 hr. For D3/10-fasted group, food was withdrawn from them for 24 hr on D3 initially and back to normal supply on D4. On D10, previous D3-fasted chicks were fasted again for 24hr. All three groups of chicks were sacrificed on D11 and PVN and FB samples were collected. For EZH2 anti-sense injected group, the treatments were exactly the same as that of the ACSF injected group.

3.4. Results

1. siRNA *in vivo* injection had no effect in protein regulation

In the FB, compared to the ACSF injection group, negative control siRNA did not inhibit either GAPDH protein or mRNA levels ($P > 0.05$) (Fig. 13) . The positive control siRNA also did not inhibit GAPDH protein and mRNA, either ($P > 0.05$).

2. EZH2 antisense oligonucleotides exhibited high effectiveness and efficiency in EZH2 protein knockdown

a. EZH2 antisense oligonucleotides effectively inhibited EZH2 protein and mRNA

Because siRNA did not work via *in vivo* injection, we substituted it with phosphorothioate oligonucleotides, which were more stable than siRNA under physiological conditions.

After the EZH2 antisense injection, in both the FB and PVN, EZH2 antisense up to 1 μg/μl did not inhibit EZH2 mRNA levels at 12 hr post injection (Fig. 14 A & C). However at 24 hr post-injection, both antisense concentrations significantly inhibited EZH2 mRNA in both tissues (Fig. 14 B & D). To confirm the effectiveness of EZH2 antisense, we also quantified the relative EZH2 protein amount in the FB and PVN at 24 hr post injection. Although a significant mRNA inhibition was observed with 0.5 μg/μl antisense, EZH2 protein was only inhibited by EZH2 antisense at 1 μg/μl in both the FB and PVN. H3K27me2, which is the product of EZH2, also showed an apparent inhibition by EZH2 antisense at 1 μg/μl in the FB. However, in the hypothalamus, H3K27me2 became significantly elevated compared to the ACSF injected group. Therefore, EZH2 antisense at 1ug/ul, but not 0.5 μg/μl, effectively inhibited EZH2 protein at 24 hr post injection in both the FB and PVN.

b. EZH2 antisense oligonucleotides selectively inhibit EZH2 protein

Following EZH2 sense injection at 1 ug/ul, EZH2 protein was not different from that of the ACSF injected group (Fig 16). On the other hand, EZH2 antisense at 1 μg/μl inhibited EZH2 protein compared to theACSF injection. Thus, we confirmed that EZH2 antisense oligonucleotides obtained a high efficiency in EZH2 protein inhibition.

3. EZH2 antisense impaired the response to early fasting in the PVN

In the previous study, D3 fasting was shown to significantly inhibit BDNF protein and mRNA expression in both the FB and PVN. This change was due to the regulation of methylation at H3K27 via the PRC2. As the only subunit containing methyltransferase capacity in the PRC2, EZH2 played an important role during the entire regulation process. Thus, interruption of EZH2 protein should significantly change the response of the body to fasting stress. As we had evaluated the effectiveness and efficiency of EZH2 antisense oligonucleotides after *in vivo* injection, we were interested to monitor the effect of changes in

the PVN after the same fasting stress but with disrupted EZH2 protein expression. First, we compared the D3-fasting to the naive group in ACSF injected group.

a. ACSF-injection overall had no effect on global methylation at H3K27 expression in FB and PVN

First, we measured the body weight changes of chicks bared with different treatment (Table 4). For the naive group, the body weight was 78.01 $\pm$ 1.44 mg on D4 and 172.6 $\pm$ 5.52 mg on D11. After D3-fasting treatment, significant decrease of body weight was observed, which was 20 mg and 21 mg lower on D4 and D11, respectively. Additional EZH2 antisense injection on D3-fasting did not change this phenomenon.

Next, we measured the changes of epigenetic markers change after D3-fasting. The previous study confirmed that after D3-fasting, the FB did not show significant changes in methylation at H3K27 and PRC2 complex key factors' level. In the current "D3-fasting + ACSF injection" group, results were overall consistent with the previous results. This suggested that ACSF injection overall had only a minimum effect in the brain (Fig. 17 E, F, G & H). On both one and eight days post "D3-fasting + ACSF injection", no changes of H3K27me2 were detected. On the other hand, both total H3 and H3K27me3 were elevated on D4 after "D3-fasting + ACSF injection" but returned to naive levels on D11. We also tested the acetylation level at the H3K27 site. H3K27ac exhibited constant inhibition after "D3-fasting + ACSF injection" on both D4 and D11 in FB.

To confirm the global acetylation and methylation level at H3K27, the mRNA levels of key factors in the PRC2 and TRX complexes in FB. No significant difference was detect in SUZ, EZH2, EED and CBP between the naive group and "D3-fasting + ACSF injection" group (Fig. 18 E, F, G & H). Again, these data confirmed that FB was not the major feeding regulation center and did not respond to feeding stress .

Next, we tested the global methylation status at H3K27 in the PVN from the same animals. In the previous finding, the PVN exhibited significant changes after D3-fasting stress alone. In the current study, after "D3-fasting + ACSF injection", we found that the PVN revealed similar changes in H3K27 methylation patterns (Fig. 17 A, B, C & D) as well as key factors in PRC2 and TRX complex (Fig. 18 A, B, C& D) compared to D3-fasting without ACSF injection. This indicated that ACSF overall had little effect in the PVN, as well. After "D3-fasting + ACSF injection", an instant surge of total H3, H3K27me2 and H3K27me3 level was observed on D4 and lasted until D11 (Fig. 17 A, B, C & D). This data agreed with previous data from D3-fasting only chicks. On the other hand, the acetylation level at H3K27 site was significantly inhibited after "D3-fasting + ACSF injection" on both D4 and D11.

Again, we tested the mRNA levels of key factors in the PRC2 and TRX to match the modification at H3K27 site (Fig. 18 A, B, C & D). After "D3-fasting + ACSF injection", EED, SUZ and EZH2 had a mRNA surge on D4. On D11, while EED remained significantly elevated, SUZ became indifferent while EZH2 was inhibited compared to control. This increased PRC2

components agreed with the increased methylation patterns at H3K27 from the protein analysis. On the other hand, CBP also exhibited an increased trend, which was insignificant, after "D3-fasting + ACSF injection".

b. BDNF protein and mRNA exhibited inhibited levels after "ACSF injection + D3-fasting"

BDNF was used as a target gene to match with the global H3K27 methylation changes after fasting stress. In the FB, after "D3-fasting + ACSF injection", we found that the BDNF protein was constantly inhibited on both D4 and D11 (Fig. 19 B & D). These changes matched the data in the FB from previous "D3-fasting only" treatment. Similarly, BDNF mRNA showed an apparent decrease on D4, but was reversed on D11.

Furthermore, we used a CHIP assay to detect the distribution of H3K27me2, H3K27me3 and total H3 along the *Bdnf* gene in the FB (Fig. 21 A-I). According to the BDNF mRNA, it was first inhibited on D4 and then elevated on D11. Thus, there should be an increase and drop of methylation at H3K27 on D4 and D11, respectively. Our results matched this hypothesis. We found that after "D3-fasting + ACSF injection", there was a constant surge of H3K27me2 at both the *Bdnf* promoter area and beginning of coding region on D4 but not 3'-UTR (Fig. 21 B, E & H). On D11, H3K27me2 level returned back to naive level. On the other hand, H3K27me3 was inhibited by "D3-fasting + ACSF injection" on D4 along *Bdnf* gene and became more depressed on D11 (Fig. 21 C, F & I). Combine the changes from both H3K27me2 and H3K27me3, it matched the changes of *Bdnf* mRNA after the treatment. We further monitored the total H3 level along the *Bdnf* gene. A constant increase in H3 was found along *Bdnf* gene, which lasted until D11 (Fig. 21 A, D & G). Because the H3K27 methylation was mainly carried by EZH2 in the PRC2, we also tested the EZH2 distribution along the *Bdnf* gene. An apparent peak of EZH2 was monitored along the *Bdnf* gene 24 hr after "D3-fasting + ACSF injection" (Fig. 22 D, E & F). On D11, while the peak remained at *Bdnf* coding beginning region, the promoter and 3'-UTR were no longer different from the naive. The dynamic changes of EZH2 distribution overall matched that of H3K27me2 but not H3K27me3.

Next, the expression of the BDNF protein/mRNA was evaluated in the PVN from the same animals. Other than a traditional neurotrophic factor, BDNF also served as an anorexigenic factor in the PVN, which inhibited feeding. Thus, fasting should inhibit the expression of the BDNF protein. As expected, BDNF protein was inhibited after "D3-fasting + ACSF injection" treatment on D4 in the PVN (Fig. 19 A). This change was compatible with the noticeable inhibition of BDNF mRNA level on D4 (Fig. 19 C). However, on D11, no difference was detected on either BDNF protein or mRNA between the naive and "D3-fasting + ACSF injection" groups (Fig. 19 A & C).

To further study the mechanism under BDNF mRNA changes, we then monitored the distribution of methylated H3K27 along the *Bdnf* gene in the PVN. We found that right after "D3-fasting + ACSF injection", both H3K27me2 and H3K27me3 instantly peaked at both the *Bdnf* promoter and coding beginning regions on D4 (Fig. 20 B, C, E & F). This peaked level remained until D11. However, no apparent change was detected at the *Bdnf* 3'-UTR region until D11 (except increased

H3K27me3 at *Bdnf* 3'-UTR on D4) (Fig. 20 H & I). Total H3 showed similar dynamic deposition along the *Bdnf* gene. It did not respond to the treatment on D4 but became noticeably increased on D11 (except inhibited level on D4 at *Bdnf* coding beginning region) (Fig. 20 A, D & G). All these changes matched with the significant drop of BDNF mRNA on D4, but not on D11. Furthermore, we tested the level of EZH2 to match up the methylation status at H3K27. After "D3-fasting + ACSF injection", EZH2 exhibited apparent elevation on D4 along *Bdnf* gene but was significantly inhibited on D11 (except EZh2 at 3'-UTR, which became same as naive level) (Fig. 22 A, B & C).

4. EZH2 antisense injection changed the response towards D3-fasting stress

a. EZH2 antisense eliminated the surge of methylation at H3K27 after D3-fasting in PVN

Because EZH2 is the only methyltransferase in the PRC2, knockdown the EZH2 protein should eliminate methylation at H3K27, and thus impair the body's response towards D3-fasting stress. Thus, we injected chicks with EZH2 antisense and monitored the changes inside the PVN and FB after D3-fasting treatment and compared them to "D3-fasting + ACSF injection".

In FB, we found that after "EZH2 antisense injection + D3-fasting", the EZh2 antisense apparently eliminated the methylation at the H3K27 site. Both H3K27me2 and H3K27me3 exhibited significantly lowered levels compared to both naive and "D3-fasting + ACSF" groups (Fig. 17 F & G). Total H3 responded the same as that of H3K27me2 and H3K27me3 (Fig. E). At the same time, EZh2 saved the noticeably inhibited H3K27ac caused by "D3-fasting + ACSF" on both D4 and D11. In addition, H3K27ac became even more elevated than naive levels (Fig. 17 H). The significant drop of both di- and tri-methylation at H3K27, led to the hypothesis that the mRNA levels of PRC2 factors would drop after the EZH2 antisense injection. PCR results agreed with this hypothesis: EZH2 antisense obviously inhibited EZH2, which via unknown mechanism also inhibited SUZ and EED (Fig. 18 E, F & G). This result matched the changes of methylation status at H3K27. In addition, CBP mRNA was also increased after EZH2 antisense injection (Fig. 18 H).

In the PVN, we previously found that D3-fasting had a tremendous effect on the methylation status at the H3K27 site, which resulted from changes of the PRC2. After EZH2 antisense injection, the PVN overall had a significant loss of methylation at the H3K27 site. On D4, compared to "ACSF injection + D3-fasting" treatment ", "EZH2 antisense + D3-fasting" was able to apparently inhibit the surge of H3K27me3 and H3K27me2 on D4 (Fig. 17 B & C). On D11, while the inhibition of H3K27me2 remained, H3K27me3 became even more elevated in the "EZH2 antisense + D3-fasting" group. Similarly, the H3 level was constantly inhibited after EZH2 antisense injection, which lasted until D11 (Fig. 17 A). However, compared to the "ACSF injection + D3-fasting" treatment, EZH2 antisense did not eliminate the significant drop of acetylation levels at H3K27 compared to the naive. On D4, H3K27ac remained the same between the ACSF and EZH2 injected groups after D3-fasting (Fig. 17 D). On D11, this inhibition of H3K27ac remained in the PVN compared to naive and "ACSF injection + D3-fasting" chicks. H3K27ac became further inhibited in the EZh2 injected group.

The mRNA level of PRC2 and TRX key factors were also tested in the PVN. CBP mRNA was not affected by EZH2 antisense as it showed no difference to that of ACSF injection (Fig. 18 D). However, factors in PRC2 changed dramatically. First, EZH2 antisense dramatically inhibited EZH2 mRNA levels starting 24 hr post injection and lasted 8 days post injection (Fig. 18 B). For EED, "EZH2 antisense injection + D3-fasting" effectively eliminated its surge led by "ACSF injection + D3-fasting" on both D4 and D11 (Fig. 18 C). For SUZ, EZH2 antisense did not changed its mRNA level from that of the ACSF injection on D4. However, SUZ mRNA was significantly lower on D11 after "EZH2 antisense + D3-fasting" when compared to that of ACSF injection (Fig. 18 A).

b. BDNF protein and mRNA expression level confirmed the fact that EZH2 antisense eliminated body's response towards D3-fasting

As the significant global inhibition of both methylation and acetylation happened at H3K27 in the FB, we suspected that BDNF protein and mRNA levels should be affected after "EZH2 antisense injection + D3-fasting". We found that on D4, EZh2 antisense not only eliminated BDNF protein inhibition led by "ACSF injection + D3-fasting" in the FB, but also brought the BDNF protein to a much higher level compared to the naive group (Fig. 19 B). BDNF mRNA on D4 was very similar to its protein changes. On D11, while "ACSF injection + D3-fasting" significantly increased BDNF mRNA compared to the naive group, "EZH2 antisense injection + D3-fasting" brought BDNF mRNA back to naive group (Fig. 19 D).

We then used CHIP assays to test the distribution of methylated H3K27 along *Bdnf* gene in FB. Compared to "ACSF injection + D3-fasting", EZH2 antisense eliminated the surge of H3K27me2 led by D3-fasting along the *Bdnf* gene on D4 (Fig. 21 B, E & H). However, a more significant peak of H3K27me2 was monitored on D11 in "EZH2 antisense injection + D3-fasting". On the other hand, EZH2 antisense restored H3K27me3 to naive group level compared to the inhibition caused by "ACSF injection + D3-fasting" along the *Bdnf* gene on both D4 and D11 (except at 3'-UTR on D4) (Fig. 21 D, F & I). These changes overall matched the changes of BDNF mRNA. On the other hand, total H3 either stayed at the same level as the naive or was more elevated after "EZH2 antisense injection + D3-fasting" compared to the "ACSF injection + D3-fasting" on D4 along *Bdnf* gene (Fig. 21 A, D & G). This pattern of H3 lasted until D11.

Next, we tested the BDNF response towards D3-fasting after EZH2 antisense injection in PVN. We hypothesized that BDNF protein and mRNA should be spared from D3-fasting stress after EZH2 fasting. We found that EZH2 antisense spared the BDNF inhibition from "ACSF + D3-fasting" and brought both BDNF protein and mRNA back to naive levels (Fig. 19 A & C). On D11, while BDNF protein was elevated after "EZH2 antisense injection + D3-fasting" when compared to the "ACSF injection + D3-fasting", no changes was found for BDNF mRNA.

We further tested the dynamic deposition of methylated H3K27 on the *Bdnf* gene in the PVN. As expected, the "rescue" pattern was detected at multiple loci of *Bdnf*. On D4 and D11, while "ACSF injection + D3-fasting" increased the

deposition of both H2K27me2 and H3K27me3 at the *Bdnf* promoter and coding beginning region, EZH2 antisense eliminated this surge and brought them closer to the naive group (Fig. 20B, C, E & F). However, on D11, not only the peak of H3K27me2 and H3K27me3 disappeared, they became further inhibited than the naive group. At the same time, the changes at *Bdnf* 3'-UTR were minimal. These changes overall matched the changes of BDNF mRNA levels. In addition, on D4, EZH2 antisense elevated the H3 deposition along *Bdnf* gene on D4 injection and significantly inhibited on D11 (Fig 20 A, D & G). Furthermore, EZh2 was also monitored to match the changes of H3K27me2 and H3K27me3 changes. We found that on D4, at the *Bdnf* promoter and coding beginning regions, the EZH2 peak resulting from the D3-fasting was eliminated and was even more inhibited than the naive group (Fig. 22 A, B & C). Additionally, the EZH2 antisense inhibited EZH2 deposition on D11 along the *Bdnf* gene as well.

5. EZH2 eliminated the "molecular memory" towards repetitive fasting stress in PVN

a. EZH2 antisense impaired "molecular memory" PVN

We again measured the changes of body weight following either D10- or D3/10-fasting treatment (Table 5). Compared to the naive group, D10-fasting significantly decreased chicks body weight. An additional D10-fasting on the top of D3-fasting further decreased body weight. On the other hand, EZH2 antisense injection overall had no effect on body weight of chicks in naive and D10-fasting group. However, Compared to "D3/10-fasting + ACSF injection" group, the body weight of the "D3/10-fasting + EZH2 antisense" group was less attenuated.

As we previously showed, fasting at D3 could protect the body by minimizing the response to the same stress in later days. We called it "molecular memory". This protection mechanism is mainly via regulating the methylation status at H3K27. As an important methyltransferase, EZH2 plays a key role in "molecular memory". Thus, interruption of the PRC2 should impair the H3K27 methylation, which causes dysfunction of this memory towards repetitive stress. To test this hypothesis, we injected EZH2 antisense into chicks and put them under repetitive fasting stress conditions.

First, we tested the FB's response toward repetitive stress. As we showed earlier, the FB had little function in feeding regulation and did not exhibit any molecular memory towards the fasting stress. In the current study, we confirmed this hypothesis again by showing that the FB did not exhibit any memory towards fasting stress. After single D10-fasting, there was overall no change in H3K27 methylation or acetylation and total H3 levels compared to the naive group (Fig 23 E, F, G & H). Repetitive D3/10-fasting only significantly inhibited H3K27me3 levels. However, after EZH2 antisense injection, EZh2 antisense non-specifically inhibited H3K27me2 and increased H3K27ac in either type of fasting stress. Total H3 and H3K27me3 did not exhibit any changes in either fasting treated groups.

We measured the mRNA levels of the PRC2 to confirm the changes of methylation at H3K27 in the FB. In the ACSF injected group, after a single D10-fasting stress, a noticeable increase and decrease of SUZ and EED were monitored,

respectively (Fig. 24 E & G). However, after D3/10-fasting, while SUZ decreased and became indifferent from the naive, EED remained noticeably inhibited. Both EZH2 and CBP mRNA levels, although elevated, were not significant compared to the naive (Fig. 24 F & H). After D3/10-fasting treatment, EZH2 became significantly elevated. CBP, on the other hand, remain silenced to the repetitive fasting. In the EZH2 antisense injected group, EZH2 mRNA was inhibited after either type of fasting stress (Fig. 24 F). After D3/10-fasting, SUZ and CBP were inhibited while EED remained unchanged (Fig. 24 E, G & H).

Next, we applied the same test towards the PVN sample. In the ACSF injected group, the PVN revealed a "molecular memory" pattern: while single fasting on D10 significantly elevated/inhibited protein level from the naive group, a D3 fasting prior to D10 fasting alleviated this elevated/inhibited level. In Western Blot testing, we found that H3K27me2, H3K27me3 and H3K27ac followed this pattern (Fig. 23 B, C &D). For H3, it exhibited constantly increased levels after either D10-fasting or D3/10-fasting (Fig. 23 A). However, after EZH2 antisense injection, "molecular memory" patterns disappeared. First, EZH2 antisense injection constantly eliminated the peak of H3K27me2 led by single fasting on D10 or repetitive fasting on D3/10 (Fig. 23 B). For H3K27me3 and H3K27ac, EZH2 antisense injection caused constant elevation compared to "ACSF injection + D10-fasting" treatment (Fig. 23 C & D). In addition, EZH2 antisense caused constant inhibition of H3 in both D10 and D3/10-fasting group (Fig. 23 A).

The mRNA levels of the PRC2 key factors agreed with the methylation status in the PVN. Compared to the ACSF injection group, EZH2 antisense constantly inhibited not only EZH2, but also SUZ and EED mRNA levels after a single fasting on D10 (Fig. 24 A, B & C). After D3/10-fasting treatment, EZH2 antisense remained effective and significantly inhibited SUZ and EZH2 while elevated the level of EED. CBP from the TRX overall was not affected by EZH2 antisense compared to that of ACSF injection (Fig. 24 D).

b. BDNF expression supports the statement that EZH2 antisense impaired "molecular memory"

We then studied BDNF protein and mRNA changes in the FB. After D10-fasting, a significant inhibition of BDNF protein was found (Fig. 25 B). After D3/10-fasting fasting, BNDF revealed a partially recovered protein level from D10-fasting, which however remained lower than the naive. BDNF mRNA levels in the FB shown no changes after D10-fasting but much inhibited levels after repetitive fasting in the ACSF injected group (Fig. 25 D).

We further used CHIP assays to study these changes in BDNF mRNA levels. Without EZH2 antisense, D3-fasting was able to elicit a surge of total H3 and H3K27me2 levels along the *Bdnf* gene (Fig. 27 A, B, D, E, G & H). After D3/10-fasting, the surge of H3 became even bigger while H3K27me2 remained the same level as that of D3-fasting. On the other hand, H3K27me3 was inhibited by D3-fasting and exhibited a more significant inhibition after D3/10-fasting (Fig. 27 C, F & I). However, after EZH2 antisense injection, H3 increased its deposition after D10-fasting along *Bdnf* but decreased its deposition after D3/10-fasting (Fig. 27 A, D & G). At the mean time, EZH2 antisense was able to decreased H3K27me2 deposition along *Bdnf* in both

single and repetitive fasting treatments (except at the *Bdnf* promoter and 3'-UTR regions) (Fig. 27 B,E & H). On the contrary, H3K27me3 deposition were constantly increased along the *Bdnf* gene after EZH2 antisense injection, in both single and repetitive fasting treatments (Fig. 27 C, F & I). EZH2 itself showed unchanged, decreased and increased levels at *Bdnf* promoter, coding beginning region and 3'-UTR regions, respectively, after D3-fasting (Fig 28 D, E & F). EZH2 antisense also inhibited EZH2 level along *Bdnf* gene after D3/10-fasting treatment (Fig 28 D, E & F).

Next, we tested the changes of BDNF in the PVN. Compared to the FB, PVN exhibited much more meaningful changes after fasting stress. In the ACSF injected group, both BDNF protein and mRNA exhibited the "molecular memory" patterns after repetitive fasting stress (Fig. 25 A & C). EZH2 antisense impaired this pattern of both BDNF protein and mRNA. After single fasting on D10, BDNF protein and mRNA exhibited significant elevated levels after EZH2 antisense injection (Fig. 25 A & C). After repetitive fasting, both BDNF protein and mRNA expression levels showed the reversal.

The results from CHIP assays agreed with that of BDNF mRNA changes in PVN. First, after ACSF injection at Bdnf promoter and coding beginning regions, both H3K27me2 and H3K27me3 exhibited the "molecular memory" pattern: while single fasting D10 significantly shifted its level from the naive, repetitive fasting on both D3 and D10 brought its level back or close to the naive group (Fig. B, C, E & F). Following EZH2 antisense injection, D10-fasting significantly inhibited H3K27me2 and H3K27me3 level at both *Bdnf* promoter and coding beginning regions (Fig. B, C, E & F). However, this pattern was reversed after D3/10-fasting (except H3K27me3 was not different between EZH2 antisense and ACSF group). 3'-UTR region remained unchanged regardless of injection and fasting(Fig. 26 H & I). On the other hand, total H3 levels tended to increase upon D3-fasting and became more increased upon D3/10-fasting without EZH2 antisense (Fig. 26 A, D & G). However, EZH2 antisense significantly increased total H3 after single D10 fasting at the *Bdnf* promoter and coding beginning region. This pattern reversed after D3/10-fasting treatment. EZH2 deposition after ACSF injection exhibited "molecular memory" only at *Bdnf* promoter region but not others (Fig28 A, B & C). After EZH2 antisense injection, EZH2 deposition was inhibited at Bdnf promoter region after single fasting on D3. In addition, EZH2 antisense also elevated EZH2 level along *Bdnf* gene (Fig28 A, B & C).

3.5. Discussion

To the author's knowledge, only limited number of publications reported the changes of histone [6] and histone modification enzymes [349] in hypothalamus after unfavorable nutritional stress. Thus, we are interested in knowing the histone covalent modification regulation after nutritional stress. In a previous study, we showed that after 24 hr fasting on D3, significant increased methylation was detected at H3K27 in PVN. In addition, PVN is able to establish so called "molecular memory", which protects the body from a future same stress. In the present study, we first confirmed that ACSF injection in lateral ventricle overall did not affect the body's response toward D3-fasting. Additionally, we also confirmed the existence of "molecular memory" inside the PVN after ACSF injection into the lateral ventricle. However, after EZH2 antisense application, the PVN lost its correct responses after a single24 hr fasting on D3. In addition, the PVN failed to develop "molecular memory" towards the fasting stress after EZH2 antisense injection.

Feeding regulation is determined by the neural-networking in the five different sub-hypothalamic nuclei [51]. Among them, PVN is one of most important nuclei and plays a pivotal role in feeding and energy homeostasis regulation. A histological study showed that the PVN received innervation fibers from almost all areas of the hypothalamus [105]. Nearly all known orexigenic and anorexigenic factors increased and decreased feeding respectively, when micro-injected into the PVN [50]. Multiple numerous neuro-peptides, including BDNF [79], was also detected in the PVN. In addition, some recent studies find that fasting stress tends to change histone methylation status inside PVN [6]. In the current study, we showed that after single 24 hr fasting on D3, there was significant increased methylation and decreased acetylation at H3K27 in PVN. This changed pattern of H3K27 covalent modification lasted until 8 days post fasting. These data suggest that histone modification is highly responsive rather than static towards nutritional stresses. As previously reported by other groups that nutritional stress could leave covalent modification on both histones [6,349] and nucleotides [350,351]. Our data provided evidence to support this hypothesis. In addition, 8 days post injection, elevation of methylation and acetylation at H3K27 remained exist. These results matched our previous finding that 24 hr fasting on D3 could keep inducing H3K27 methylation and methylation machinery, i.e. PRC2, up to at least 38 days. This suggests that single nutritional stress during early brain development could induce long term covalent modification on histones. This durable histone modification can lead to changing of both chromatin structure and gene transcription and, thus, increased risk towards some diseases such as obesity. Some recent epidemiological studies claimed that nutritional stress in early life period is able to cause long term disturbance in energy and metabolic homeostasis in humans [376]. Thus, our data supported this hypothesis by showing that long term histone modification deposition on chromosome could be the potential mechanism.

We were also interested in investigating the meaning of this long term modification on histone. Previous studies showed that animals became more resistant towards heat challenge later in life if exposed to heat stress during thermal-control establishment period [377,378]. It is mainly due to adaption of histones modification in the preoptic and

anterior hypothalamus (PO/AH) [7]. We suspected the histone modification in PVN after fasting had the same the function as that of PO/AH after heat stress. Thus, we compared a repetitive 24 hr fasting stress (on both D3 and D10) to the single 24 hr fasting (on D3) in chicks. Similarly, we found that the body exhibits a less disrupted methylation as well as acetylation at H3K27 after repetitive fasting stress compared to a single fasting stress. We called this change of pattern as the "molecular memory". We used BDNF protein, BDNF mRNA and H3K27me2/3 lying on *Bdnf* gene to support this finding as well. This indicates that the long term histone covalent modification serves as a protective mechanism for the body toward future same stress type. Importantly, this is the first study series reporting that repetitive fasting during feeding-control establishment develops a "molecular memory" and protects the body from future same fasting stress. In addition, this "molecular memory" utilizes histone covalent modification via PRC2. However, it remains elusive how neurons in the PVN could develop "molecular memory" in the first place. Additionally, it is not clear whether the body could build a "cross molecular-memory" towards different types of stress.

It is very surprising to see that not all factors inside PRC2 obtained "molecular memory": in the PVN while repetitive fasting induce the memory for EED and SUZ, EZH2 kept increasing in both single and repetitive fasting situation. PRC2 is a huge H3K27 methylation machinery [213]. In its functional core, three key factors have been discovered, which are EZH2, SUZ and extra-sex comb EED [213]. As EZH2 is the only methyltransferase inside PRC2, its expression level increasing suggested the same trend for H3K27 methylation [242]. However, H3K27me2 /me3 exhibited the similar "molecular memory" pattern as well after repetitive fasting stress. Literature review suggested that EZH2 had barely no function if presented alone without other non-catalytic subunits in PRC2 [248]. This is because EZH2 does not have a DNA binding domain, which prevent EZH2 from histone binding [259,355]. So far EZH2 had been shown to have direct connection with EED in [251,259,357] and SUZ[252,259,358], which forms a triplet model that EZH2 sits in the middle[259]. EED binds to histones [255,356] while SUZ connects proteins on chromosome, such as heterochromatin protein 1alpha [252]. These linkages insure the EZH2 to have full contact with histones and proceed methylation. Mutation or knockout SUZ [259,357,358] and EED [259,277,359] depleted the function of PRC2. These data suggest that both catalytic (EZH2) and non-catalytic subunit (EED and SUZ) are pivotal to PRC2. In the current study, we reported that "molecular memory" exhibited in EED and SUZ, but not EZH2. This indicates that although body responds to the fasting stress through EZH2-methylating-H3K27, it is indeed via regulating of EED and SUZ. Thus, via regulating EED and SUZ only could determine level of H3K27 methylation. However, we are not clear how the body instills memory toward SUZ and EED and why EZH2 does not.

BDNF is initially known for its function in neuron proliferation, differentiation, growth and interaction [125]. Recently, it is also categorized as an anorexigenic factor [75,159]. Both acute injection [159,160] (including at the PVN [161]) or long term intracerebroventricular injection [162] of BDNF inhibited the feeding and increased energy expenditure in tested

animals. While fasting inhibited BDNF level inside in the ventromedial hypothalamus [75] and dorsal vagal complex of hinder brain [159], re-fed led to recovered BDNF [159]. In female humans with either bulimia nervosa (BN) or anorexia nervosa (AN), a significantly lowered serum BDNF level was observed [163]. All these data highlighted the importance of BDNF in feeding regulation. In our current study, we identified a drop in both the BDNF protein and mRNA levels and a long term BDNF mRNA inhibition after a single 24 hr fasting on D3. This finding agreed with the findings from previous studies. But more importantly, we were able to match the BDNF mRNA changes with the H3K27me2/3 distribution along the *Bdnf* gene. It is widely accepted that H3K27 methylation compacts nucleosomes and thus blocks transcriptional elongation on gene templates [361,362]. Thus, increased H3K27me2/3 after fasting indicated massive gene transcription inhibition in the PVN. However, it remained out of clue that when and where of H3K27me2/3 deposition will lead to induce specific gene inhibition. We picked three areas on *Bdnf* gene, which are promoter (-869 to -801 bp), coding starting region (+91 to +190 bp) and 3'-UTR side (+1623 to +1698 bp). Same as the global changes in PVN, instant increased level of H3K27 me2/me3 was deposited mainly happened at *Bdnf* promoter and coding beginning region (but sometimes *Bdnf* 3'-UTR as well). EZH2, on the other hand, was also significantly changes but along *Bdnf* gene. This indicates that fasting inhibits *Bdnf* gene transcription mainly via regulating depositing PRC2 along *Bdnf* gene.

The PRC2 is known for its capacity to di- and tri methylate H3K27 site [242,243,247,248]. Because chicks' PVN showed increased H3K27 methylation levels after fasting stress, we were interested to investigate what happened if PRC2 was impaired. We picked EZH2 as our target because it is the only methyltransferases inside PRC2 [242]. An early study reported that an EZH2 *null* mutation is lethal towards animals [379]. Thus, EZH2 could only be knockdown via siRNA and oligodeoxyribonucleotide. First, we tried to test the effectiveness of siRNA knockdown on the target mRNA. We picked siRNA targeting GAPDH as our test and performed *in vivo* intracerebroventricular injection. However, even at 27173.9 nM (final concentration in chick CSF, suggested concentration > 5 nM, chick at D3 had 4u µl CSF) and with the help of Invivofectamine® 2.0 Reagent, which was more than the 5400 fold higher than suggested concentration, no effect on GAPDH protein and mRNA levels in the chick FB was observed 24 hr after 6 µl siRNA exhibited. Literature review did find some successful studies to induce gene knockdown in the CNS via *in vivo* siRNA intracerebroventricular injection. But siRNA was either injected topically [380,381,382] or newly remodeled which is more resistant to degradation [383]. In our case, we suspected the failure was due to the combination of following factors: 1) premature ending of siRNA reaction in FB (suggested time by manufacture is 48 hr) [384,385], 2) naked signal quick degradation in CSF [386] and 3) difficult penetration into deeper brain tissue [385] even with the presence of Invivofectamine® 2.0 Reagent.

Next we adopted the method from an earlier study, using oligodeoxyribonucleotides targeting the EZH2 to knockdown the EZH2 protein [7]. Compared to normal oligonucleotides, the oligodeoxyribonucleotide had a nonbridging oxygen replaced by a sulfur atom at every single phosphorus, which makes them highly resistant towards endonucleases. In addition, the double-

phosphorothiolation at both the 3'-end and 5'-end of the deoxyribonucleotide further protects it from exonucleases. Thus, EZH2 oligodeoxyribonucleotides antisense should be very stable after *in vivo* intracerebroventricular injection. As expected, EZH2 oligodeoxyribonucleotide antisense at 1 μg/μl effectively and selectively inhibited EZH2 protein and mRNA expression after 24 hr post injection. So far, two mechanisms have introduced to explain how oligodeoxyribonucleotide antisense work inside cell. These mechanisms are the RNase H pathway [369,370,371], blocking transcription initiator progression [372] and inhibiting mRNA splicing [368]. The RNase H pathway utilizes RNase H enzyme to hydrolyze the RNA/DNA complex, which significantly inhibits mRNA of target gene [368]. However, other two pathways are expected to inhibit mRNA translation rather than hydrolyze and decrease mRNA [372]. Thus, in our case, EZH2 oligodeoxyribonucleotides antisense should utilize RNase H pathway as we observed significant inhibition of EZH2 mRNA.

We evaluated the effect of EZH2-antisense inhibition by monitoring the methylation status at H3K27 in the PVN. Whereas the D3-fasting significantly increased the EZH2 mRNA on D4, EZH2 antisense eliminated this response. In addition to the inhibition of EZH2 mRNA, the peak of H3K27me2/3 protein was also eliminated. This indicates that EZH2 knockdown depletes the function of PRC2 and thus impairs the changes of H3K27 methylation. In other words, the body's response towards D3-fasting was impaired. On D11, EZH2 mRNA remained inhibited in "EZH2 antisense + D3-fasting" group compared to "ACSF + D3-fasting" group. This observation indicated that EZH2 antisense remained effective even 8 days after injection. The EZH2 antisense we used is phosphorothioated oligonucleotides, which are fairly resistant to the intracellular endonucleases and exonucleases [368]. This explained a constant inhibition of EZH2 mRNA in PVN neurons, which led to constant inhibition of methylation at H3K27. Interestingly, SUZ and EED mRNA also shown changed level after EZH2 antisense injection. As we have blasted the EZH2 antisense sequence, it could not bind to SUZ and EED mRNA. Literature review found that phosphorothioated oligonucleotides are capable of causing non-specific mRNA inhibition [368]. However, individual cell have a intact biological environment where interruption of one molecule could affect the level of the others, especially they have collaboration. Thus, this phenomenon could either be the response of PVN to EZH2 antisense or non-specific inhibition caused by EZH2 antisense. Monitoring the changes of BDNF protein mRNA and deposition on *Bdnf* gene agreed with the effect of EZH2 antisense at global level.

Furthermore, EZH2 antisense also eliminated D3/10-fasting induced long-term H3K27 methylation modification. We showed that this long-term modification was beneficial for the body and protect body from future fasting stress. As H3K27 specific methyltransferase, EZH2 played a pivotal role during this process, although EZH2 itself does not obtain "molecular memory". To provide more evidence, we again applied EZH2 antisense towards the repetitive fasting test. We found that after the injection, EZH2 mRNA was constantly inhibited compared to non-EZH2 injected group. In addition, the "molecular memory" pattern was totally eliminated for EED, but not SUZ. As a key factor for PRC2 functioning, lost of "molecular memory" for EED was expected to eliminate "molecular memory" pattern for products of PRC2. Accordingly, H3K27me2/me3

no longer exhibited any "molecular memory" as well. These data indicate that interrupting EZH2 expression impaired neurons in the PVN to obtain memory toward fasting, which eliminated a protection in the PVN. This hypothesis was later supported by the results of the BDNF protein, mRNA and H3K27me2/3 distribution on the *Bdnf* gene as well.

We also monitored some discrepancies in our data. For example, in "ACSF injected + D3-fasting" group, although EZH2 deposition matched perfectly of H3K27me2/me3 level in PVN on D4, it did not matched perfectly well of H3K27me2/me3 on D11. We do not understand why this happened. It could be due to the co-effect of other PcG complex [245], chromosome proteins, nucleotide covalent modification or histone covalent modification at 3'-UTR that blocks the function of PRC2 at this area. In addition, H3K27me3 and H3K27ac were found to have the exactly same patterns in repetitive fasting study, but no after single D3-fasting. H3K27me3 and H3K27ac are the products of PRC2 [245] and TRX [387], respectively. They antagonize each other to regulate gene transcription level under different circumstance [295,363]. Most of the time, H3K27me3 and H3K27ac are reversely parallel to each other [226,388]. In our situation, because all chicks had been fasting before, this parallel H3K27me3 and H3K27ac effect could be fasting specific. It is also possible that the significant increased H3K27me3 and H3K27ac could be deposited into different area of the chromosome, affecting different genes.

Overall, our data showed that the PVN is capable of responding to fasting stress quickly and methylates H3K27 via regulating of PRC2. These changes last for a fairly long time because it protected the body from interrupted inner environment after a future same fasting stress. Upon impairment of the PRC2 via knockdown of EZH2, the PVN is no longer capable of responding to fasting correctly, thus it cannot establish any memory to protect homeostasis from future fasting.

	D4			D11		
D3-fasting	-	+	+	-	+	+
antisense	-	-	+	-	-	+
Body weight	78.01 [a]	58.84 [b]	59.39 [b]	172.6 [a]	151 [b]	154.8 [b]
SEM	1.44	0.89	0.71	5.52	3.24	5.66

Table 5 Changes in body weight of chicks following fasting. At three days of age, eighteen birds were injected with ACSF into lateral ventricle of brain and fed *ad libitum* (naïve). Eighteen birds were injected with ACSF and another eighteen birds were injected with EZH2 antisense oligonucleotides. Right after injection, these birds were fasted for 24 hours (D3-fasted). Data from the same sacrifice day bared different letters indicate significant different. Naïve controls and fasted chicks (from both ACSF and antisense injected group) were sacrificed on day 4 (D4) and day 11 (D11). Before sacrificing, body weight was measured. There was a significant decrease in the body weight between naïve and "D3-fasting + ACSF" chicks on 24 hrs and 8 days post fast. This pattern of body weight remained same on D11.

	D11					
D3-fasting	-	-	-	-	+	+
D10-fasting	-	-	+	+	+	+
antisense	-	+	-	+	-	+
Body weight	175	177.1	151.6	153.6	121.4	141.3 *
SEM	5.47	4.97	2.37	5.28	2.94	3.51

Table 6 Changes in body weight of chicks following D10-fasting or D3/10-fasting. At three days of age, eighteen birds were injected with ACSF into the lateral ventricle and then randomly and evenly divided into three groups. One group was randomly picked and fed *ad libitum* until D11 (na ïve). For D3- and D10- double fasting group (called D3/10-fasting in the following paragraph), food was withdrawn for 24 hr on D3. On D4, food was back to normal supply to the fasted group. On D10, D3/10-fasting groups were fasted again for 24hr. For single fasting on D10 group (called D10-fasting), food was only withdrawn on D10 for 24 hr. All three groups of chicks were sacrificed on D11 and PVN and FB samples were collected. In EZH2 antisense injected group, all treatments remained the same as that of the ACSF injected group, except ACSF was replaced with EZH2 antisense. Data bared asterisk mark indicates significant difference between ACSF and EZH2 antisense injected group. Data bared Greek letter indicates significant difference among a group which receives the same injection chemicals. . In ACSF injected group, D10-fasing significantly inhibited chick body weight. If applied a fasting on D3 prior to D10 fasting, chick body weight was significantly decreased compared to both the naive group and 10-fasting group. EZH2 antisense injected group showed a similar pattern compared to that of ACSF group: there was an overall down regulation of body weight with increased fasting time. In between EZH2 antisense injected group, while EZH2 antisense had no effect on the naive and D10-fasting group, it significantly increased body weight of D3/10-fasting group compared to ACSF injected group.

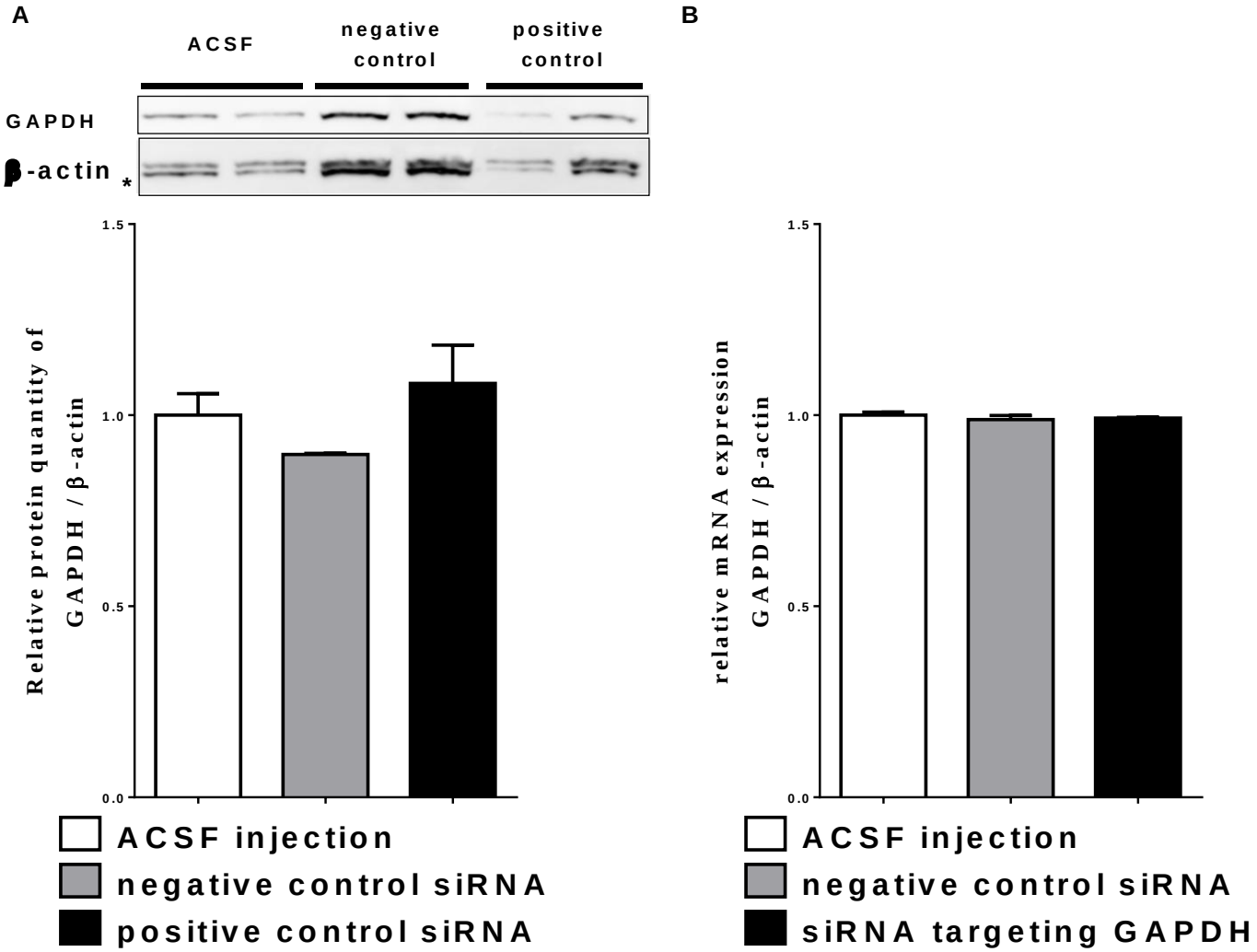
A
ACSF
negative control
positive control
GAPDH
β-actin
*
B
Relative protein quantity of GAPDH / β-actin
1.5
1.0
0.5
0.0
ACSF injection
negative control siRNA
positive control siRNA
relative mRNA expression GAPDH / β-actin
1.5
1.0
0.5
0.0
ACSF injection
negative control siRNA
siRNA targeting GAPDH

Figure 11. Changes in protein and mRNA levels of GAPDH in the chick forebrain (FB) (A & B) following anti-GAPDH siRNA injection. At three days of age, birds were injected with ACSF, GAPDH sense and GAPDH antisense siRNA into 3rd ventricle of brain. 24 hr after injection, all chicks were sacrificed and FB was extracted. Total protein was isolated and evaluated by Western blot using the antibody against GAPDH. Blot density were compared with β-actin. Each value is the mean ± standard error of the mean of 6 individual chicks. GAPDH protein shown no difference among GAPDH sense and GAPDH antisense siRNA injection group (A). Total mRNA was isolated and evaluated by real-time polymerase chain reaction (PCR) using the Sybr green method with *Gapdh* gene-specific primers (see Table 1). Gene expression levels were compared with β-actin. Each value is the mean ± standard error of the mean of 6 individual chicks. GAPDH mRNA shown no difference among GAPDH sense and GAPDH antisense siRNA injection group, either (B).

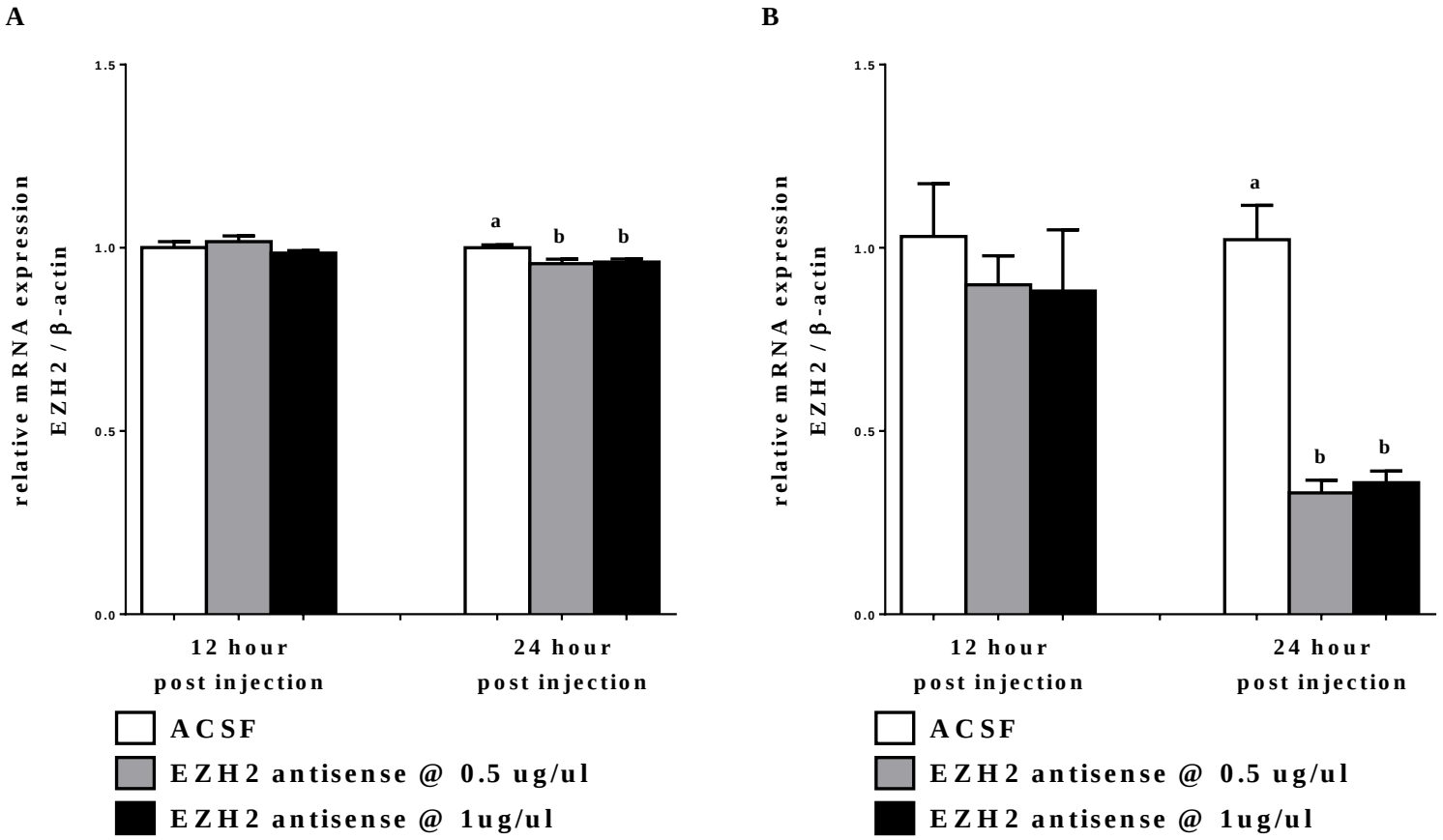
A
B
relative mRNA expression
EZH2 / β-actin
1.5
1.0
0.5
0.0
a
b
b
12 hour
post injection
24 hour
post injection
ACSF
EZH2 antisense @ 0.5 ug/ul
EZH2 antisense @ 1ug/ul

Figure 12. Changes in mRNA levels of EZH2 in the chick's FB (A) and hypothalamus (B) following EZH2 antisense injection. At three days of age, birds were injected with ACSF and EZh2 antisense oligonucleotides at 0.5 ug/ul and 1 ug/ul into lateral ventricle of the brain. Chicks were sacrificed at 12 hr or 24 hr post injection. FB and hypothalamic tissues were collected. Total mRNA was isolated and evaluated by PCR using the Sybr green method with *Ezh2* gene-specific primers (see Table 1). Gene expression levels were compared with β-actin. Each value is the mean ± standard error of the mean of 6 individual chicks. EZH2 mRNA showed no difference after EZH2 antisense at 12 hr post injection in the FB (A) and hypothalamus at both 0.5 ug/ul and 1ug/ul. However, at 24 hr post injection, EZH2 mRNA was significantly inhibited at both 0.5 ug/ul and 1ug/ul in both FB (B) and hypothalamus (D) histogram with same letter indicated insignificant difference ($P > 0.05$) while histogram with different letter indicated significant difference ($P< 0.05$).

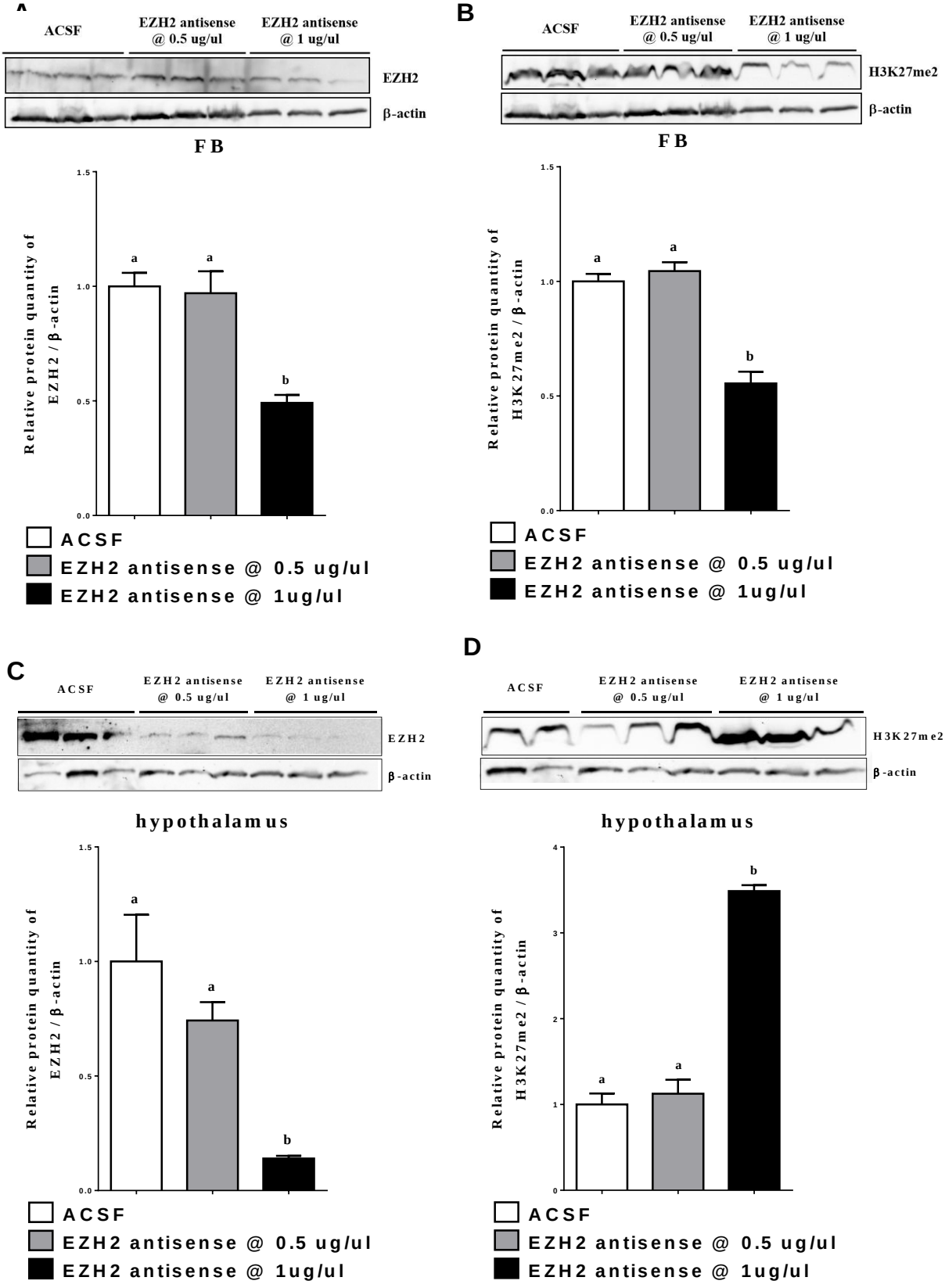
A
ACSF
EZH2 antisense @ 0.5 ug/ul
EZH2 antisense @ 1 ug/ul
EZH2
β-actin
F B
Relative protein quantity of EZH2 / β-actin
a
a
b
ACSF
EZH2 antisense @ 0.5 ug/ul
EZH2 antisense @ 1ug/ul
B
ACSF
EZH2 antisense @ 0.5 ug/ul
EZH2 antisense @ 1 ug/ul
H3K27me2
β-actin
F B
Relative protein quantity of H3K27me2 / β-actin
a
a
b
ACSF
EZH2 antisense @ 0.5 ug/ul
EZH2 antisense @ 1ug/ul
C
ACSF
EZH2 antisense @ 0.5 ug/ul
EZH2 antisense @ 1 ug/ul
EZH2
β-actin
hypothalamus
Relative protein quantity of EZH2 / β-actin
a
a
b
ACSF
EZH2 antisense @ 0.5 ug/ul
EZH2 antisense @ 1ug/ul
D
ACSF
EZH2 antisense @ 0.5 ug/ul
EZH2 antisense @ 1 ug/ul
H3K27me2
β-actin
hypothalamus
Relative protein quantity of H3K27me2 / β-actin
a
a
b
ACSF
EZH2 antisense @ 0.5 ug/ul
EZH2 antisense @ 1ug/ul

Figure 13. Changes in protein and mRNA levels of EZH2 in the chick's FB (A & B) and PVN (C & D) following EZH2 antisense injection. At three days of age, birds were injected with ACSF and EZh2 antisense oligonucleotides at 0.5 ug/ul and 1 ug/ul into lateral ventricle of brain. 24 hr after injection, all chicks were sacrificed and FB and hypothalamus tissues were collected. Total protein was isolated and evaluated by Western Blot. Protein expression levels were compared with β-actin. Each value is the mean ± standard error of the mean of 6 individual chicks. In FB, although EZH2 mRNA was inhibited by both 0.5 and 1 ug/ul EZH2 antisens after 24 hours as shown previously, EZH2 protein was only inhibited by EZH2 antisense at 1 ug/ul (A). The product of EZH2, H3K27me2, followed the same trend as EZH2 in FB (B). In the hypothalamus, EZH2 protein was inhibited by EZH2 antisense at 1 ug/ul but not 0.5 ug/ul (C). However, H3K27me2 revealed a significant increased level after 1ug/ul EZH2 antisense injection while 0.5 ugl/ul did not affect its level (D). Histogram with same letter indicated insignificant difference ($P > 0.05$) while histogram with different letter indicated significant difference ($P< 0.05$).

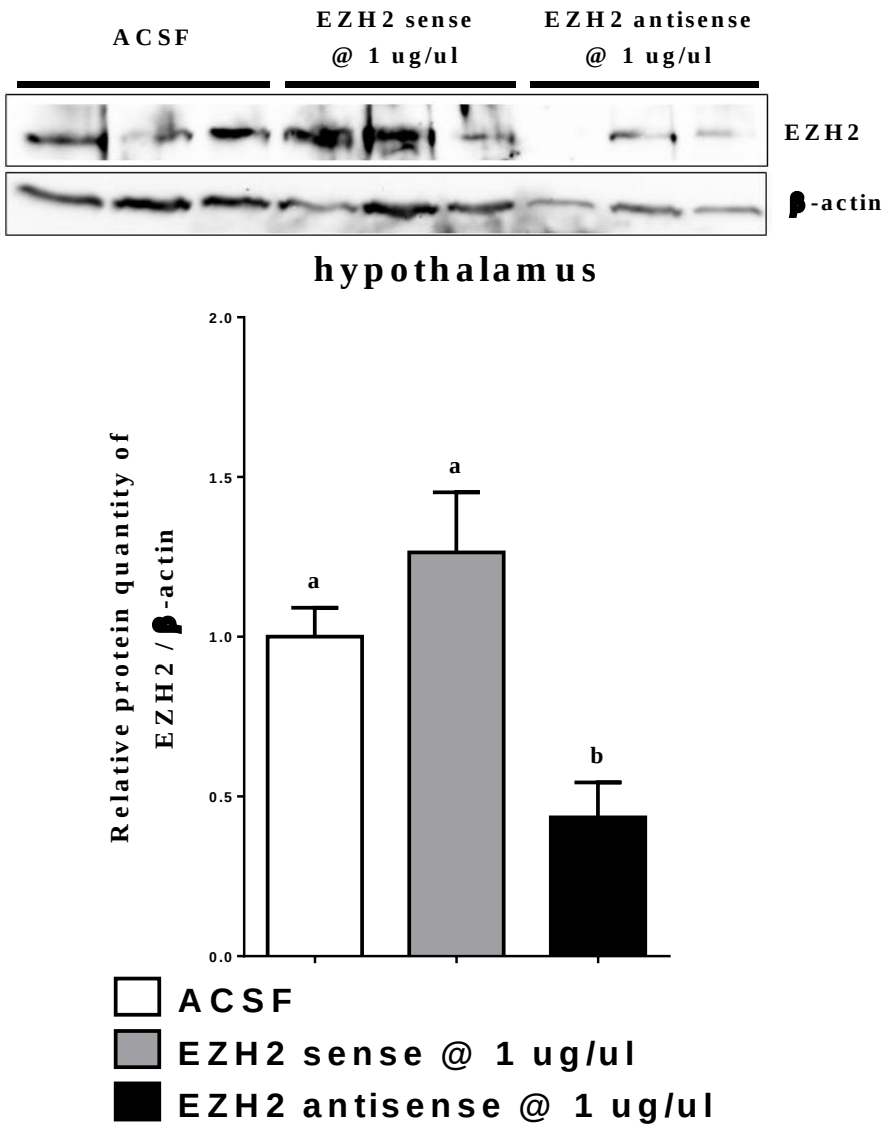

Figure 14. Changes in protein levels of EZH2 in the chick's PVN (C & D) following ACSF, EZH2 sense (1 ug/ul) and EZH2 antisense (1 ug/ul) injection. At three days of age, birds were injected with ACSF, EZh2 sense and EZH2 antisense oligonucleotides into lateral ventricle of brain. 24 hr after injection, all chicks were sacrificed and hypothalamus was extracted. Total protein was isolated and evaluated by Western Blot. Gene expression levels were compared with β-actin. Each value is the mean ± standard error of the mean of 6 individual chicks. EZH2 protein showed no difference between ACSF and EZH2 sense injected group at 24 hr post injection. However, EZH2 antisense significantly inhibited EZH2 protein compared to ACSF injected group. Histogram with same letter indicated insignificant difference ($P > 0.05$) while histogram with different letter indicated significant difference ($P< 0.05$).

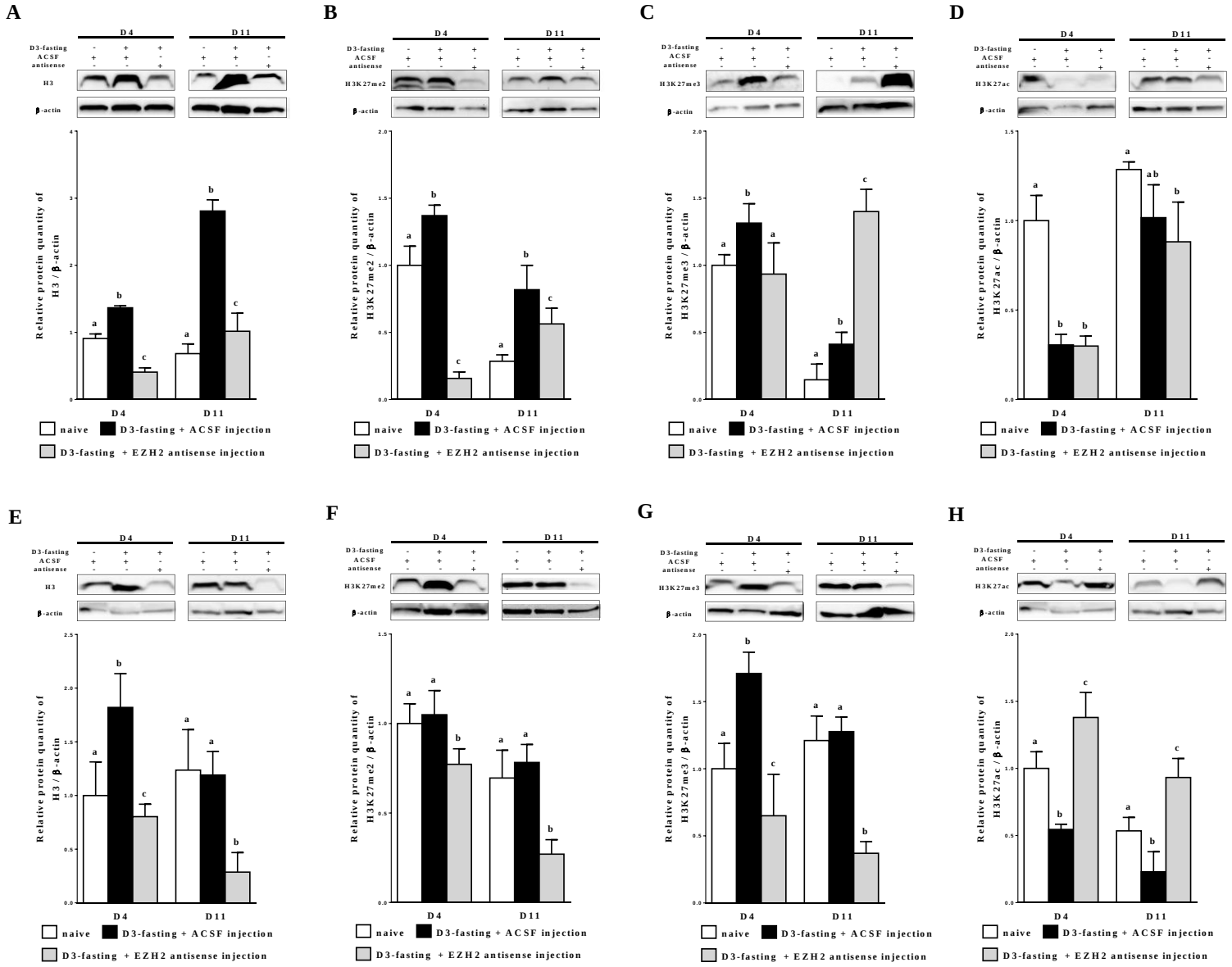
A
B
C
D
E
F
G
H
D4
D11
D3-fasting
ACSF
antisense
H3
H3K27me2
H3K27me3
H3K27ac
β-actin
Relative protein quantity of H3 / β-actin
Relative protein quantity of H3K27me2 / β-actin
Relative protein quantity of H3K27me3 / β-actin
Relative protein quantity of H3K27ac / β-actin
naive
D3-fasting + ACSF injection
D3-fasting + EZH2 antisense injection

Figure 15. Changes in protein levels of H3, H3K27me2, H3K27me3 and H3K27ac in chick's paraventricular nucleus (PVN) (A, B, C & D) and the forebrain (FB) (E, F, G & H) following fasting. At three days of age, eighteen birds were injected with ACSF into lateral ventricle of brain and fed *ad libitum* (naïve). Eighteen birds were injected with ACSF and another eighteen birds were injected with EZH2 antisense oligonucleotides. Right after injection, these birds were fasted for 24 hours (D3-fasted). Naïve controls and fasted chicks (from both ACSF and antisense injected group) were sacrificed on day 4 (D4) and day 11 (D11). Total protein was isolated and evaluated by Western blot using the antibody against H3, H3K27me2, H3K27me3 and H3K27ac. Blot density were compared with β-actin. Each value is the mean ± standard error of the mean of 6 to 12 individual chicks. Histogram with different letters indicated a significant difference. There was an overall significant increase in the levels of global H3 (A), H3K27me2 (B) and H3K27me3 (C) between naïve and "D3-fasting + ACSF" chicks on 24 hrs and 8 days post fast (A). Global acetylated lysine 27 levels on H3 were significantly decreased at 24 hours post "D3-fasting + ACSF", but became insignificant on D11 (D). After EZH2 antisense injection, the surge of H3 and H3K27me2 were inhibited on both 24 hrs and 8 days post fast (A). EZH2 antisense also blocked the surge of H3K27me3 at 24 hr post fast but showed a reversal on 8 days post fast (C). However, H3K27ac did not seem to be affected by EZH2 antisense (D). In FB, after "D3-fasting +ACSF" treatment, the global H3 (E) and H3K27me3 (G) levels were significantly increased on D4 but not D11. While H3K27me2 (F) was not affected by "D3-fasting + ACSF" at all, H3K27ac (H) was constantly inhibited on both D4 and D11. After EZH2 antisense injection, total H3 (E) , H3K27me2 (F) and H3K27me3 (G) all exhibited significant inhibited levels. On the contrary, H3K27ac was significantly elevated (H).

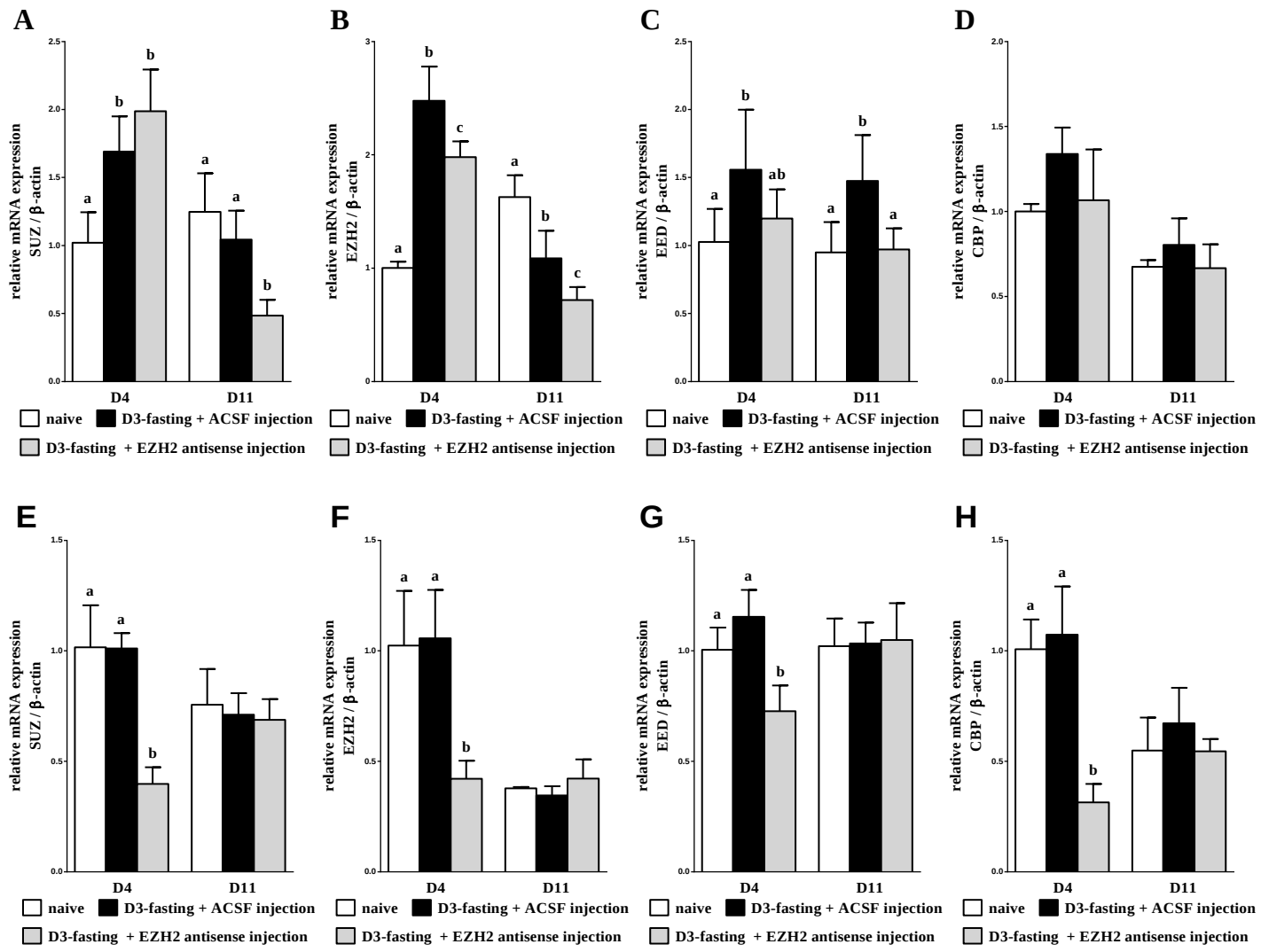
A
B
C
D
E
F
G
H
relative mRNA expression
SUZ / β-actin
EZH2 / β-actin
EED / β-actin
CBP / β-actin
D4
D11
naive
D3-fasting + ACSF injection
D3-fasting + EZH2 antisense injection

Figure 16. Changes in mRNA levels of key factors in the Polycomb repressive complex 2 (PRC2) and a histone acetyltransferase (HAT) in the chick paraventricular nucleus (PVN) (A, B, C & D) and the forebrain (FB) (E, F, G & H) following fasting and injection. At three days of age, eighteen birds were injected with ACSF into the lateral ventricle of the brain and fed *ad libitum* (naïve). Eighteen birds were injected with ACSF and another eighteen birds were injected with EZH2 antisense oligonucleotides. Right after injection, these birds were fasted for 24 hours (D3-fasted). Naïve controls and fasted chicks (from both ACSF and antisense injected group) were sacrificed on day 4 (D4) and day 11 (D11). Total mRNA was isolated and evaluated by real-time polymerase chain reaction (PCR) using the Sybr green method with *SUZ*, *EZh2*, *EED*, and *CBP* gene-specific primers (see Table 1). Gene expression levels were compared with β-actin. Each value is the mean ± standard error of the mean of 6 to 12 individual chicks. Histogram with different letters indicated a significant difference. Abbreviations: *SUZ* (suppressor of zeste), *EZh2* (enhancer of zeste 2); *EED* (embryonic ectoderm development); *CBP* (CREB [cAMP response element binding] protein). In PVN, after "D3-fasting +ACSF" treatment, there was an instant increase in the levels of SUZ (A), EZH2 (B), EED (C) but not CBP (D) on 24 hrs post fasting. On D11, while "D3-fasting +ACSF" no longer caused any effect on SUZ and CBP, it inhibited EZH2 and further elevated EED in the PVN. After EZH2 antisense injection, it blocked the surge of EZH2 and EED mRNA on both D4 and D11 (B). While EZH2 antisense did not show any effect on SUZ at 24 hr post injection, it did inhibit SUZ mRNA on 8 days post injection (A). CBP, on the other hand, was not affect by EZH2 antisense at all (D). In FB, "D3-fasting +ACSF" had no effect on SUZ (E), EZH2 (F), EED (G) and CBP (H). However, after EZH2 injection, all of them became significantly inhibited.

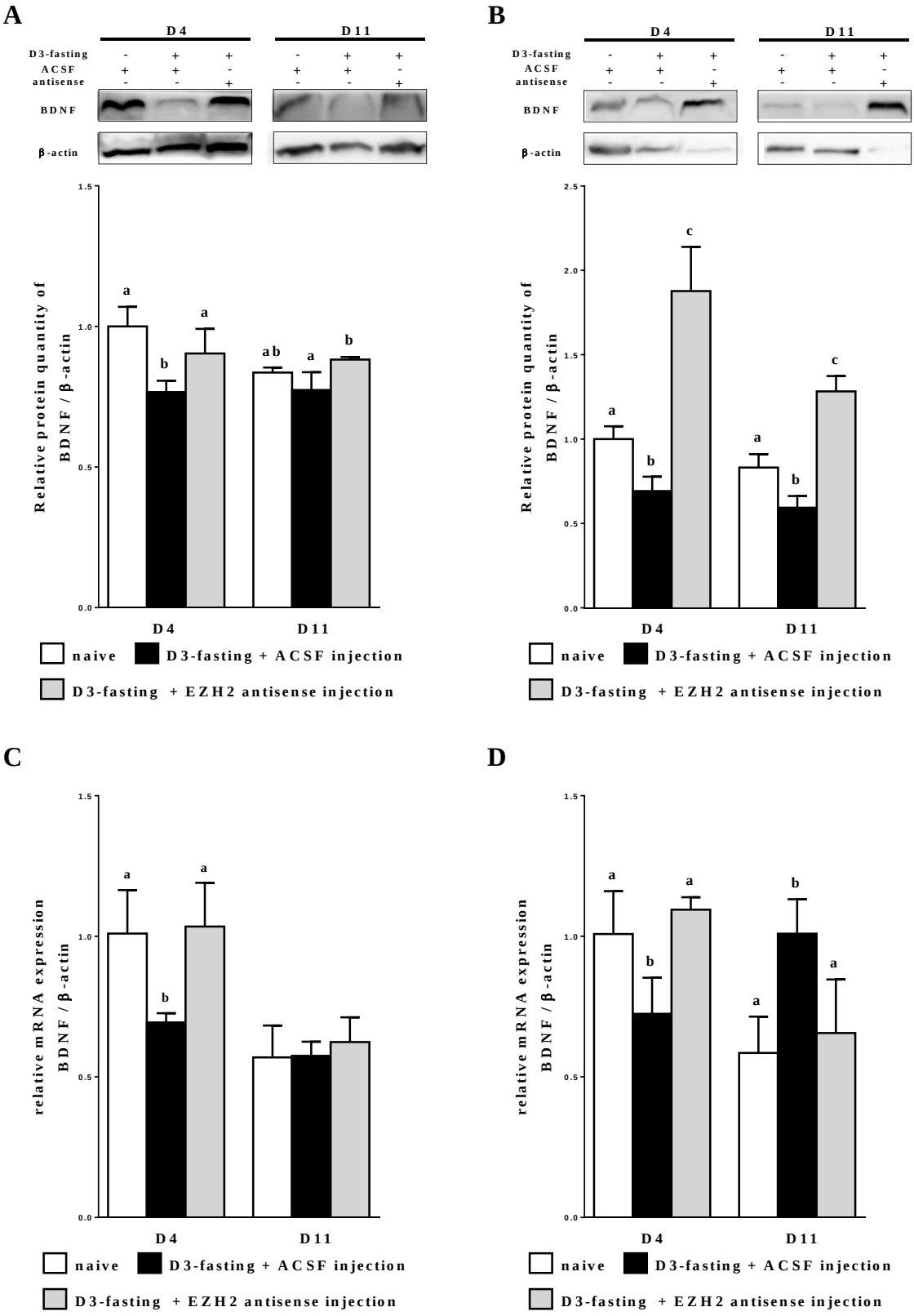
A
D4
D11
D3-fasting
ACSF
antisense
BDNF
β-actin
Relative protein quantity of BDNF / β-actin
naive
D3-fasting + ACSF injection
D3-fasting + EZH2 antisense injection
B
C
relative mRNA expression BDNF / β-actin
D

Figure 17. Changes in protein and mRNA levels of BDNF in chick's PVN (A & C) and FB (B & D) following fasting and injection. At three days of age, eighteen birds were injected with ACSF into the lateral ventricle of the brain and fed *ad libitum* (naïve). Eighteen birds were injected with ACSF and another eighteen birds were injected with EZH2 antisense oligonucleotides. Right after injection, these birds were fasted for 24 hours (D3-fasted). Naïve controls and fasted chicks (from both ACSF and antisense injected group) were sacrificed on day 4 (D4) and day 11 (D11). Total protein was isolated and evaluated by Western blot using the antibody against BDNF. Blot density were compared with β-actin. Total mRNA was isolated and evaluated by real-time PCR using the Sybr green method with *BDNF* (see Table 1). Gene expression levels were compared with β-actin. Each value is the mean ± standard error of the mean of 6 to 12 individual chicks. Histogram with different letters indicated a significant difference. After "D3-fasting + ACSF", a significant drop of BDNF protein was detected at 24 hr post fasting in both PVN (A) and FB (B). On D11, BDNF protein in both tissues went back to the naive level. In addition, BDNF mRNA was instantly inhibited by "D3-fasting + ACSF" but went back to naive on D11 in PVN (C). However in FB, while BDNF mRNA was inhibited on D4, it showed a reversal on D11 (D). After EZH2 antisense injection, both BDNF protein (A) and mRNA (C) no longer showed the drop and became non-shifted from naive level in PVN. In FB, EZH2 antisense reversed the inhibition/elevation of BDNF protein and mRNA after D3-fasting (B).

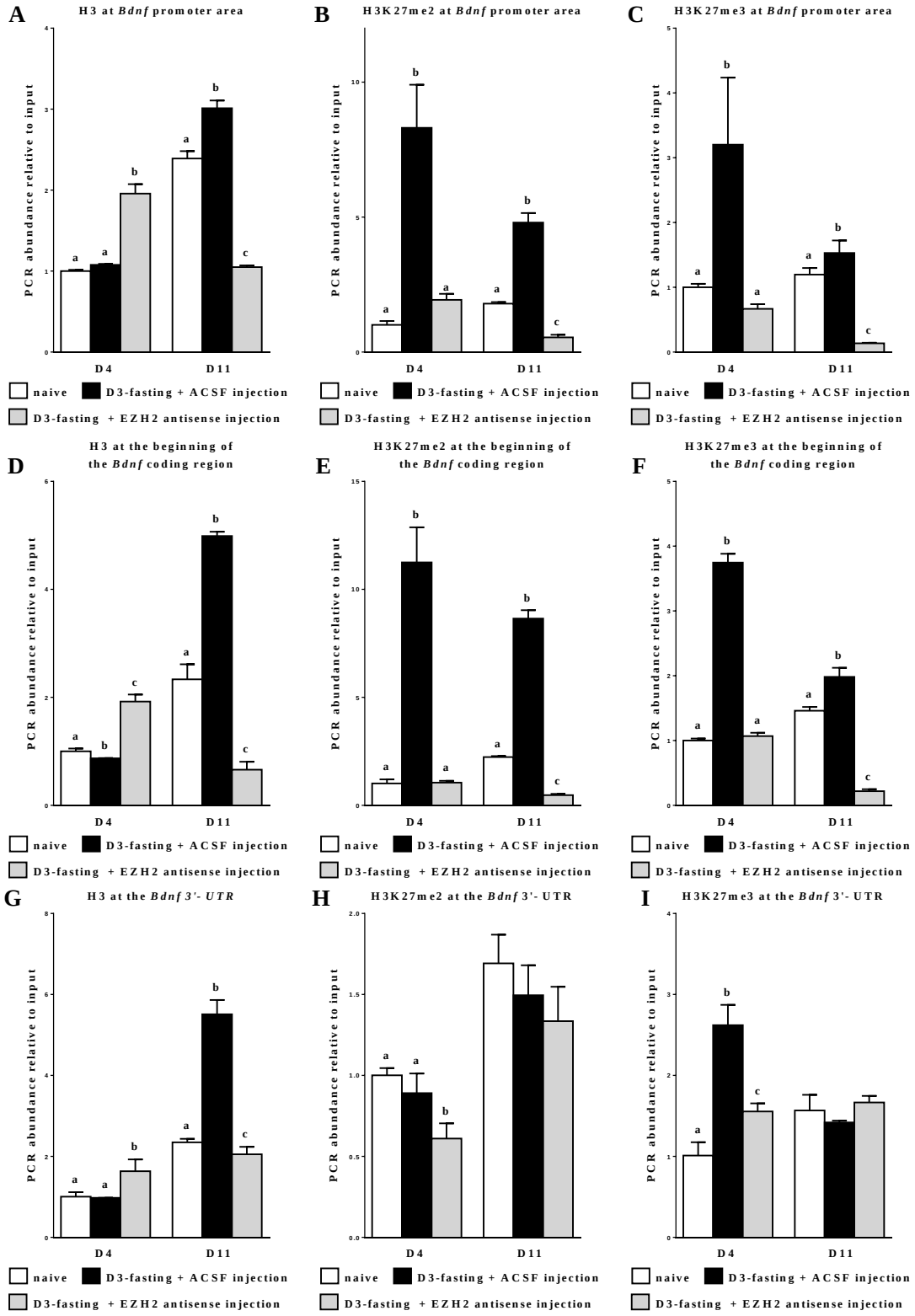
A
H3 at Bdnf promoter area
B
H3K27me2 at Bdnf promoter area
C
H3K27me3 at Bdnf promoter area
D
H3 at the beginning of the Bdnf coding region
E
H3K27me2 at the beginning of the Bdnf coding region
F
H3K27me3 at the beginning of the Bdnf coding region
G
H3 at the Bdnf 3'- UTR
H
H3K27me2 at the Bdnf 3'- UTR
I
H3K27me3 at the Bdnf 3'- UTR
PCR abundance relative to input
D4
D11
naive
D3-fasting + ACSF injection
D3-fasting + EZH2 antisense injection

Figure 18. Alterations in dimethylation and trimethylation levels of H3K27 along the *Bdnf* gene in the PVN following a 24 hour fast on day 3 with injection. To assess the histone modifications present at the *Bdnf* gene, ChIP assays were performed. Eighteen birds were injected with ACSF and another eighteen birds were injected with EZH2 antisense oligonucleotides into the latral ventricle. Right after injection, these birds were fasted for 24 hours (D3-fasted). Na ïve controls and fasted chicks (from both ACSF and antisense injected groups) were sacrificed on day 4 (D4) and day 11 (D11). PVN samples were collected and immuno-precipitated with antibodies against H3 (positive control), H3K27me2, H3K27me3 and IgG (as negative control). PCR results with *Bdnf*-specific primers (see Table 1) aligning at the promoter region and producing amplicon -869 to -801 bp upstream of the coding region. (D, E & F). PCR results with *Bdnf*-specific primers aligning at the transcription start site and producing amplicon +91 to +190 bp. (G, H and I). PCR results with *Bdnf*-specific primers aligning at the 3'-UTR and producing amplicon +1623 to +1698 bp. Each value (PCR abundance relative to input) is the mean ± standard error of the mean of 6 individual chicks minus the background signal (IgG) and then normalized to that of age comparable control na ïve chicks. Histogram with different letters indicated a significant difference.

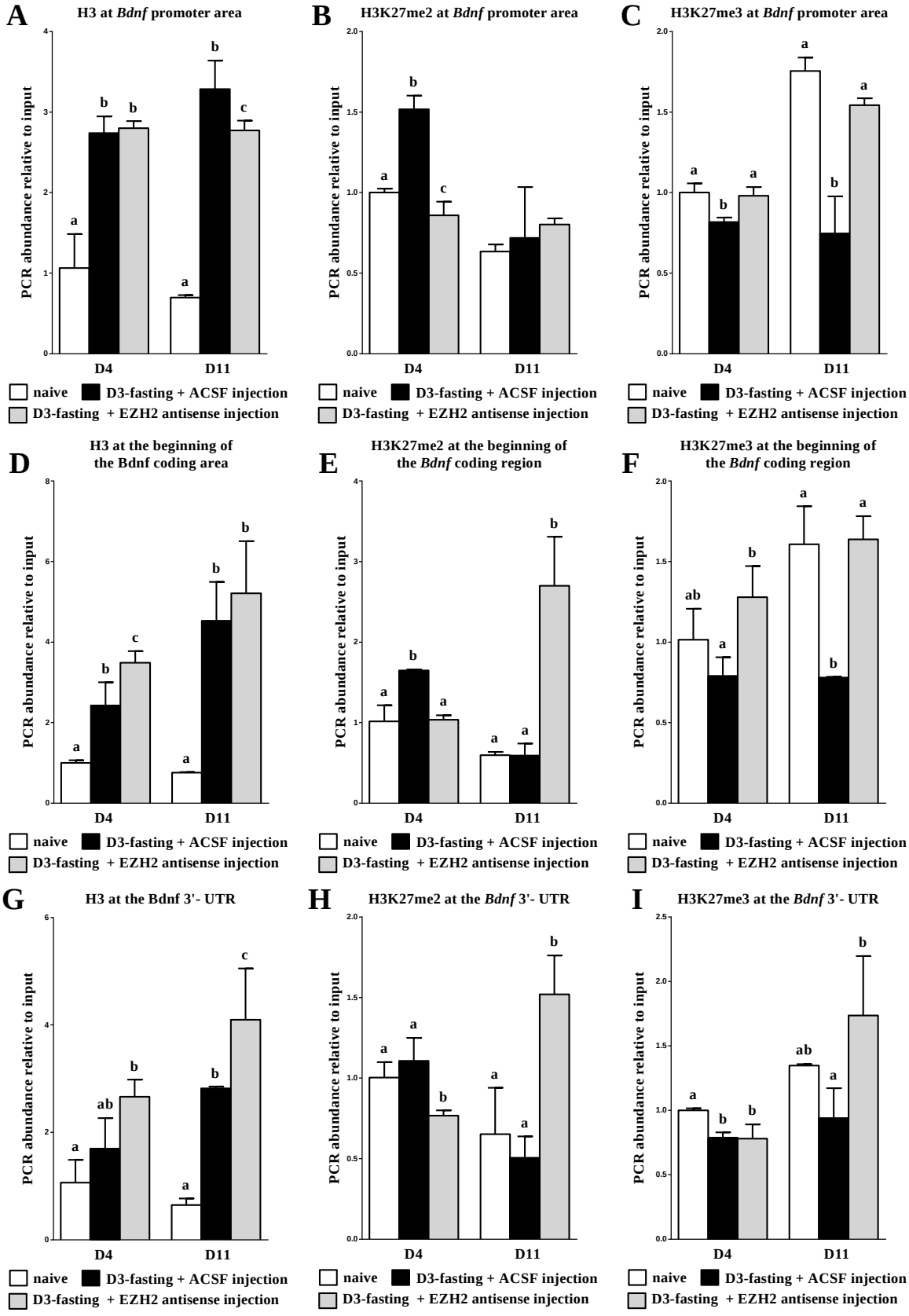
A
H3 at *Bdnf* promoter area
B
H3K27me2 at *Bdnf* promoter area
C
H3K27me3 at *Bdnf* promoter area
D
H3 at the beginning of the Bdnf coding area
E
H3K27me2 at the beginning of the *Bdnf* coding region
F
H3K27me3 at the beginning of the *Bdnf* coding region
G
H3 at the Bdnf 3'- UTR
H
H3K27me2 at the *Bdnf* 3'- UTR
I
H3K27me3 at the *Bdnf* 3'- UTR
PCR abundance relative to input
D4
D11
naive
D3-fasting + ACSF injection
D3-fasting + EZH2 antisense injection

Figure 19. Alterations in dimethylation and trimethylation levels of H3K27 along the *Bdnf* gene in the FB following a 24 hour fast on day 3 with injection. To assess the histone modifications present at the *Bdnf* gene, ChIP assays were performed. Eighteen birds were injected with ACSF and another eighteen birds were injected with EZH2 antisense oligonucleotides into the lateral ventricle. Right after injection, these birds were fasted for 24 hours (D3-fasted). Naïve controls and fasted chicks (from both ACSF and antisense injected groups) were sacrificed on day 4 (D4) and day 11 (D11). PVN samples were collected and immuno-precipitated with antibodies against H3 (positive control), H3K27me2, H3K27me3 and IgG (as negative control). PCR results with *Bdnf*-specific primers (see Table 1) aligning at the promoter region and producing amplicon -869 to -801 bp upstream of the coding region. (D, E & F). PCR results with *Bdnf*-specific primers aligning at the transcription start site and producing amplicon +91 to +190 bp. (G, H and I). PCR results with *Bdnf*-specific primers aligning at the 3'-UTR and producing amplicon +1623 to +1698 bp. Each value (PCR abundance relative to input) is the mean ± standard error of the mean of 6 individual chicks minus the background signal (IgG) and then normalized to that of age comparable control naïve chicks. Histogram with different letters indicated a significant difference.

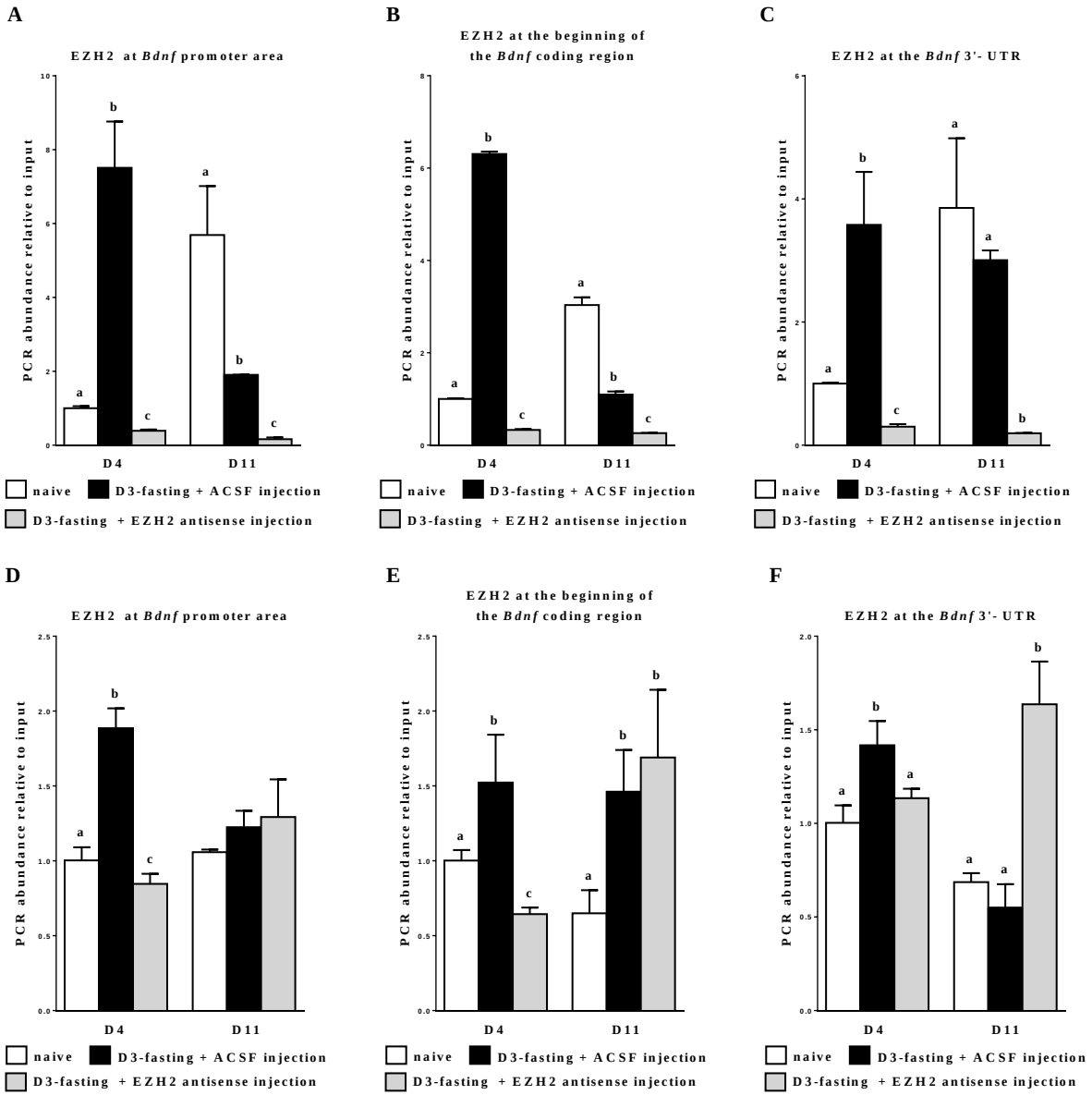
A
EZH2 at Bdnf promoter area
PCR abundance relative to input
D4
D11
naive
D3-fasting + ACSF injection
D3-fasting + EZH2 antisense injection
B
EZH2 at the beginning of the Bdnf coding region
C
EZH2 at the Bdnf 3'- UTR
D
E
F

Figure 20. Alterations in EZH2 along the *Bdnf* gene in the PVN (A, B & C) and FB (D, E & F) following a 24 hour fast on day 3 with injection. To assess the histone modifications present at the *Bdnf* gene, ChIP assays were performed. Eighteen birds were injected with ACSF and another eighteen birds were injected with EZH2 antisense oligonucleotides. Right after injection, these birds were fasted for 24 hours (D3-fasted). Naïve controls and fasted chicks (from both ACSF and antisense injected groups) were sacrificed on day 4 (D4) and day 11 (D11). PVN samples were collected and immuno-precipitated with antibodies against H3 (positive control), EZH2 and IgG (as negative control). PCR results with *Bdnf*-specific primers (see Table 1) aligning at the promoter region and producing amplicon -869 to -801 bp upstream of the coding region. PCR results with *Bdnf*-specific primers aligning at the transcription start site and producing amplicon +91 to +190 bp. (B & E). PCR results with *Bdnf*-specific primers aligning at the 3'-UTR and producing amplicon +1623 to +1698 bp (C & F). Each value (PCR abundance relative to input) is the mean ± standard error of the mean of 6 individual chicks minus the background signal (IgG) and then normalized to that of age comparable control naïve chicks. Histogram with different letters indicated a significant difference.

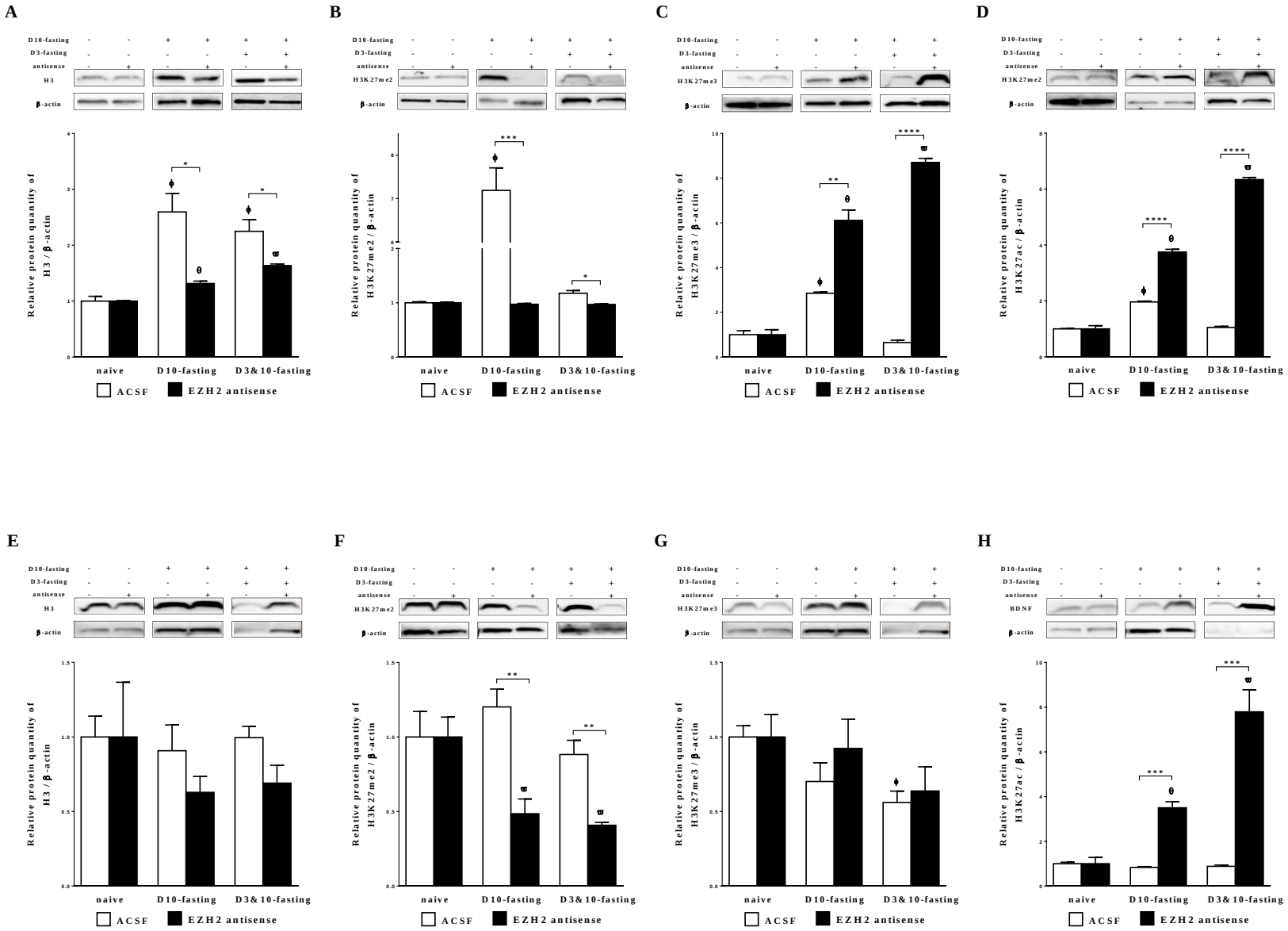
A
B
C
D
E
F
G
H
D10-fasting
D3-fasting
antisense
H3
H3K27me2
H3K27me3
BDNF
β-actin
Relative protein quantity of H3 / β-actin
Relative protein quantity of H3K27me2 / β-actin
Relative protein quantity of H3K27me3 / β-actin
Relative protein quantity of H3K27ac / β-actin
naive
D10-fasting
D3&10-fasting
ACSF
EZH2 antisense

Figure 21. Changes in protein levels of H3, H3K27me2, H3K27me3 and H3K27ac in chick's PVN (A, B, C & D) and FB (E, F, G & H) following fasting and injection. At three days of age, eighteen birds were injected with ACSF into the lateral ventricle and then randomly and evenly divided into three groups. One group was randomly picked and fed *ad libitum* until D11 (naïve). For D3- and D10- double fasting group (called D3/10-fasting in the following paragraph), food was withdrawn for 24 hr on D3. On D4, food was back to normal supply to the fasted group. On D10, D3/10-fasting groups were fasted again for 24hr. For single fasting on D10 group (called D10-fasting), food was only withdrawn on D10 for 24 hr. All three groups of chicks were sacrificed on D11 and PVN and FB samples were collected. In EZH2 antisense injected group, all treatments remained the same as that of the ACSF injected group, except ACSF was replaced with EZH2 antisense. Total protein was isolated and evaluated by Western blot using the antibody against H3, H3K27me2, H3K27me3 and H3K27ac. Blot density were compared with β-actin. Each value is the mean ± standard error of the mean of 6 to 12 individual chicks. Histogram with different asterisks indicated a significant difference. In the ACSF injected group, D10-fasting was able to significantly increase global H3 (A), H3K27me2 (B), H3K27me3 (C) and H3K27ac (D) level in the PVN. However, if applied a fasting on D3 prior to D10 fasting, H3K27me2, H3K27me3 and H3K27ac went back to the level of naive groups. H3, on the other hand, was more elevated. After EZH2 antisense injection, H3K27me2 no longer showed a peak after single D10 fasting (B). On the other hand, H3K27me3 (C) and H3K27ac (D) were more elevated after D10-fasting and even more elevated after D3/10-fasting. Total H3 was significantly inhibited after EZH2 antisense after either D10-fasting or D3/10-fasting (A). In FB, EZH2 antisense only significantly inhibited H3K27me2 (F) and elevated H3K27ac (H) after both D3 and D3/10-fasting treatment. However, it had no effect on total H3 (E) and H3K27me3 (G).

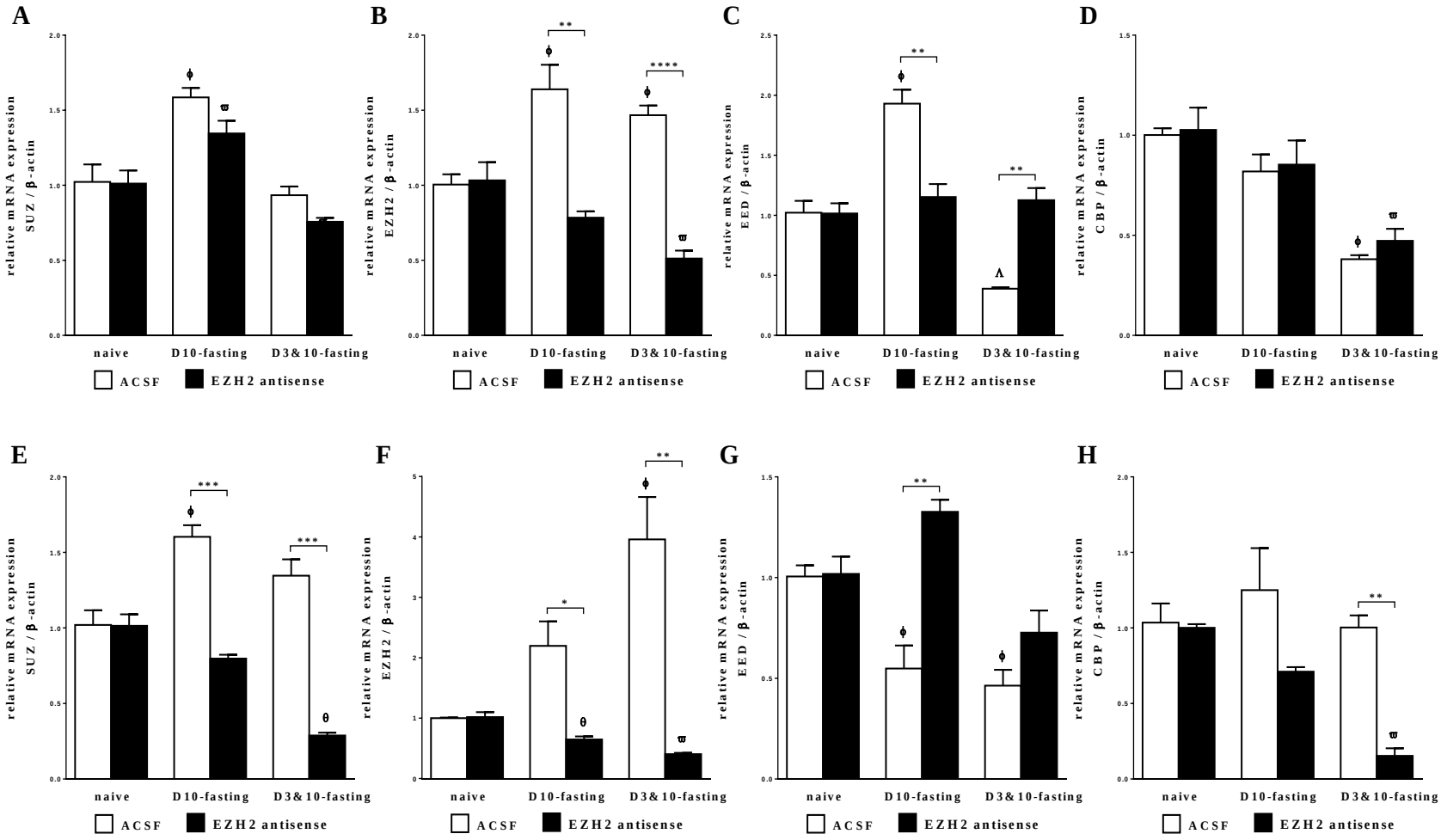
A
B
C
D
E
F
G
H
relative mRNA expression
SUZ / β-actin
EZH2 / β-actin
EED / β-actin
CBP / β-actin
naive
D10-fasting
D3&10-fasting
ACSF
EZH2 antisense

Figure 22. Changes in mRNA levels of key factors in Polycomb repressive complex 2 (PRC2) and a histone acetyltransferase (HAT) in the chick PVN (A, B, C & D) and FB (E, F, G & H) following fasting and injection. At three days of age, eighteen birds were injected with ACSF into the lateral ventricle and then randomly and evenly divided into three groups. One group was randomly picked and fed *ad libitum* until D11 (naïve). For D3- and D10- double fasting group (called D3/10-fasting in the following paragraph), food was withdrawn for 24 hr on D3. On D4, food was back to normal supply to the fasted group. On D10, D3/10-fasting groups were fasted again for 24hr. For single fasting on D10 group (called D10-fasting), food was only withdrawn on D10 for 24 hr. All three groups of chicks were sacrificed on D11 and PVN and FB samples were collected. In EZH2 antisense injected group, all treatments remained the same as that of the ACSF injected group, except ACSF was replaced with EZH2 antisense. Total mRNA was isolated and evaluated by real-time polymerase chain reaction (PCR) using the Sybr green method with *SUZ*, *EZh2*, *EED*, and *CBP* gene-specific primers (see Table 1). Gene expression levels were compared with β-actin. Each value is the mean ± standard error of the mean of 6 to 12 individual chicks. Histogram with different asterisks indicated a significant difference. Abbreviations: *SUZ* (suppressor of zeste), *EZh2* (enhancer of zeste 2); *EED* (embryonic ectoderm development); *CBP* (CREB [cAMP response element binding] protein). In PVN, after "D10-fasting +ACSF" treatment, there was an instant increase in the levels of SUZ (A), EZH2 (B), EED (C) but not CBP (D) on 24 hrs post fasting. If applied a fasting on D3 prior D10-fasting, SUZ (A), EZH2 (B) and EED (C) mRNA were constantly inhibited (except EED after D3/10-fasting) and the "molecular memory" pattern no long existed. CBP, on the other hand, was not affected by EZH2 antisense (D). In FB, although no apparent pattern of "molecular memory" existed, EZH2 antisense significantly inhibited levels of SUZ and EZH2 after either kind of fasting. On the other hand, EZH2 antisense injection elevated EED mRNA levels after D10-fasting while inhibiting CBP mRNA level after D3/10-fasting.

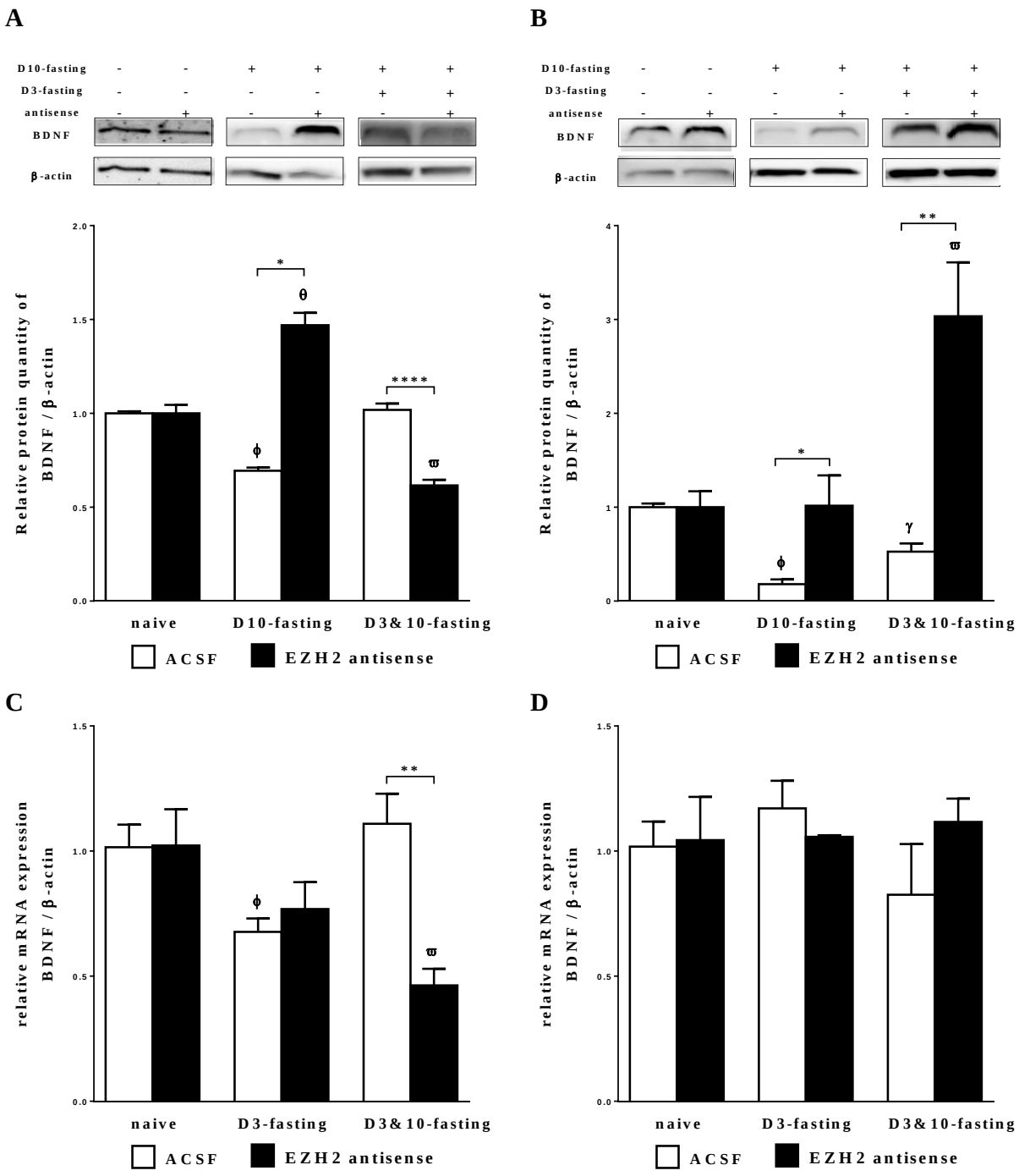
A
B
D10-fasting
D3-fasting
antisense
BDNF
β-actin
Relative protein quantity of BDNF / β-actin
naive
D10-fasting
D3&10-fasting
ACSF
EZH2 antisense
C
D
relative mRNA expression BDNF / β-actin
D3-fasting

Figure 23. Changes in protein and mRNA levels of BDNF in chick's PVN (A & C) and FB (B & D) following fasting and injection. At three days of age, eighteen birds were injected with ACSF into the lateral ventricle and then randomly and evenly divided into three groups. One group was randomly picked and fed *ad libitum* until D11 (naïve). For the D3- and D10- double fasting group (called D3/10-fasting in the following paragraph), food was withdrawn for 24 hr on D3. On D4, food was back to normal supply to the fasted group. On D10, D3/10-fasting groups were fasted again for 24hr. For single fasting on D10 group (called D10-fasting), food was only withdrawn on D10 for 24 hr. All three groups of chicks were sacrificed on D11 and PVN and FB samples were collected. In EZH2 antisense injected group, all treatments remained the same as that of the ACSF injected group, except ACSF was replaced with EZH2 antisense. Total protein was isolated and evaluated by Western blot using the antibody against H3, H3K27me2, H3K27me3 and H3K27ac. Blot density were compared with β-actin. Each value is the mean ± standard error of the mean of 6 to 12 individual chicks. Histogram with different asterisks indicated a significant difference. In ACSF injected group, D10-fasing significantly inhibited both BDNF protein and mRNA in PVN. However, if applied a fasting on D3 prior to D10 fasting, both BDNF protein and mRNA became not different to the naive groups (A & C). Both BDNF protein and mRNA revealed a perfect pattern, which we refer to as "molecular memory". However, after EZH2 antisense injection, the "molecular memory" pattern was impaired: BDNF protein and mRNA were increased after D10-fasting while decreased after D3/10-fasting. In the FB, BDNF protein also obtained this molecular memory after ACSF injection, which became elevated after EZH2 antisense injection (B & D). BDNF mRNA in FB was only increased after D3/10-fasting + EZH2 antisense injection.

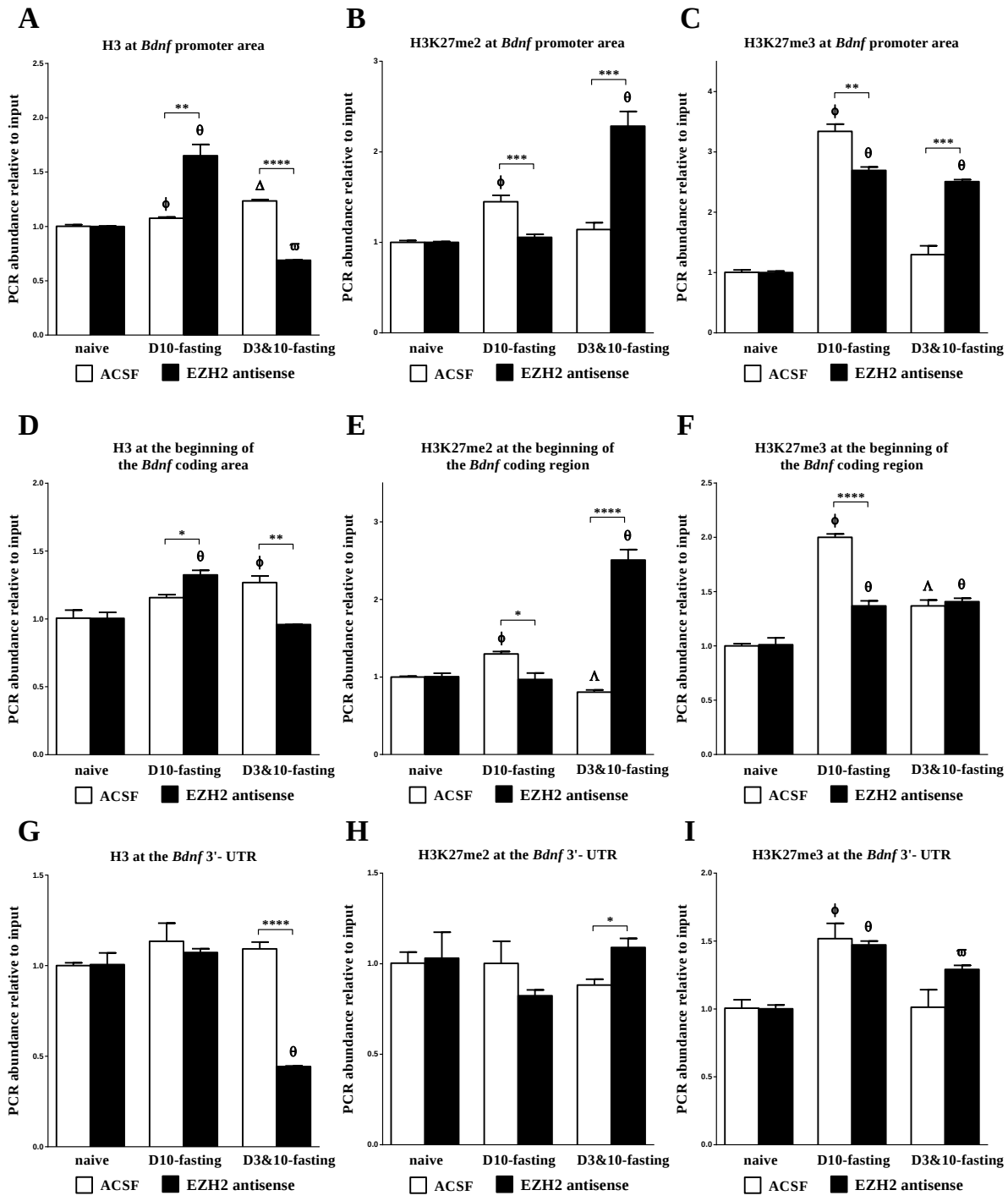
A
H3 at *Bdnf* promoter area
B
H3K27me2 at *Bdnf* promoter area
C
H3K27me3 at *Bdnf* promoter area
D
H3 at the beginning of the *Bdnf* coding area
E
H3K27me2 at the beginning of the *Bdnf* coding region
F
H3K27me3 at the beginning of the *Bdnf* coding region
G
H3 at the *Bdnf* 3'- UTR
H
H3K27me2 at the *Bdnf* 3'- UTR
I
H3K27me3 at the *Bdnf* 3'- UTR
PCR abundance relative to input
naive
D10-fasting
D3&10-fasting
ACSF
EZH2 antisense

Figure 24. Alterations in dimethylation and trimethylation levels of H3K27 along the *Bdnf* gene in the PVN following a 24 hour fast on day 3 with injection. To assess the histone modifications present at the *Bdnf* gene, ChIP assays were performed. At three days of age, eighteen birds were injected with ACSF into the lateral ventricle and then randomly and evenly divided into three groups. One group was randomly picked and fed *ad libitum* until D11 (naïve). For D3- and D10- double fasting group (called D3/10-fasting in the following paragraph), food was withdrawn for 24 hr on D3. On D4, food was back to normal supply to the fasted group. On D10, D3/10-fasting groups were fasted again for 24hr. For single fasting on D10 group (called D10-fasting), food was only withdrawn on D10 for 24 hr. All three groups of chicks were sacrificed on D11 and PVN samples were collected. In the EZH2 antisense injected group, all treatments remained the same as that of the ACSF injected group, except ACSF was replaced with EZH2 antisense. PVN samples were immuno-precipitated with antibodies against H3 (positive control), H3K27me2, H3K27me3 and IgG (as negative control). PCR results with *Bdnf*-specific primers (see Table 1) aligning at the promoter region and producing amplicon -869 to -801 bp upstream of the coding region (D, E & F). PCR results with *Bdnf*-specific primers aligning at the transcription start site and producing amplicon +91 to +190 bp (G, H and I). PCR results with *Bdnf*-specific primers aligning at the 3'-UTR and producing amplicon +1623 to +1698 bp. Each value (PCR abundance relative to input) is the mean ± standard error of the mean of 6 individual chicks minus the background signal (IgG) and then normalized to that of age comparable control naïve chicks. Histogram with different asterisks indicated a significant difference.

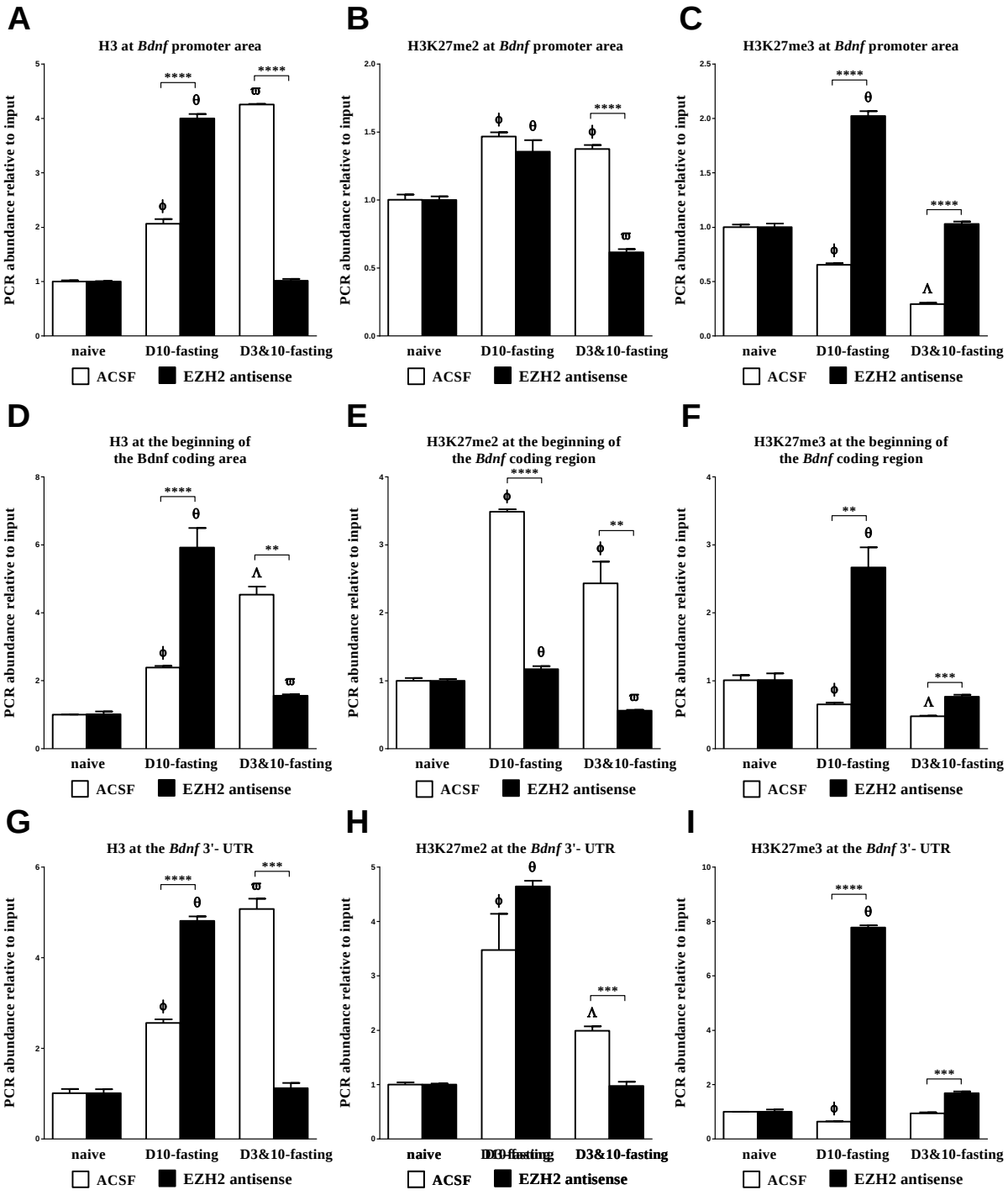
A
H3 at *Bdnf* promoter area
B
H3K27me2 at *Bdnf* promoter area
C
H3K27me3 at *Bdnf* promoter area
D
H3 at the beginning of the Bdnf coding area
E
H3K27me2 at the beginning of the *Bdnf* coding region
F
H3K27me3 at the beginning of the *Bdnf* coding region
G
H3 at the *Bdnf* 3'- UTR
H
H3K27me2 at the *Bdnf* 3'- UTR
I
H3K27me3 at the *Bdnf* 3'- UTR
PCR abundance relative to input
naive
D10-fasting
D3&10-fasting
ACSF
EZH2 antisense

Figure 25. Alterations in dimethylation and trimethylation levels of H3K27 along the *Bdnf* gene in the FB following a 24 hour fast on day 3 with injection. To assess the histone modifications present at the *Bdnf* gene, ChIP assays were performed. At three days of age, eighteen birds were injected with ACSF into the lateral ventricle and then randomly and evenly divided into three groups. One group was randomly picked and fed *ad libitum* until D11 (naïve). For D3- and D10- double fasting group (called D3/10-fasting in the following paragraph), food was withdrawn for 24 hr on D3. On D4, food was back to normal supply to the fasted group. On D10, D3/10-fasting groups were fasted again for 24hr. For single fasting on D10 group (called D10-fasting), food was only withdrawn on D10 for 24 hr. All three groups of chicks were sacrificed on D11 and FB samples were collected. In EZH2 antisense injected group, all treatments remained same as that of ACSF injected group, except ACSF was replaced with EZH2 antisense. FB samples were immuno-precipitated with antibodies against H3 (positive control), H3K27me2, H3K27me3 and IgG (as negative control). PCR results with *Bdnf*-specific primers (see Table 1) aligning at the promoter region and producing amplicon -869 to -801 bp upstream of the coding region (D, E & F). PCR results with *Bdnf*-specific primers aligning at the transcription start site and producing amplicon +91 to +190 bp (G, H and I). PCR results with *Bdnf*-specific primers aligning at the 3'-UTR and producing amplicon +1623 to +1698 bp. Each value (PCR abundance relative to input) is the mean ± standard error of the mean of 6 individual chicks minus the background signal (IgG) and then normalized to that of age comparable control naïve chicks. Histogram with different asterisks indicated a significant difference.

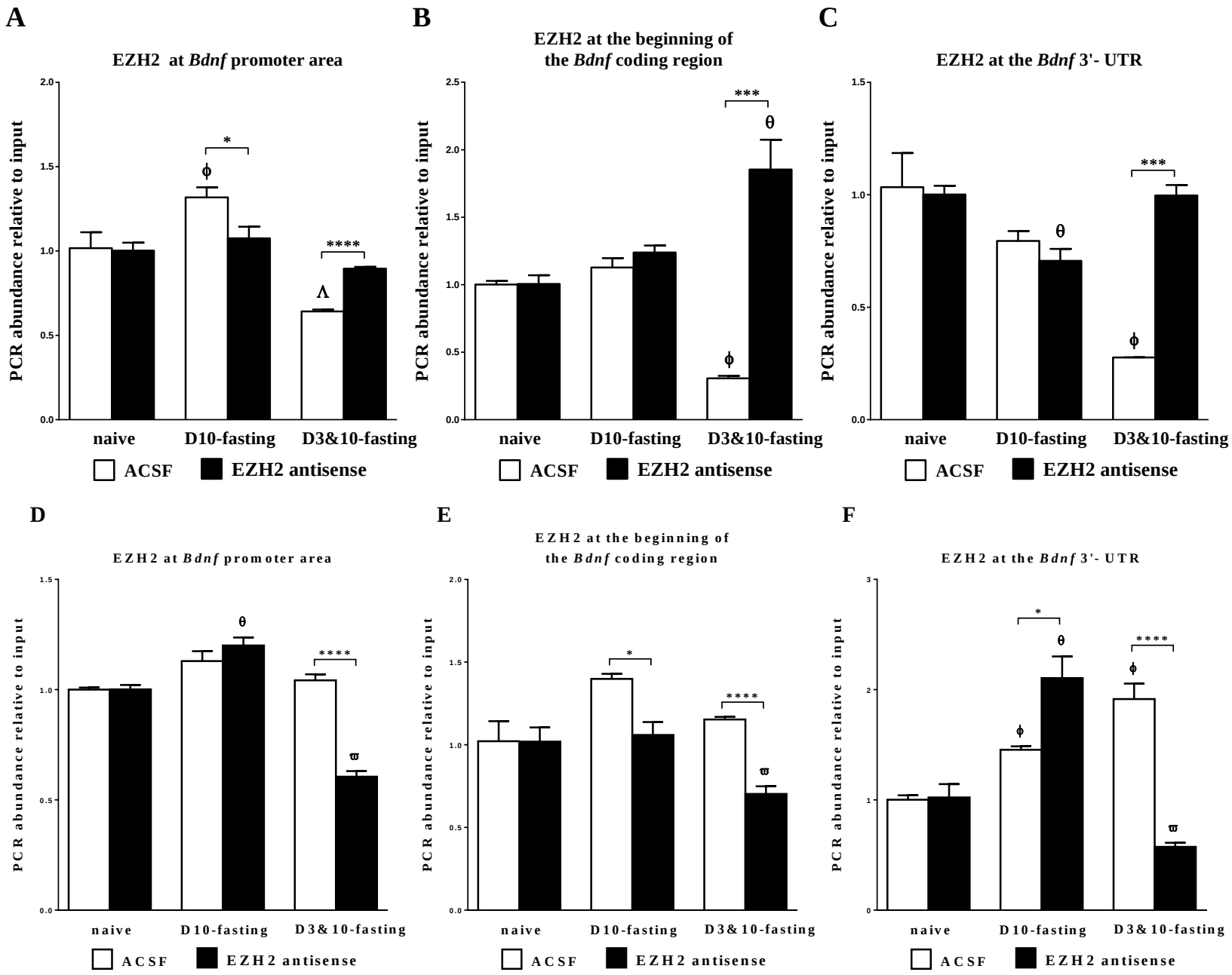
A
EZH2 at Bdnf promoter area
PCR abundance relative to input
naive
D10-fasting
D3&10-fasting
ACSF
EZH2 antisense
B
EZH2 at the beginning of the Bdnf coding region
C
EZH2 at the Bdnf 3'- UTR
D
E
F

Figure 26. Alterations in EZH2 along the *Bdnf* gene in the PVN (A, B & C) and FB (D, E & F) following a 24 hour fast on day 3 with injection. To assess the histone modifications present at the *Bdnf* gene, ChIP assays were performed. At three days of age, eighteen birds were injected with ACSF into the lateral ventricle and then randomly and evenly divided into three groups. One group was randomly picked and fed *ad libitum* until D11 (naïve). For D3- and D10- double fasting group (called D3/10-fasting in the following paragraph), food was withdrawn for 24 hr on D3. On D4, food was back to normal supply to the fasted group. On D10, D3/10-fasting groups were fasted again for 24hr. For single fasting on D10 group (called D10-fasting), food was only withdrawn on D10 for 24 hr. All three groups of chicks were sacrificed on D11 and FB samples were collected. In the EZH2 antisense injected group, all treatments remained the same as that of the ACSF injected group, except ACSF was replaced with EZH2 antisense. FB samples were immuno-precipitated with antibodies against H3 (positive control), EZH2 and IgG (as negative control). PCR results with *Bdnf*-specific primers aligning at the transcription start site and producing amplicon +91 to +190 bp (B & E). PCR results with *Bdnf*-specific primers aligning at the 3'-UTR and producing amplicon +1623 to +1698 bp (C & F). PCR results with *Bdnf*-specific primers aligning at the 3'-UTR and producing amplicon +1623 to +1698 bp. Each value (PCR abundance relative to input) is the mean ± standard error of the mean of 6 individual chicks minus the background signal (IgG) and then normalized to that of age comparable control naïve chicks. Histogram with different asterisks indicated a significant difference.

CHAPTER 4: Summary and conclusion

This dissertation project investigated the hypothesis that fasting stress during the early brain developmental period is able to change histone modifications in the paraventricular nucleus (PVN) in chicks, which is catalyzed by the methyltransferase machinery, called polycomb repressive complex 2 (PRC2). We monitored the changes of key components of the PRC2, including embryonic ectoderm development (EED) protein, enhancer of zeste 2 (EZH2) and suppressor of zeste (SUZ), and its product, di- (me2) and tri-methylated (me3) histone 3 (H3) lysine 27 (K27). Specific findings in current study included:

1) We found that after 24 hour fasting stress on 3 day-of-age chicks, the PVN exhibited significant increases of PRC2 key components as well as H3K27me2/me3. Some of these changes last at least for 38 days post fast.

2) The PVN is able to develop "epigenetic memory", which utilizes PRC2 to protect the body from the future same stress, thus keeping inner environment homeostasis.

3) EZH2 antisense oligonucleotides (5.5 ul at 1ug/ul) *in vivo* injections into the lateral ventricle of chick brains successfully induced EZH2 protein and mRNA knockdown.

4) EZH2 knockdown impaired the proper response of the PVN to the 24 hour fasting on D3

5) EZH2 knockdown impaired the "epigenetic memory" development

Future works:

This study linked fasting stress to histone posttranslational modifications. In the current study, however, we only studied the methylation modification at H3K27, but not at other locations with other modifications. Neither did we calculate the food intake amount and linked that to the "epigenetic memory" finding in the PVN. Thus, in future studies, specific research should be carried out to include:

1) Measurement of the other modifications (acetylation, phosphorylation, etc) at different histone (H1 - H4) residues.

2) A nucleotide methylation study linked to that of histone modification, which gives a better understanding of the entire picture

4) The use of immunohistochemical staining to visualize the histone deposition location on the chromosome.

5) Electrophysiology and histology study of neurons in the PVN, which could offer a better understanding of fasting induced epigenetic changes.

References

1. Shalev U, Tylor A, Schuster K, Frate C, Tobin S, Woodside B (2010) Long-term physiological and behavioral effects of exposure to a highly palatable diet during the perinatal and post-weaning periods. Physiol Behav 101: 494-502.
2. Singhal A, Kennedy K, Lanigan J, Fewtrell M, Cole TJ, Stephenson T, Elias-Jones A, Weaver LT, Ibhanesebhor S, MacDonald PD, Bindels J, Lucas A (2010) Nutrition in infancy and long-term risk of obesity: evidence from 2 randomized controlled trials. Am J Clin Nutr 92: 1133-1144.
3. Boullu-Ciocca S, Dutour A, Guillaume V, Achard V, Oliver C, Grino M (2005) Postnatal diet-induced obesity in rats upregulates systemic and adipose tissue glucocorticoid metabolism during development and in adulthood: its relationship with the metabolic syndrome. Diabetes 54: 197-203.
4. Stettler N, Bovet P, Shamlaye H, Zemel BS, Stallings VA, Paccaud F (2002) Prevalence and risk factors for overweight and obesity in children from Seychelles, a country in rapid transition: the importance of early growth. Int J Obes Relat Metab Disord 26: 214-219.
5. Stettler N, Stallings VA, Troxel AB, Zhao J, Schinnar R, Nelson SE, Ziegler EE, Strom BL (2005) Weight gain in the first week of life and overweight in adulthood: a cohort study of European American subjects fed infant formula. Circulation 111: 1897-1903.
6. Xu P, Denbow CJ, Meiri N, Denbow DM (2012) Fasting of 3-day-old chicks leads to changes in histone H3 methylation status. Physiol Behav 105: 276-282.
7. Kisliouk T, Meiri N (2009) A critical role for dynamic changes in histone H3 methylation at the Bdnf promoter during postnatal thermotolerance acquisition. Eur J Neurosci 30: 1909-1922.
8. Plagemann A, Harder T, Brunn M, Harder A, Roepke K, Wittrock-Staar M, Ziska T, Schellong K, Rodekamp E, Melchior K, Dudenhausen JW (2009) Hypothalamic proopiomelanocortin promoter methylation becomes altered by early overfeeding: an epigenetic model of obesity and the metabolic syndrome. J Physiol 587: 4963-4976.
9. Waterland RA, Michels KB (2007) Epigenetic epidemiology of the developmental origins hypothesis. Annu Rev Nutr 27: 363-388.
10. Bannister AJ, Kouzarides T (2011) Regulation of chromatin by histone modifications. Cell Res 21: 381-395.
11. Zentner GE, Henikoff S (2013) Regulation of nucleosome dynamics by histone modifications. Nat Struct Mol Biol 20: 259-266.
12. Young NL, Dimaggio PA, Garcia BA (2010) The significance, development and progress of high-throughput combinatorial histone code analysis. Cell Mol Life Sci 67: 3983-4000.
13. Okamoto I, Otte AP, Allis CD, Reinberg D, Heard E (2004) Epigenetic dynamics of imprinted X inactivation during early mouse development. Science 303: 644-649.
14. Ebert A, Schotta G, Lein S, Kubicek S, Krauss V, Jenuwein T, Reuter G (2004) Su(var) genes regulate the balance between euchromatin and heterochromatin in Drosophila. Genes Dev 18: 2973-2983.
15. Wang Z, Zang C, Rosenfeld JA, Schones DE, Barski A, Cuddapah S, Cui K, Roh TY, Peng W, Zhang MQ, Zhao K (2008) Combinatorial patterns of histone acetylations and methylations in the human genome. Nat Genet 40: 897-903.
16. Schwartz MW, Woods SC, Porte D, Seeley RJ, Baskin DG (2000) Central nervous system control of food intake. Nature 404: 661-671.
17. Brobeck JR, Tepperman J, Long CN (1943) Experimental hypothalamic hyperphagia in the albino rat. Yale J Biol Med 15: 831-853.
18. King BM (2006) The rise, fall, and resurrection of the ventromedial hypothalamus in the regulation of feeding behavior and body weight. Physiol Behav 87: 221-244.
19. Frohlich A (1901) A case involving a tumor of the hypophysis cerebri without acromegaly. Wien Klin Rundsch 15: 883-886.

20. Erdheim J (1904) Ober Hypophysenganggeschwtilste und Hirncholesteatome. S B Akad Wiss Wien 113 537-726.
21. Hetherington AW (1943) The production of hypothalamic obesity in rats already displaying chronic hypopituitarism. Am J Physiol 140: 89-92.
22. Camus J, Roussy G (1920) Experimental researches on the pituitary body. Endocrinology 4: 507-522.
23. Bailey P, Bremer F (1921) Experimental diabetes insipidus. Arch Intern Med 28: 773–803.
24. Macnalty A (1957) Sir Victor Horsley: his life and work. Br Med J 1: 910-916.
25. Hetherington AW, Ranson SW (1939) Experimental hypothalamico-hypophyseal obesity in the rat. Proc Soc Exp Biol Med 41: 465-466.
26. Hetherington AW, Ranson SW (1941) The relation of various hypothalamic lesions to adiposity and other phenomena in the rat. Am J Physiol 133: 326-327.
27. Hetherington AW, Ranson SW (1942a) Effect of early hypophysectomy on hypothalamic obesity. Endocrinology 31: 30-34.
28. Anand BK, Brobeck JR (1951) Hypothalamic controls of food intake in rats and cats. Yale J Biol Med 24: 123-139.
29. Richter CP, Eckert JF (1936) Behavior changes produced in the rat by hypophysectomy. Proc Assoc Res Nerv Ment Dis 17: 561-571.
30. Kenndy GC (1950) The hypothalamic control of food intake in rats. Proc R Soc Lond B Biol Sci 137: 535-549.
31. Wyrwicka W, Dobrzecka C (1960) Relationship between feeding and satiation centers of the hypothalamus. Science 132: 805-806.
32. Brobeck JR, Larsson S, Reyes E (1956) A study of the electrical activity of the hypothalamic feeding mechanism. J Physiol 132: 358–364.
33. Hetherington AW, Ranson SW (1942b) The spontaneous activity and food intake of rats with hypothalamic lesions. Am J Physiol 136: 609-617.
34. Brobeck JR (1948) Food intake as a mechanism of temperature regulation. Yale J Biol Med 6: 545-552.
35. Mayer J (1955) Regulation of energy intake and the body weight: the glucostatic theory and the lipostatic hypothesis. Ann N Y Acad Sci 63: 15-43.
36. Kenndy GC (1953) The role of depot fat in the hypothalamic control of food intake in the rat. Proc R Soc Lond B Biol Sci 140: 578-596.
37. Ranson SW (1940) Regulation of body temperature. Res Publ AssocRes Nerv Ment Dis 20: 342-399.
38. Mayer J (1953) Genetic, traumatic and environmental factors in the etiology of obesity. Physiol Rev 33: 472-508.
39. Mayer J, Bates MW (1952) Blood glucose and food intake in normal and hypophysectomized, alloxan-treated rats. Am J Physiol 168: 812-819.
40. Dunn JS, McLetchie NGB (1943) Experimental alloxan diabetes in the rat. Lancet 245: 384-387.
41. Weaver DC, McDaniel ML, Lacy PE (1978) Alloxan uptake by isolated rat islets of Langerhans. Endocrinology 102: 1847-1855.
42. Gorus FK, Malaisse WJ, Pipeleers DG (1982) Selective uptake of alloxan by pancreatic B-cells. Biochem J 208: 513-515.
43. Lenzen S (2008) The mechanisms of alloxan- and streptozotocin-induced diabetes. Diabetologia 51: 216-226.
44. Hervey GR (1959) The effects of lesions in the hypothalamus in parabiotic rats. J Physiol 145: 336-352.
45. Olney JW (1969) Brain lesions, obesity, and other disturbances in mice treated with monosodium glutamate. Science 164: 719-721.
46. Holzwarth-McBride MA, Hurst EM, Knigge KM (1976) Monosodium glutamate induced lesions of the arcuate nucleus. I. Endocrine deficiency and ultrastructure of the median eminence. Anat Rec 186: 185-205.

47. Abraham R, Dougherty W, Golberg L, Coulston F (1971) The response of the hypothalamus to high doses of monosodium glutamate in mice and monkeys. Cytochemistry and ultrastructural study of lysosomal changes. Exp Mol Pathol 15: 43-60.
48. Simpson KA, Martin NM, Bloom SR (2009) Hypothalamic regulation of food intake and clinical therapeutic applications. Arq Bras Endocrinol Metabol 53: 120-128.
49. Stephens TW, Basinski M, Bristow PK, Bue-Valleskey JM, Burgett SG, Craft L, Hale J, Hoffmann J, Hsiung HM, Kriauciunas A (1995) The role of neuropeptide Y in the antiobesity action of the obese gene product. Nature 377: 530-532.
50. Kalra SP, Dube MG, Pu S, Xu B, Horvath TL, Kalra PS (1999) Interacting appetite-regulating pathways in the hypothalamic regulation of body weight. Endocr Rev 20: 68-100.
51. Elmquist JK, Elias CF, Saper CB (1999) From lesions to leptin: hypothalamic control of food intake and body weight. Neuron 22: 221-232.
52. Horvath TL, Bechmann I, Naftolin F, Kalra SP, Leranth C (1997) Heterogeneity in the neuropeptide Y-containing neurons of the rat arcuate nucleus: GABAergic and non-GABAergic subpopulations. Brain Res 756 283-286.
53. Cowley MA, Smart JL, Rubinstein M, Cerdán MG, Diano S, Horvath TL, Cone RD, Low MJ (2001) Leptin activates anorexigenic POMC neurons through a neural network in the arcuate nucleus. Nature 411: 480-484.
54. Baskin D, Breininger J, Schwartz M (1999) Leptin receptor mRNA identifies a subpopulation of neuropeptide Y neurons activated by fasting in rat hypothalamus. . Diabetes 48: 828-833.
55. Cheung CC, Clifton DK, Steiner RA (1997) Proopiomelanocortin neurons are direct targets for leptin in the hypothalamus. Endocrinology 138: 4489-4492.
56. Pandit R, de Jong JW, Vanderschuren LJ, Adan RA (2011) Neurobiology of overeating and obesity: the role of melanocortins and beyond. Eur J Pharmacol 660: 28-42.
57. Hetherington AW, Ranson SW (1942a) Effect of early hypophysectomy on hypothalamic obesity. . Endocrinology 31: 30-34.
58. King BM (1980) A re-examination of the ventromedial hypothalamic paradox. Neurosci Biobehav Rev 4: 151-160.
59. Sakaguchi T, Arase K, Bray GA (1988) Sympathetic activity and food intake of rats with ventromedial hypothalamic lesions. Int J Obes 12: 285-291.
60. Magrani J, de Castro e Silva E, Varjao B, Duarte G, Ramos AC, Athanazio R, Barbetta M, Luz P, Fregoneze JB (2004) Histaminergic H1 and H2 receptors located within the ventromedial hypothalamus regulate food and water intake in rats. Pharmacol Biochem Behav 79: 189-198.
61. Hikiji K, Inoue K, Iwasaki S, Ichihara K, Kiriike N (2004) Local perfusion of mCPP into ventromedial hypothalamic nucleus, but not into lateral hypothalamic area and frontal cortex, inhibits food intake in rats. Psychopharmacology (Berl) 174: 190-196.
62. Ohata H, Suzuki K, Oki Y, Shibasaki T (2000) Urocortin in the ventromedial hypothalamic nucleus acts as an inhibitor of feeding behavior in rats. Brain Res 861: 1-7.
63. Kelly J, Alheid GF, Newberg A, Grossman SP (1977) GABA stimulation and blockade in the hypothalamus and midbrain: effects on feeding and locomotor activity. Pharmacol Biochem Behav 7: 537-541.
64. Blevins JE, Stanley BG, Reidelberger RD (2000) Brain regions where cholecystokinin suppresses feeding in rats. Brain Res 860: 1-10.
65. Masaki T, Yoshimichi G, Chiba S, Yasuda T, Noguchi H, Kakuma T, Sakata T, Yoshimatsu H (2003) Corticotropin-releasing hormone-mediated pathway of leptin to regulate feeding, adiposity, and uncoupling protein expression in mice. Endocrinology 144: 3547-3554.
66. Strubbe JH, Mein CG (1977) Increased feeding in response to bilateral injection of insulin antibodies in the VMH. Physiol Behav 19: 309-313.

67. Kong WM, Martin NM, Smith KL, Gardiner JV, Connoley IP, Stephens DA, Dhillo WS, Ghatei MA, Small CJ, Bloom SR (2004) Triiodothyronine stimulates food intake via the hypothalamic ventromedial nucleus independent of changes in energy expenditure. Endocrinology 145: 5252-5258.
68. Shimazu T, Noma M, Saito M (1986) Chronic infusion of norepinephrine into the ventromedial hypothalamus induces obesity in rats. Brain Res 369: 215-233.
69. Bouali SM, Fournier A, St-Pierre S, Jolicoeur FB (1995) Effects of NPY and NPY2-36 on body temperature and food intake following administration into hypothalamic nuclei. Brain Res Bull 36: 131-135.
70. Jolicoeur FB, Bouali SM, Fournier A, St-Pierre S (1995) Mapping of hypothalamic sites involved in the effects of NPY on body temperature and food intake. Brain Res Bull 36: 125-129.
71. Fahrbach SE, Morrell JI, Pfaff DW (1989) Studies of ventromedial hypothalamic afferents in the rat using three methods of HRP application. Exp Brain Res 77: 221-233.
72. Saper CB, Swanson LW, Cowan WM (1979) An autoradiographic study of the efferent connections of the lateral hypothalamic area in the rat. J Comp Neurol 183: 689-706.
73. Ter Horst GJ, Luiten PG (1987) Phaseolus vulgaris leuco-agglutinin tracing of intrahypothalamic connections of the lateral, ventromedial, dorsomedial and paraventricular hypothalamic nuclei in the rat. Brain Res Bull 18: 191-203.
74. Canteras NS, Simerly RB, Swanson LW (1994) Organization of projections from the ventromedial nucleus of the hypothalamus: a Phaseolus vulgaris-leucoagglutinin study in the rat. J Comp Neurol 348: 41-79.
75. Xu B, Goulding EH, Zang K, Cepoi D, Cone RD, Jones KR, Tecott LH, Reichardt LF (2003) Brain-derived neurotrophic factor regulates energy balance downstream of melanocortin-4 receptor. Nat Neurosci 6: 736-742.
76. Bagnol D, Lu XY, Kaelin CB, Day HE, Ollmann M, Gantz I, Akil H, Barsh GS, Watson SJ (1999) Anatomy of an endogenous antagonist: relationship between Agouti-related protein and proopiomelanocortin in brain. J Neurosci 19: 1-7.
77. Sternson SM, Shepherd GM, Friedman JM (2005) Topographic mapping of VMH --> arcuate nucleus microcircuits and their reorganization by fasting. Nat Neurosci 8: 1356-1363.
78. Katoh-Semba R, Takeuchi IK, Semba R, Kato K (1997) Distribution of brain-derived neurotrophic factor in rats and its changes with development in the brain. J Neurochem 69: 34-42.
79. Kernie SG, Liebl DJ, Parada LF (2000) BDNF regulates eating behavior and locomotor activity in mice. EMBO J 19: 1290-1300.
80. Beinfeld MC, Palkovits M (1981) Distribution of cholecystokinin (CCK) in the hypothalamus and limbic system of the rat. Neuropeptides 2: 123-129.
81. Bellinger LL, Bernardis LL (2002) The dorsomedial hypothalamic nucleus and its role in ingestive behavior and body weight regulation: lessons learned from lesioning studies. Physiol Behav 76: 431-442.
82. Larsson S (1954) On the hypothalamic organization of the nervous mechanisms regulating food intake. Acta Physiol Scand 32: 7-61.
83. Delgado JM, Anand BK (1953) Increase of food intake induced by electrical stimulation of the lateral hypothalamus. Am J Physiol 172: 162-168.
84. Bernardis LL (1970) Participation of the dorsomedial hypothalamic nucleus in the "feeding center" and water intake circuitry of the weanling rat. J Neurovisc Relat 31: 387-398.
85. Bellinger LL (1987) Ingestive behavior of rats with ibotenic acid lesions of the dorsomedial hypothalamus. Am J Physiol 252: 938-946.
86. Bellinger LL, Bernardis LL (1999) Effect of dorsomedial hypothalamic nuclei knife cuts on ingestive behavior. Am J Physiol 276: R1772-1779.
87. Bellinger LL, Castonguay TW, Bernardis LL (1994) Hormone and somatic changes in rats pair-fed to growth retarded dorsomedial hypothalamic nuclei-lesioned rats. . Brain Res Bull 34: 117-124.

88. Bellinger LL, Bernardis LL, McCusker RH, Campion DR (1985) Plasma hormone levels in growth-retarded rats with dorsomedial hypothalamic lesions. Physiol Behav 34: 783-790.
89. Bellinger LL, Bernardis LL, Mendel VE (1976) Effect of ventromedial and dorsomedial hypothalamic lesions on circadian corticosterone rhythms. Neuroendocrinology 22: 216-222.
90. Bernardis LL, Bellinger LL (1976) Production of weanling rat ventromedial and dorsomedial hypothalamic syndromes by electrolytic lesions with platinum–iridium electrodes. Neuroendocrinology 22: 97-106.
91. Ivy AC, Kloster G, Drewyer GE, Leuth MC (1930) The preparation of a secretin concentrate. Am J Physiol 95: 35-39.
92. Lee SY, Soltesz I (2011) Cholecystokinin: a multi-functional molecular switch of neuronal circuits. Dev Neurobiol 71: 83-91.
93. Matzinger D, Degen L, Drewe J, Meuli J, Duebendorfer R, Ruckstuhl ND, Amato M, Rovati L, Beglinger C (2000) The role of long chain fatty acids in regulating food intake and cholecystokinin release in humans. . Gut 46: 688-693.
94. Raybould HE, Glatzle J, Freeman SL, Whited K, Darcel N, Liou A, Bohan D (2006) Detection of macronutrients in the intestinal wall. Auton Neurosci 30: 28-33.
95. Crawley JN (1985) Comparative distribution of cholecystokinin and other neuropeptides. Why is this peptide different from all other peptides? . Ann N Y Acad Sci 448: 1-8.
96. Beinfeld MC, Meyer DK, Eskay RL, Jensen RT, Brownstein MJ (1981) The distribution of cholecystokinin immunoreactivity in the central nervous system of the rat as determined by radioimmunoassay. Brain Res 212: 51-57.
97. Robberecht P, Deschodt-Lanckman M, Vanderhaeghen JJ (1978) Demonstration of biological activity of brain gastrin-like peptidic material in the human: its relationship with the COOH-terminal octapeptide of cholecystokinin. Proc Natl Acad Sci U S A 75: 524-528.
98. Innis RB, Corr ê FM, Uhl GR, Schneider B, Snyder SH (1979) Cholecystokinin octapeptide-like immunoreactivity: histochemical localization in rat brain. Proc Natl Acad Sci U S A 1979 Jan;76(1):521-5 76: 521-525.
99. Day NC, Hall MD, Clark CR, Hughes J (1986) High concentration of cholecystokinin receptor binding sites in the ventromedial hypothalamic nucleus. . Neuropeptides 8: 1-18.
100. Hill DR, Shaw TM, Graham W, Woodruff GN (1990) Autoradiographical detection of cholecystokinin-A receptors in primate brain using 125I-Bolton Hunter CCK-8 and 3H-MK-329. J Neurosci 10: 1070-1081.
101. Smith GP, Jerome C, Cushin BJ, Eterno R, Simansky KJ (1981) Abdominal vagotomy blocks the satiety effect of cholecystokinin in the rat. Science 213: 1036-1037.
102. Bittencourt JC (2011) Anatomical organization of the melanin-concentrating hormone peptide family in the mammalian brain. Gen Comp Endocrinol 172: 185-197.
103. Saper CB, Swanson LW, Cowan WM (1979) An autoradiographic study of the efferent connections of the lateral hypothalamic area in the rat. J Comp Neurol 183: :689-706.
104. Peyron C, Tighe DK, van den Pol AN, de Lecea L, Heller HC, Sutcliffe JG, Kilduff TS (1998) Neurons containing hypocretin (orexin) project to multiple neuronal systems. J Neurosci 18: 9996-10015.
105. Sawchenko PE, Swanson LW (1983) The organization of forebrain afferents to the paraventricular and supraoptic nuclei of the rat. J Comp Neurol 218: 121-144.
106. Stanley BG, Chin AS, Leibowitz SF (1985) Feeding and drinking elicited by central injection of neuropeptide Y: evidence for a hypothalamic site(s) of action. Brain Res Bull 14: 521-524.
107. Kim MS, Rossi M, Abusnana S, Sunter D, Morgan DG, Small CJ, Edwards CM, Heath MM, Stanley SA, Seal LJ, Bhatti JR, Smith DM, Ghatei MA, Bloom SR (2000) Hypothalamic localization of the feeding effect of agouti-related peptide and alpha-melanocyte-stimulating hormone. Diabetes 49: 177-182.
108. Coppola JD, Horwitz BA, Hamilton J, Blevins JE, McDonald RB (2005) Reduced feeding response to muscimol and neuropeptide Y in senescent F344 rats. Am J Physiol Regul Integr Comp Physiol 288: R1492-1498.

109. Kyrkouli SE, Stanley BG, Leibowitz SF (1986) Galanin: Stimulation o f feeding induced by medial hypothalamic injection o f this novel peptide. Eur J Pharmacol 122: 159-160.
110. Kyrkouli SE, Stanley BG, Seirafi RD, Leibowitz SF (1990) Stimulation of feeding by galanin: anatomical localization and behavioral specificity of this peptide's effects in the brain. Peptides 11: 995-1001.
111. Dube MG, Kalra SP, Kalra PS (1999) Food intake elicited by central administration of orexins/hypocretins: identification of hypothalamic sites of action. Brain Res 842: 473-477.
112. Fedeli A, Braconi S, Economidou D, Cannella N, Kallupi M, Guerrini R, Calò G, Cifani C, Massi M, Ciccocioppo R (2009) The paraventricular nucleus of the hypothalamus is a neuroanatomical substrate for the inhibition of palatable food intake by neuropeptide S. Eur J Neurosci 30: 1594-1602.
113. Bishop C, Parker GC, Coscina DV (2002) Nicotine and its withdrawal alter feeding induced by paraventricular hypothalamic injections of neuropeptide Y in Sprague-Dawley rats. Psychopharmacology 162: 265-272.
114. Kamdi SP, Nakhate KT, Dandekar MP, Kokare DM, Subhedar NK (2009) Participation of corticotropin-releasing factor type 2 receptors in the acute, chronic and withdrawal actions of nicotine associated with feeding behavior in rats. Appetite 53: 354-362.
115. Pelleymounter MA, Joppa M, Carmouche M, Cullen MJ, Brown B, Murphy B, Grigoriadis DE, Ling N, Foster AC (2000) Role of corticotropin-releasing factor (CRF) receptors in the anorexic syndrome induced by CRF. J Pharmacol Exp Ther 293: 799-806.
116. Swanson LW, Sawchenko PE (1983) Hypothalamic integration: organization of the paraventricular and supraoptic nuclei. Annu Rev Neurosci 6: 269-324.
117. Brownstein MJ, Russell JT, Gainer H (1980) Synthesis, transport, and release of posterior pituitary hormones. Science 207: 373-378.
118. Lechan RM, Jackson IM (1982) Immunohistochemical localization of thyrotropin-releasing hormone in the rat hypothalamus and pituitary. Endocrinology 111: 55-65.
119. Shibusawa N, Hashimoto K, Yamada M (2008) Thyrotropin-releasing hormone (TRH) in the cerebellum. Cerebellum 7: 84-95.
120. Swanson LW, Sawchenko PE, Rivier J, Vale WW (1983) Organization of ovine corticotropin-releasing factor immunoreactive cells and fibers in the rat brain: an immunohistochemical study. Neuroendocrinology 36: 165-186.
121. Ludwig M (1998) Dendritic release of vasopressin and oxytocin. J Neuroendocrinol 10: 881-895.
122. Sabatier N, Caquineau C, Douglas AJ, Leng G (2003) Oxytocin released from magnocellular dendrites: a potential modulator of alpha-melanocyte-stimulating hormone behavioral actions? Ann N Y Acad Sci 994: 218-224.
123. Swanson LW, Sawchenko PE (1983a) Hypothalamic integration: organization of the paraventricular and supraoptic nuclei. Annu Rev Neurosci 6: 269-324.
124. Ishikawa K, Taniguchi Y, Inoue K, Kurosumi K, Suzuki M (1988) Immunocytochemical delineation of thyrotrophic area: origin of thyrotropin-releasing hormone in the median eminence. Neuroendocrinology 47: 384-388.
125. Reichardt LF (2006) Neurotrophin-regulated signalling pathways. Philos Trans R Soc Lond B Biol Sci 361: 1545-1564.
126. Cohen S (1960) Purification of a nerve-growth promoting protein from the mouse salivary gland and its neuro-cytotoxic antiserum. Proc Natl Acad Sci U S A 46: 302–311.
127. Barde YA, Edgar D, Thoenen H (1982) Purification of a new neurotrophic factor from mammalian brain. EMBO J 1: 549-553.
128. Hohn A, Leibrock J, Bailey K, Barde YA (1990) Identification and characterization of a novel member of the nerve growth factor/brain-derived neurotrophic factor family. Nature 344: 339-341.
129. Hallböök F, Ibáñez CF, Persson H (1991) Evolutionary studies of the nerve growth factor family reveal a novel member abundantly expressed in Xenopus ovary. Neuron 6: 845-858.

130. Gärtner A, Shostak Y, Hackel N, Ethell IM, Thoenen H (2000) Ultrastructural identification of storage compartments and localization of activity-dependent secretion of neurotrophin 6 in hippocampal neurons. Mol Cell Neurosci 15: 215-234.
131. Lai KO, Fu WY, Ip FC, Ip NY (1998) Cloning and expression of a novel neurotrophin, NT-7, from carp. Mol Cell Neurosci 11: 64-76.
132. Nilsson AS, Fainzilber M, Falck P, Ibáñez CF (1998) Neurotrophin-7: a novel member of the neurotrophin family from the zebrafish. FEBS Lett 424: 285-290.
133. Leibrock J, Lottspeich F, Hohn A, Hofer M, Hengerer B, Masiakowski P, Thoenen H, Barde YA (1989) Molecular cloning and expression of brain-derived neurotrophic factor. Nature 341: 149-152.
134. Rosas-Vargas H, Martínez-Ezquerro JD, Bienvenu T (2011) Brain-derived Neurotrophic Factor, Food Intake Regulation, and Obesity. Arch Med Res 42: 482-494.
135. Davies AM, Thoenen H, Barde YA (1986) Different factors from the central nervous system and periphery regulate the survival of sensory neurones. Nature 319: 497-499.
136. Hofer MM, Barde YA (1988) Brain-derived neurotrophic factor prevents neuronal death *in vivo*. Nature 331: 261-262.
137. Jones KR, Reichardt LF (1990) Molecular cloning of a human gene that is a member of the nerve growth factor family. Proc Natl Acad Sci U S A 87: 8060-8064.
138. Timmusk T, Belluardo N, Metsis M, Persson H (1993) Widespread and developmentally regulated expression of neurotrophin-4 mRNA in rat brain and peripheral tissues. Eur J Neurosci 5: 605-613.
139. Rodriguez-Tébar A, Barde YA (1988) Binding characteristics of brain-derived neurotrophic factor to its receptors on neurons from the chick embryo. J Neurosci 8: 3337-3342.
140. Patapoutian A, Reichardt LF (2001) Trk receptors: mediators of neurotrophin action. Curr Opin Neurobiol 11: 272-280.
141. Chao MV (2003) Neurotrophins and their receptors: a convergence point for many signalling pathways. Nat Rev Neurosci 4: 299-309.
142. Chao MV, Hempstead BL (1995) p75 and Trk: a two-receptor system. Trends Neurosci 18: 321-326.
143. Smith CA, Farrah T, Goodwin RG (1994) The TNF receptor superfamily of cellular and viral proteins: activation, costimulation, and death. Cell 76: 959-962.
144. Rodríguez-Tébar A, Dechant G, Götz R, Barde YA (1992) Binding of neurotrophin-3 to its neuronal receptors and interactions with nerve growth factor and brain-derived neurotrophic factor. EMBO J 11: 917-922.
145. Rodriguez-Tebar A, Dechant G, Barde YA (1990) Binding of brain-derived neurotrophic factor to the nerve growth factor receptor. Neuron 4: 487-492.
146. Bibel M, Hoppe E, Barde YA (1999) Biochemical and functional interactions between the neurotrophin receptors trk and p75NTR. EMBO J 18: 616-622.
147. Hempstead BL (2002) The many faces of p75NTR. Curr Opin Neurobiol 12: 260-267.
148. Roux PP, Barker PA (2002) Neurotrophin signaling through the p75 neurotrophin receptor. Prog Neurobiol 67: 203-233.
149. Liepinsh E, Llag LL, Otting G, Ibáñez CF (1997) NMR structure of the death domain of the p75 neurotrophin receptor. EMBO J 16: 4999-5005.
150. Casaccia-Bonnefil P, Kong H, Chao MV (1998) Neurotrophins: the biological paradox of survival factors eliciting apoptosis. Cell Death Differ 5: 357-364.
151. Dobrowsky RT, Werner MH, Castellino AM, Chao MV, Hannun YA (1994) Activation of the sphingomyelin cycle through the low-affinity neurotrophin receptor. Science 265: 1596-1599.
152. Dobrowsky RT, Jenkins GM, Hannun YA (1995) Neurotrophins induce sphingomyelin hydrolysis. Modulation by co-expression of p75NTR with Trk receptors. J Biol Chem 270: 22135-22142.

153. Dobrowsky RT, Carter BD (2000) p75 neurotrophin receptor signaling: mechanisms for neurotrophic modulation of cell stress? J Neurosci Res 61: 237-243.

154. Lee FS, Kim AH, Khursigara G, Chao MV (2001) The uniqueness of being a neurotrophin receptor. Curr Opin Neurobiol 11: 281-286.

155. Nawa H, Carnahan J, Gall C (1995) BDNF protein measured by a novel enzyme immunoassay in normal brain and after seizure: partial disagreement with mRNA levels. Eur J Neurosci 7: 1527-1535.

156. Lapchak PA, Hefti F (1992) BDNF and NGF treatment in lesioned rats: effects on cholinergic function and weight gain. Neuroreport 3: 405-408.

157. Williams LR (1991) Hypophagia is induced by intracerebroventricular administration of nerve growth factor. Exp Neurol 113: 31-37.

158. Plata-Salamán CR (1988) Food intake suppression by growth factors and platelet peptides by direct action in the central nervous system. Neurosci Lett 94: 161-166.

159. Bariohay B, Lebrun B, Moyse E, Jean A (2005) Brain-derived neurotrophic factor plays a role as an anorexigenic factor in the dorsal vagal complex. Endocrinology 146: 5612-5620.

160. Wang CB, E; Levine, A; Billington, C; Kotz, CM (2007a) Brain-derived neurotrophic factor in the ventromedial nucleus of the hypothalamus reduces energy intake. Am J Physiol Regul Integr Comp Physiol 293: R1037-1045.

161. Wang C, Bomberg E, Billington C, Levine A, Kotz CM (2007b) Brain-derived neurotrophic factor in the hypothalamic paraventricular nucleus increases energy expenditure by elevating metabolic rate. Am J Physiol Regul Integr Comp Physiol 293: R992-1002.

162. Pelleymounter MA, Cullen MJ, Wellman CL (1995) Characteristics of BDNF-induced weight loss. Exp Neurol 131: 229-238.

163. Nakazato M, Hashimoto K, Shimizu E, Kumakiri C, Koizumi H, Okamura N, Mitsumori M, Komatsu N, Iyo M (2003) Decreased levels of serum brain-derived neurotrophic factor in female patients with eating disorders. Biol Psychiatry 54: 485-490.

164. Jones KR, Fariñas I, Backus C, Reichardt LF (1994) Targeted disruption of the BDNF gene perturbs brain and sensory neuron development but not motor neuron development. Cell 76: 989-999.

165. Gray J, Yeo GS, Cox JJ, Morton J, Adlam AL, Keogh JM, Yanovski JA, El Gharbawy A, Han JC, Tung YC, Hodges JR, Raymond FL, O'rahilly S, Farooqi IS (2006) Hyperphagia, severe obesity, impaired cognitive function, and hyperactivity associated with functional loss of one copy of the brain-derived neurotrophic factor (BDNF) gene. Diabetes 55: 3366-3371.

166. Unger TJ, Calderon GA, Bradley LC, Sena-Esteves M, Rios M (2007) Selective deletion of Bdnf in the ventromedial and dorsomedial hypothalamus of adult mice results in hyperphagic behavior and obesity. J Neurosci 27: 14265-14274.

167. Rizk NM, Joost HG, Eckel J (2001) Increased hypothalamic expression of the p75 tumor necrosis factor receptor in New Zealand obese mice. Horm Metab Res 33: 520-524.

168. Schreyer SA, Chua SC, LeBoeuf RC (1998) Obesity and diabetes in TNF-alpha receptor- deficient mice. J Clin Invest 102: 402-411.

169. Catts VS, Al-Menhali N, Burne TH, Colditz MJ, Coulson EJ (2008) The p75 neurotrophin receptor regulates hippocampal neurogenesis and related behaviours. Eur J Neurosci 28: 883-892.

170. Uysal KT, Wiesbrock SM, Hotamisligil GS (1998) Functional analysis of tumor necrosis factor (TNF) receptors in TNF-alpha-mediated insulin resistance in genetic obesity. Endocrinology 139: 4832-4838.

171. Mercer JG, Hoggard N, Williams LM, Lawrence CB, Hannah LT, Trayhurn P (1996) Localization of leptin receptor mRNA and the long form splice variant (Ob-Rb) in mouse hypothalamus and adjacent brain regions by in situ hybridization. FEBS Lett 387: 113-116.

172. Storlien LH, Bellingham WP, Martin GM (1975) Localization of CNS glucoregulatory insulin receptors within the ventromedial hypothalamus. Brain Res 96: 156-160.
173. Trivedi P, Yu H, MacNeil DJ, Van der Ploeg LH, Guan XM (1998) Distribution of orexin receptor mRNA in the rat brain. FEBS Lett 438: 71-75.
174. Kokkotou EG, Tritos NA, Mastaitis JW, Slieker L, Maratos-Flier E (2001) Melanin-concentrating hormone receptor is a target of leptin action in the mouse brain. Endocrinology 142: 680-686.
175. Komori T, Morikawa Y, Nanjo K, Senba E (2006) Induction of brain-derived neurotrophic factor by leptin in the ventromedial hypothalamus. Neuroscience 139: 1107-1115.
176. Xu AW, Kaelin CB, Takeda K, Akira S, Schwartz MW, Barsh GS (2005) PI3K integrates the action of insulin and leptin on hypothalamic neurons. J Clin Invest 115: 951-958.
177. Nakagawa T, Ogawa Y, Ebihara K, Yamanaka M, Tsuchida A, Taiji M, Noguchi H, Nakao K (2003) Antiobesity and antidiabetic effects of brain-derived neurotrophic factor in rodent models of leptin resistance. Int J Obes Relat Metab Disord 27: 557-565.
178. Toriya M, Maekawa F, Maejima Y, Onaka T, Fujiwara K, Nakagawa T, Nakata M, Yada T (2010) Long-term infusion of brain-derived neurotrophic factor reduces food intake and body weight via a corticotrophin-releasing hormone pathway in the paraventricular nucleus of the hypothalamus. J Neuroendocrinol 22: 987-995.
179. Pruunsild P, Kazantseva A, Aid T, Palm K, Timmusk T (2007) Dissecting the human BDNF locus: bidirectional transcription, complex splicing, and multiple promoters. Genomics 90: 397-406.
180. Timmusk T, Palm K, Metsis M, Reintam T, Paalme V, Saarma M, Persson H (1993) Multiple promoters direct tissue-specific expression of the rat BDNF gene. Neuron 10: 475-489.
181. Goodman LJ, Valverde J, Lim F, Geschwind MD, Federoff HJ, Geller AI, Hefti F (1996) Regulated release and polarized localization of brain-derived neurotrophic factor in hippocampal neurons. Mol Cell Neurosci 7: 222-238.
182. Aid T, Kazantseva A, Piirsoo M, Palm K, Timmusk T (2007) Mouse and rat BDNF gene structure and expression revisited. J Neurosci Res 85: 525-535.
183. Yossifoff M, Kisliouk T, Meiri N (2008) Dynamic changes in DNA methylation during thermal control establishment affect CREB binding to the brain-derived neurotrophic factor promoter. Eur J Neurosci 28: 2267-2277.
184. Yu Y, Zhang H, Byerly MS, Bacon LD, Porter TE, Liu GE, Song J (2009) Multiple promoters direct tissue-specific expression of the rat BDNF gene. Brain Res 1269: 1-10.
185. Bird A (2007) Perceptions of epigenetics. Nature 447: 396-398.
186. Annunziato AT (2008) DNA Packaging: Nucleosomes and Chromatin. Nature Education.
187. Luger K, Mäder AW, Richmond RK, Sargent DF, Richmond TJ (1997) Crystal structure of the nucleosome core particle at 2.8 A resolution. Nature 389: 251-260.
188. Davey CA, Sargent DF, Luger K, Maeder AW, Richmond TJ (2002) Solvent mediated interactions in the structure of the nucleosome core particle at 1.9 Å resolution. J Mol Biol 319: 1097-1113.
189. Richmond TJ, Finch JT, Rushton B, Rhodes D, Klug A (1984) Structure of the nucleosome core particle at 7 A resolution. Nature 311: 532-537.
190. Arents G, Burlingame RW, Wang BC, Love WE, Moudrianakis EN (1991) The nucleosomal core histone octamer at 3.1 Å resolution: a tripartite protein assembly and a left-handed superhelix. Proc Natl Acad Sci USA 88: 10148-10152.
191. Zlatanova J, Bishop TC, Victor JM, Jackson V, van Holde K (2009) The nucleosome family: dynamic and growing. Structure 17: 160-171.
192. Kaplan N, Moore IK, Fondufe-Mittendorf Y, Gossett AJ, Tillo D, Field Y, LeProust EM, Hughes TR, Lieb JD, Widom J, Segal E (2009) The DNA-encoded nucleosome organization of a eukaryotic genome. Nature 458: 362-366.
193. Grunstein M (1997) Histone acetylation in chromatin structure and transcription. Nature 389: 349-352.

194. Lorch Y, LaPointe JW, Kornberg RD (1987) Nucleosomes inhibit the initiation of transcription but allow chain elongation with the displacement of histones. Cell 49: 203-210.
195. Han M, Grunstein M (1988) Nucleosome loss activates yeast downstream promoters in vivo. Cell 55: 1137-1145.
196. Andrews AJ, Luger K (2011) Nucleosome structure(s) and stability: variations on a theme. Annu Rev Biophys 40: 99-117.
197. Ausio J, Dong F, van Holde KE (1989) Use of selectively trypsinized nucleosome core particles to analyze the role of the histone "tails" in the stabilization of the nucleosome. J Mol Biol 206: 451-463.
198. Kurdistani SK, Grunstein M (2003) Histone acetylation and deacetylation in yeast. Nat Rev Mol Cell Biol 4: 276-284.
199. Kuo MH, Allis CD (1998) Roles of histone acetyltransferases and deacetylases in gene regulation. Bioessays 20: 615-626.
200. Bernstein E, Allis CD (2005) RNA meets chromatin. Genes Dev 19: 1635-1655.
201. Garcia BA, Hake SB, Diaz RL, Kauer M, Morris SA, Recht J, Shabanowitz J, Mishra N, Strahl BD, Allis CD, Hunt DF (2007) Organismal differences in post-translational modifications in histones H3 and H4. J Biol Chem 282: 7641-7655.
202. Mosammaparast N, Shi Y (2010) Reversal of histone methylation: biochemical and molecular mechanisms of histone demethylases. Annu Rev Biochem 79: 155-179.
203. Allfrey VG, Faulkner RM, Mirsky AE (1964) Acetylation and methylation of histones and their possible role in the regulation of RNA synthesis. Proc Natl Acad Sci U S A 51: 786-794.
204. Strahl BD, Allis CD (2000) The language of covalent histone modifications. Nature 403: 41-45.
205. Martin C, Zhang Y (2005) The diverse functions of histone lysine methylation. Nat Rev Mol Cell Biol 6: 838-849.
206. Lai AY, Wade PA (2011) Cancer biology and NuRD: a multifaceted chromatin remodelling complex. Nat Rev Cancer 11: 588-596.
207. Byvoet P, Shepherd GR, Hardin JM, Noland BJ (1972) The distribution and turnover of labeled methyl groups in histone fractions of cultured mammalian cells. Arch Biochem Biophys 148: 558-567.
208. Santos-Rosa H, Schneider R, Bannister AJ, Sherriff J, Bernstein BE, Emre NC, Schreiber SL, Mellor J, Kouzarides T (2002) Active genes are tri-methylated at K4 of histone H3. Nature 419: 407-411.
209. Wang H, An W, Cao R, Xia L, Erdjument-Bromage H, Chatton B, Tempst P, Roeder RG, Zhang Y (2003) mAM facilitates conversion by ESET of dimethyl to trimethyl lysine 9 of histone H3 to cause transcriptional repression. Mol Cell 12: 475-487.
210. Wu SC, Zhang Y (2009) Minireview: role of protein methylation and demethylation in nuclear hormone signaling. Mol Endocrinol 23: 1323-1334.
211. Black JC, Whetstine JR (2011) Chromatin landscape: methylation beyond transcription. Epigenetics 6: 9-15.
212. Feng Q, Wang H, Ng HH, Erdjument-Bromage H, Tempst P, Struhl K, Zhang Y (2002) Methylation of H3-lysine 79 is mediated by a new family of HMTases without a SET domain. Curr Biol 12: 1052-1058.
213. Margueron R, Reinberg D (2011) The Polycomb complex PRC2 and its mark in life. Nature 469: 343-349.
214. Barski A, Cuddapah S, Cui K, Roh TY, Schones DE, Wang Z, Wei G, Chepelev I, Zhao K (2007) High-resolution profiling of histone methylations in the human genome. Cell 129: **823-837**.
215. Sarma K, Margueron R, Ivanov A, Pirrotta V, Reinberg D (2008) Ezh2 requires PHF1 to efficiently catalyze H3 lysine 27 trimethylation in vivo. Mol Cell Biol 28: 2718-2731.
216. Peters AH, Kubicek S, Mechtler K, O'Sullivan RJ, Derijck AA, Perez-Burgos L, Kohlmaier A, Opravil S, Tachibana M, Shinkai Y, Martens JH, Jenuwein T (2003) Partitioning and plasticity of repressive histone methylation states in mammalian chromatin. Mol Cell 12: 1577-1589.

217. Jacob Y, Feng S, LeBlanc CA, Bernatavichute YV, Stroud H, Cokus S, Johnson LM, Pellegrini M, Jacobsen SE, Michaels SD (2009) ATXR5 and ATXR6 are H3K27 monomethyltransferases required for chromatin structure and gene silencing. Nat Struct Mol Biol 16: 763-768.

218. Shen X, Liu Y, Hsu YJ, Fujiwara Y, Kim J, Mao X, Yuan GC, Orkin SH (2008) EZH1 mediates methylation on histone H3 lysine 27 and complements EZH2 in maintaining stem cell identity and executing pluripotency. Mol Cell 32: 491-502.

219. Montgomery ND, Yee D, Chen A, Kalantry S, Chamberlain SJ, Otte AP, Magnuson T (2005) The murine polycomb group protein Eed is required for global histone H3 lysine-27 methylation. Curr Biol 15: 942-947.

220. Vakoc CR, Sachdeva MM, Wang H, Blobel GA (2006) Profile of histone lysine methylation across transcribed mammalian chromatin. Mol Cell Biol 26: 9185-9195.

221. Jeddeloh JA, Stokes TL, Richards EJ (1999) Maintenance of genomic methylation requires a SWI2/SNF2-like protein. Nat Genet 22: 94-97.

222. Fransz P, ten Hoopen R, Tessadori F (2006) Composition and formation of heterochromatin in Arabidopsis thaliana. Chromosome Res 14: 71-82.

223. Naumann K, Fischer A, Hofmann I, Krauss V, Phalke S, Irmler K, Hause G, Aurich AC, Dorn R, Jenuwein T, Reuter G (2005) Pivotal role of AtSUVH2 in heterochromatic histone methylation and gene silencing in Arabidopsis. EMBO J 24: 1418-1429.

224. Shilatifard A (2006) Chromatin modifications by methylation and ubiquitination: implications in the regulation of gene expression. Annu Rev Biochem 75: 243-269.

225. Lu F, Cui X, Zhang S, Jenuwein T, Cao X (2011) Arabidopsis REF6 is a histone H3 lysine 27 demethylase. Nat Genet 43: 715-719.

226. Stepanik VA, Harte PJ (2012) A mutation in the E(Z) methyltransferase that increases trimethylation of histone H3 lysine 27 and causes inappropriate silencing of active Polycomb target genes. Dev Biol 364: 249-258.

227. Strahl BD, Ohba R, Cook RG, Allis CD (1999) Methylation of histone H3 at lysine 4 is highly conserved and correlates with transcriptionally active nuclei in Tetrahymena. Proc Natl Acad Sci U S A 96: 14967-14972.

228. Schneider R, Bannister AJ, Myers FA, Thorne AW, Crane-Robinson C, Kouzarides T (2004) Histone H3 lysine 4 methylation patterns in higher eukaryotic genes. Nat Cell Biol 6: 73-77.

229. Liang G, Lin JC, Wei V, Yoo C, Cheng JC, Nguyen CT, Weisenberger DJ, Egger G, Takai D, Gonzales FA, Jones PA (2004) Distinct localization of histone H3 acetylation and H3-K4 methylation to the transcription start sites in the human genome. Proc Natl Acad Sci U S A 101: 7357-7362.

230. Rice JC, Briggs SD, Ueberheide B, Barber CM, Shabanowitz J, Hunt DF, Shinkai Y, Allis CD (2003) Histone methyltransferases direct different degrees of methylation to define distinct chromatin domains. Mol Cell 12: 1591-1598.

231. Barski A, Pregizer S, Frenkel B (2008) Identification of transcription factor target genes by ChIP display. Methods Mol Biol 455: 177-190.

232. Heintzman ND, Hon GC, Hawkins RD, Kheradpour P, Stark A, Harp LF, Ye Z, Lee LK, Stuart RK, Ching CW, Ching KA, Antosiewicz-Bourget JE, Liu H, Zhang X, Green RD, Lobanenkov VV, Stewart R, Thomson JA, Crawford GE, Kellis M, Ren B (2009) Histone modifications at human enhancers reflect global cell-type-specific gene expression. Nature 459: 108-112.

233. Schotta G, Lachner M, Sarma K, Ebert A, Sengupta R, Reuter G, Reinberg D, Jenuwein T (2004) A silencing pathway to induce H3-K9 and H4-K20 trimethylation at constitutive heterochromatin. Genes Dev 18: 1251-1262.

234. Plath K, Fang J, Mlynarczyk-Evans SK, Cao R, Worringer KA, Wang H, de la Cruz CC, Otte AP, Panning B, Zhang Y (2003) Role of histone H3 lysine 27 methylation in X inactivation. Science 300: 131-135.

235. Xu L, Zhao Z, Dong A, Soubigou-Taconnat L, Renou JP, Steinmetz A, Shen WH (2008) Di- and tri- but not monomethylation on histone H3 lysine 36 marks active transcription of genes involved in flowering time regulation and other processes in Arabidopsis thaliana. Mol Cell Biol 28: 1348-1360.
236. Guenther MG, Levine SS, Boyer LA, Jaenisch R, Young RA (2007) A chromatin landmark and transcription initiation at most promoters in human cells. Cell 130: 77-88.
237. Tschiersch B, Hofmann A, Krauss V, Dorn R, Korge G, Reuter G (1994) The protein encoded by the Drosophila position-effect variegation suppressor gene Su(var)3-9 combines domains of antagonistic regulators of homeotic gene complexes. EMBO J 13: 3822-3831.
238. Alkema MJ, Bronk M, Verhoeven E, Otte A, van 't Veer LJ, Berns A, van Lohuizen M (1997) Identification of Bmi1-interacting proteins as constituents of a multimeric mammalian polycomb complex. Genes Dev 11: 226-240.
239. Satijn DP, Hamer KM, den Blaauwen J, Otte AP (2001) The polycomb group protein EED interacts with YY1, and both proteins induce neural tissue in Xenopus embryos. Mol Cell Biol 21: 1360-1369.
240. Levine SS, Weiss A, Erdjument-Bromage H, Shao Z, Tempst P, Kingston RE (2002) The core of the polycomb repressive complex is compositionally and functionally conserved in flies and humans. Mol Cell Biol 22: 6070-6078.
241. Saurin AJ, Shao Z, Erdjument-Bromage H, Tempst P, Kingston RE (2001) A Drosophila Polycomb group complex includes Zeste and dTAFII proteins. Nature 412: 655-660.
242. Cao R, Wang L, Wang H, Xia L, Erdjument-Bromage H, Tempst P, Jones RS, Zhang Y (2002) Role of histone H3 lysine 27 methylation in Polycomb-group silencing. Science 298: 1039-1043.
243. Czermin B, Melfi R, McCabe D, Seitz V, Imhof A, V. P (2002) Drosophila Enhancer of Zeste/ESC complexes have a histone H3 methyltransferase activity thatmarks chromosomalPolycomb sites. Cell 111: 185-196.
244. Franke A, DeCamillis M, Zink D, Cheng N, Brock HW, Paro R (1992) Polycomb and polyhomeotic are constituents of a multimeric protein complex in chromatin of Drosophila melanogaster. EMBO J 11: 2941-2950.
245. Schwartz YB, Pirrotta V (2007) Polycomb silencing mechanisms and the management of genomic programmes. Nat Rev Genet 8: 9-22.
246. Jones A, Wang H (2010) Polycomb repressive complex 2 in embryonic stem cells: an overview. Protein Cell 1: 1056-1062.
247. Kuzmichev A, Nishioka K, Erdjument-Bromage H, Tempst P, Reinberg D (2002) Histone methyltransferase activity associated with a human multiprotein complex containing the Enhancer of Zeste protein. Genes Dev 16: 2893-2905.
248. Müller J, Hart CM, Francis NJ, Vargas ML, Sengupta A, Wild B, Miller EL, O'Connor MB, Kingston RE, Simon JA (2002) Histone methyltransferase activity of a Drosophila Polycomb group repressor complex. Cell 111: 197-208.
249. Zee BM, Levin RS, Xu B, LeRoy G, Wingreen NS, Garcia BA (2010) In vivo residue-specific histone methylation dynamics. J Biol Chem 285: 3341-3350.
250. Fujii S, Ito K, Ito Y, Ochiai A (2008) Enhancer of zeste homologue 2 (EZH2) down-regulates RUNX3 by increasing histone H3 methylation. J Biol Chem 283: 17324-17332.
251. Tie F, Furuyama T, Harte PJ (1998) The Drosophila Polycomb-group proteins ESC and E(Z) bind directly to each other and co-localize at multiple chromosomal sites. Development 125: 3483-3496.
252. Yamamoto K, Sonoda M, Inokuchi J, Shirasawa S, Sasazuki T (2004) Polycomb group suppressor of zeste 12 links heterochromatin protein 1alpha and enhancer of zeste 2. J Biol Chem 279: 401-406.
253. Tyler JK, Bulger M, Kamakaka RT, Kobayashi R, Kadonaga JT (1996) The p55 subunit of Drosophila chromatin assembly factor 1 is homologous to a histone deacetylase-associated protein. Mol Cell Biol 16: 6149-6159.
254. Ohno K, McCabe D, Czermin B, Imhof A, Pirrotta V (2008) ESC, ESCL and their roles in Polycomb Group mechanisms. Mech Dev 125: 527-541.

255. Tie F, Stratton CA, Kurzhals RL, Harte PJ (2007) The N terminus of Drosophila ESC binds directly to histone H3 and is required for E(Z)-dependent trimethylation of H3 lysine 27. Mol Cell Biol 27: 2014-2026.
256. Simon J, Bornemann D, Lunde K, Schwartz C (1995) The extra sex combs product contains WD40 repeats and its time of action implies a role distinct from other Polycomb group products. Mech Dev 53: 197-208.
257. Faust C, Schumacher A, Holdener B, Magnuson T (1995) The eed mutation disrupts anterior mesoderm production in mice. Development 121: 273-285.
258. Struhl G, Brower D (1982) Early role of the esc+ gene product in the determination of segments in Drosophila. Cell 31: 285-292.
259. Ketel CS, Andersen EF, Vargas ML, Suh J, Strome S, Simon JA (2005) Subunit contributions to histone methyltransferase activities of fly and worm polycomb group complexes. Mol Cell Biol 25: 6857-6868.
260. Mohrmann L, Verrijzer CP (2005) Composition and functional specificity of SWI2/SNF2 class chromatin remodeling complexes. Biochim Biophys Acta 1681: 59-73.
261. Tie F, Furuyama T, Prasad-Sinha J, Jane E, Harte PJ (2001) The Drosophila Polycomb Group proteins ESC and E(Z) are present in a complex containing the histone-binding protein p55 and the histone deacetylase RPD3. Development 128: 275-286.
262. Van der Vlag J, Otte AP (1999) Transcriptional repression mediated by the human Polycomb-group protein EED involves histone deacetylation. Nat Genet 23: 474-478.
263. Birve A, Sengupta AK, Beuchle D, Larsson J, Kennison JA, Rasmuson-Lestander A, Müller J (2001) Su(z)12, a novel Drosophila Polycomb group gene that is conserved in vertebrates and plants. Development 128: 3371-3379.
264. Chen S, Birve A, Rasmuson-Lestander A (2008) In vivo analysis of Drosophila SU(Z)12 function. Mol Genet Genomics 279: 159-170.
265. Nowak AJ, Alfieri C, Stirnimann CU, Rybin V, Baudin F, Ly-Hartig N, Lindner D, Müller CW (2011) Chromatin-modifying complex component Nurf55/p55 associates with histones H3 and H4 and polycomb repressive complex 2 subunit Su(z)12 through partially overlapping binding sites. J Biol Chem 286: 23388-23396.
266. Verreault A, Kaufman PD, Kobayashi R, Stillman B (1996) Nucleosome assembly by a complex of CAF-1 and acetylated histones H3/H4. Cell 87: 95-104.
267. Verreault A, Kaufman PD, Kobayashi R, Stillman B (1998) Nucleosomal DNA regulates the core-histone-binding subunit of the human Hat1 acetyltransferase. Curr Biol 8: 96-108.
268. Song JJ, Garlick JD, Kingston RE (2008) Structural basis of histone H4 recognition by p55. Genes Dev 22: 1313-1318.
269. Nekrasov M, Wild B, Müller J (2005) Nucleosome binding and histone methyltransferase activity of Drosophila PRC2. EMBO Rep 6: 348-353.
270. Anderson AE, Karandikar UC, Pepple KL, Chen Z, Bergmann A, Mardon G (2011) The enhancer of trithorax and polycomb gene Caf1/p55 is essential for cell survival and patterning in Drosophila development. Development 138: 1957-1966.
271. Wen P, Quan Z, Xi R (2012) The biological function of the WD40 repeat-containing protein p55/Caf1 in drosophila. Dev Dyn 241: 455-464.
272. Vermaak D, Wade PA, Jones PL, Shi YB, Wolffe AP (1999) Functional analysis of the SIN3-histone deacetylase RPD3-RbAp48-histone H4 connection in the Xenopus oocyte. Mol Cell Biol 19: 5847-5860.
273. Brown JL, Mucci D, Whiteley M, Dirksen ML, Kassis JA (1998) The Drosophila Polycomb group gene pleiohomeotic encodes a DNA binding protein with homology to the transcription factor YY1. Mol Cell 1: 1057-1064.
274. Wysocka J, Swigut T, Xiao H, Milne TA, Kwon SY, Landry J, Kauer M, Tackett AJ, Chait BT, Badenhorst P, Wu C, Allis CD (2006) A PHD finger of NURF couples histone H3 lysine 4 trimethylation with chromatin remodelling. Nature 442: 86-90.

275. Rastelli L, Chan CS, Pirrotta V (1993) Related chromosome binding sites for zeste, suppressors of zeste and Polycomb group proteins in Drosophila and their dependence on Enhancer of zeste function. EMBO J 12: 1513-1522.
276. Benson M, Pirrotta V (1988) The Drosophila zeste protein binds cooperatively to sites in many gene regulatory regions: implications for transvection and gene regulation. EMBO J 7: 3907-3915.
277. Schuettengruber B, Cavalli G (2009) Recruitment of polycomb group complexes and their role in the dynamic regulation of cell fate choice. Development 136: 3531-3542.
278. Brownell JE, Allis CD (1996) Special HATs for special occasions: linking histone acetylation to chromatin assembly and gene activation. Curr Opin Genet Dev 6: 176-184.
279. Wolffe AP, Pruss D (1996) Targeting chromatin disruption: Transcription regulators that acetylate histones. Cell 84: 817-819.
280. Hebbes TR, Thorne AW, Crane-Robinson C (1988) A direct link between core histone acetylation and transcriptionally active chromatin. EMBO J 7: 1395-1402.
281. Durrin LK, Mann RK, Kayne PS, Grunstein M (1991) Yeast histone H4 N-terminal sequence is required for promoter activation in vivo. Cell 65: 1023-1031.
282. Pokholok DK, Harbison CT, Levine S, Cole M, Hannett NM, Lee TI, Bell GW, Walker K, Rolfe PA, Herbolsheimer E, Zeitlinger J, Lewitter F, Gifford DK, Young RA (2005) Genome-wide map of nucleosome acetylation and methylation in yeast. Cell 122: 517-527.
283. Suka N, Suka Y, Carmen AA, Wu J, Grunstein M (2001) Highly specific antibodies determine histone acetylation site usage in yeast heterochromatin and euchromatin. Mol Cell 8: 473-479.
284. Creyghton MP, Cheng AW, Welstead GG, Kooistra T, Carey BW, Steine EJ, Hanna J, Lodato MA, Frampton GM, Sharp PA, Boyer LA, Young RA, Jaenisch R (2010) Histone H3K27ac separates active from poised enhancers and predicts developmental state. Proc Natl Acad Sci U S A 107: 21931-21936.
285. Rada-Iglesias A, Bajpai R, Swigut T, Brugmann SA, Flynn RA, Wysocka J (2011) A unique chromatin signature uncovers early developmental enhancers in humans. Nature 470: 279-283.
286. Jung HR, Pasini D, Helin K, Jensen ON (2010) Quantitative mass spectrometry of histones H3.2 and H3.3 in Suz12-deficient mouse embryonic stem cells reveals distinct, dynamic post-translational modifications at Lys-27 and Lys-36. Mol Cell Proteomics 9: 838-850.
287. Tie F, Banerjee R, Strattonk CA, Prasad-Sinha J, Stepanik V, Zlobin A, Diaz MO, Scacheri PC, Harte PJ (2009) CBP-mediated acetylation of histone H3 lysine 27 antagonizes Drosophila Polycomb silencing. Development 136: 3131-3141.
288. Brownell JE, Zhou J, Ranalli T, Kobayashi R, Edmondson DG, Roth SY, Allis CD (1996) Tetrahymena histone acetyltransferase A: a homolog to yeast Gcn5p linking histone acetylation to gene activation. Cell 84: 843-851.
289. Petruk S, Sedkov Y, Smith S, Tillib S, Kraevski V, Nakamura T, Canaani E, Croce CM, Mazo A (2001) Trithorax and dCBP acting in a complex to maintain expression of a homeotic gene. Science 294: 1331-1334.
290. Papp B, Müller J (2006) Histone trimethylation and the maintenance of transcriptional ON and OFF states by trxG and PcG proteins. Genes Dev 20: 2041-2054.
291. Hallson G, Hollebakken RE, Li T, Syrzycka M, Kim I, Cotsworth S, Fitzpatrick KA, Sinclair DA, Honda BM (2012) dSet1 is the main H3K4 di- and tri-methyltransferase throughout Drosophila development. Genetics 190: 91-100.
292. Smolik S, Jones K (2007) Drosophila dCBP is involved in establishing the DNA replication checkpoint. Mol Cell Biol 27: 135-146.
293. Schuettengruber B, Martinez AM, Iovino N, Cavalli G (2011) Trithorax group proteins: switching genes on and keeping them active. Nat Rev Mol Cell Biol 12: 799-814.
294. Ringrose L, Paro R (2004) Epigenetic regulation of cellular memory by the Polycomb and Trithorax group proteins. Annu Rev Genet 38: 413-443.

295. Poux S, Horard B, Sigrist CJ, Pirrotta V (2002) The Drosophila trithorax protein is a coactivator required to prevent re-establishment of polycomb silencing. Development 129: 2483-2493.
296. Rozovskaia T, Tillib S, Smith S, Sedkov Y, Rozenblatt-Rosen O, Petruk S, Yano T, Nakamura T, Ben-Simchon L, Gildea J, Croce CM, Shearn A, Canaani E, Mazo A (1999) Trithorax and ASH1 interact directly and associate with the trithorax group-responsive bxd region of the Ultrabithorax promoter. Mol Cell Biol 19: 6441-6447.
297. Chinwalla V, Jane EP, Harte PJ (1995) The Drosophila trithorax protein binds to specific chromosomal sites and is co-localized with Polycomb at many sites. EMBO J 14: 2056-2065.
298. Ogryzko VV, Schiltz RL, Russanova V, Howard BH, Nakatani Y (1996) The transcriptional coactivators p300 and CBP are histone acetyltransferases. Cell 87: 953-959.
299. Akimaru H, Chen Y, Dai P, Hou DX, Nonaka M, Smolik SM, Armstrong S, Goodman RH, Ishii S (1997) Drosophila CBP is a co-activator of cubitus interruptus in hedgehog signalling. Nature 386: 735-738.
300. Ludlam WH, Taylor MH, Tanner KG, Denu JM, Goodman RH, Smolik SM (2002) The acetyltransferase activity of CBP is required for wingless activation and H4 acetylation in Drosophila melanogaster. Mol Cell Biol 22: 3832-3841.
301. Tie F, Banerjee R, Conrad PA, Scacheri PC, Harte PJ (2012) Histone demethylase UTX and chromatin remodeler BRM bind directly to CBP and modulate acetylation of histone H3 lysine 27. Mol Cell Biol 32: 2323-2334.
302. Workman J, Kingston R (1998) Alteration of nucleosome structure as a mechanism of transcriptional regulation. Annu Rev Biochem 67: 545-579.
303. Owen-Hughes T, Workman JL (1994) Experimental analysis of chromatin function in transcription control. Crit Rev Eukaryot Gene Expr 4: 403-441.
304. Fairman-Williams ME, Guenther UP, Jankowsky E (2010) SF1 and SF2 helicases: family matters. Curr Opin Struct Biol 20: 313-324.
305. Clapier CR, Cairns BR (2009) The biology of chromatin remodeling complexes. Annu Rev Biochem 78: 273-304.
306. Norton VG, Imai BS, Yau P, Bradbury EM (1989) Histone acetylation reduces nucleosome core particle linking number change. Cell 57: 449-457.
307. Mutskov V, Gerber D, Angelov D, Ausio J, Workman J, Dimitrov S (1998) Persistent interactions of core histone tails with nucleosomal DNA following acetylation and transcription factor binding. Mol Cell Biol 18: 6293-6304.
308. Hecht A, Laroche T, Strahl-Bolsinger S, Gasser SM, Grunstein M (1995) Histone H3 and H4 N-termini interact with SIR3 and SIR4 proteins: a molecular model for the formation of heterochromatin in yeast. Cell 80: 583-592.
309. Edmondson DG, Smith MM, Roth SY (1996) Repression domain of the yeast global repressor Tup1 interacts directly with histones H3 and H4. Genes Dev 10: 1247-1259.
310. Johnson LM, Kayne PS, Kahn ES, Grunstein M (1990) Genetic evidence for an interaction between SIR3 and histone H4 in the repression of the silent mating loci in Saccharomyces cerevisiae. Proc Natl Acad Sci U S A 87: 6286-6290.
311. Tse C, Sera T, Wolffe AP, Hansen JC (1998) Disruption of higher-order folding by core histone acetylation dramatically enhances transcription of nucleosomal arrays by RNA polymerase III. Mol Cell Biol 18: 4629-4638.
312. Ogiwara H, Ui A, Otsuka A, Satoh H, Yokomi I, Nakajima S, Yasui A, Yokota J, Kohno T (2011) Histone acetylation by CBP and p300 at double-strand break sites facilitates SWI/SNF chromatin remodeling and the recruitment of non-homologous end joining factors. Oncogene 30: 2135-2146.
313. Hassan AH, Awad S, Al-Natour Z, Othman S, Mustafa F, Rizvi TA (2007) Selective recognition of acetylated histones by bromodomains in transcriptional co-activators. Biochem J 402: 125-133.
314. Chandy M, Gutiérrez JL, Prochasson P, Workman JL (2006) SWI/SNF displaces SAGA-acetylated nucleosomes. Eukaryot Cell 5: 1738-1747.
315. Struhl K (1998) Histone acetylation and transcriptional regulatory mechanisms. Genes Dev 12: 599-606.

316. Nagy Z, Tora L (2007) Distinct GCN5/PCAF-containing complexes function as co-activators and are involved in transcription factor and global histone acetylation. Oncogene 26: 5341-5357.

317. Vignali M, Steger DJ, Neely KE, Workman JL (2000) Distribution of acetylated histones resulting from Gal4-VP16 recruitment of SAGA and NuA4 complexes. EMBO J 19: 2629-2640.

318. Kasten M, Szerlong H, Erdjument-Bromage H, Tempst P, Werner M, Cairns BR (2004) Tandem bromodomains in the chromatin remodeler RSC recognize acetylated histone H3 Lys14. EMBO J 23: 1348-1359.

319. Vogelauer M, Wu J, Suka N, Grunstein M (2000) Global histone acetylation and deacetylation in yeast. Nature 408: 495-498.

320. Simon JA, Kingston RE (2009) Mechanisms of polycomb gene silencing: knowns and unknowns. Nat Rev Mol Cell Biol 10: 697-708.

321. Min J, Zhang Y, Xu RM (2003) Structural basis for specific binding of Polycomb chromodomain to histone H3 methylated at Lys 27. Genes Dev 17: 1823-1828.

322. Fischle W, Wang Y, Jacobs SA, Kim Y, Allis CD, Khorasanizadeh S (2003) Molecular basis for the discrimination of repressive methyl-lysine marks in histone H3 by Polycomb and HP1 chromodomains. Genes Dev 17: 1870-1881.

323. Lee MG, Villa R, Trojer P, Norman J, Yan KP, Reinberg D, Di Croce L, Shiekhattar R (2007) Demethylation of H3K27 regulates polycomb recruitment and H2A ubiquitination. Science 318: 447-450.

324. Schwartz YB, Kahn TG, Nix DA, Li XY, Bourgon R, Biggin M, Pirrotta V (2006) Genome-wide analysis of Polycomb targets in Drosophila melanogaster. Nat Genet 38: 700-705.

325. Mikkelsen TS, Ku M, Jaffe DB, Issac B, Lieberman E, Giannoukos G, Alvarez P, Brockman W, Kim TK, Koche RP, Lee W, Mendenhall E, O'Donovan A, Presser A, Russ C, Xie X, Meissner A, Wernig M, Jaenisch R, Nusbaum C, Lander ES, Bernstein BE (2007) Genome-wide maps of chromatin state in pluripotent and lineage-committed cells. Nature 448: 553-560.

326. Kanhere A, Viiri K, Araújo CC, Rasaiyaah J, Bouwman RD, Whyte WA, Pereira CF, Brookes E, Walker K, Bell GW, Pombo A, Fisher AG, Young RA, Jenner RG (2010) Short RNAs are transcribed from repressed polycomb target genes and interact with polycomb repressive complex-2. Mol Cell 38: 675-688.

327. Pan G, Tian S, Nie J, Yang C, Ruotti V, Wei H, Jonsdottir GA, Stewart R, Thomson JA (2007) Whole-genome analysis of histone H3 lysine 4 and lysine 27 methylation in human embryonic stem cells. Cell Stem Cell 1: 299-312.

328. Bernstein BE, Mikkelsen TS, Xie X, Kamal M, Huebert DJ, Cuff J, Fry B, Meissner A, Wernig M, Plath K, Jaenisch R, Wagschal A, Feil R, Schreiber SL, Lander ES (2006) A bivalent chromatin structure marks key developmental genes in embryonic stem cells. Cell 125: 315-326.

329. Stock JK, Giadrossi S, Casanova M, Brookes E, Vidal M, Koseki H, Brockdorff N, Fisher AG, Pombo A (2007) Ring1-mediated ubiquitination of H2A restrains poised RNA polymerase II at bivalent genes in mouse ES cells. Nat Cell Biol 9: 1428-1435.

330. Zhao XD, Han X, Chew JL, Liu J, Chiu KP, Choo A, Orlov YL, Sung WK, Shahab A, Kuznetsov VA, Bourque G, Oh S, Ruan Y, Ng HH, Wei CL (2007) Whole-genome mapping of histone H3 Lys4 and 27 trimethylations reveals distinct genomic compartments in human embryonic stem cells. Cell Stem Cell 1: 286-298.

331. Eberlin A, Grauffel C, Oulad-Abdelghani M, Robert F, Torres-Padilla ME, Lambrot R, Spehner D, Ponce-Perez L, Würtz JM, Stote RH, Kimmins S, Schultz P, Dejaegere A, Tora L (2008) Histone H3 tails containing dimethylated lysine and adjacent phosphorylated serine modifications adopt a specific conformation during mitosis and meiosis. Mol Cell Biol 28: 1739-1754.

332. Garcia-Bassets I, Kwon YS, Telese F, Prefontaine GG, Hutt KR, Cheng CS, Ju BG, Ohgi KA, Wang J, Escoubet-Lozach L, Rose DW, Glass CK, Fu XD, Rosenfeld MG (2007) Histone methylation-dependent mechanisms impose ligand dependency for gene activation by nuclear receptors. Cell 128: 505-518.

333. Björntorp P, Rosmond R (2000) Obesity and cortisol. Nutrition 16: 924-936.

334. Guillaume-Gentil C, Rohner-Jeanrenaud F, Abramo F, Bestetti GE, Rossi GL, Jeanrenaud B (1990) Abnormal regulation of the hypothalamo-pituitary-adrenal axis in the genetically obese fa/fa rat. Endocrinology 126: 1873-1879.
335. Suderman M, McGowan PO, Sasaki A, Huang TC, Hallett MT, Meaney MJ, Turecki G, Szyf M (2012) Conserved epigenetic sensitivity to early life experience in the rat and human hippocampus. Proc Natl Acad Sci U S A 109: 17266-17272.
336. McGowan PO, Sasaki A, D'Alessio AC, Dymov S, Labonté B, Szyf M, Turecki G, Meaney MJ (2009) Epigenetic regulation of the glucocorticoid receptor in human brain associates with childhood abuse. Nat Neurosci 12.
337. McGowan PO, Meaney MJ, Szyf M (2008) Diet and the epigenetic (re)programming of phenotypic differences in behavior. Brain Res 1237: 12-24.
338. Gibney ER, Nolan CM (2010) Epigenetics and gene expression. Heredity (Edinb) 105: 4-13.
339. Kouzarides T (2007) Chromatin modifications and their function. Cell 128: 693-705.
340. Czermin B, Melfi R, McCabe D, Seitz V, Imhof A, V. P (2002) Drosophila Enhancer of Zeste/ESC complexes have a histone H3 methyltransferase activity thatmarks chromosomalPolycomb sites. Cell 111: 185096.
341. Wang C, Bomberg E, Levine A, Billington C, Kotz CM (2007) Brain-derived neurotrophic factor in the ventromedial nucleus of the hypothalamus reduces energy intake. Am J Physiol Regul Integr Comp Physiol 293: R1037-1045.
342. Grove KL, Grayson BE, Glavas MM, Xiao XQ, Smith MS (2005) Development of metabolic systems. Physiol Behav 86: 646-660.
343. Roth TL, Lubin FD, Funk AJ, Sweatt JD (2009) Lasting epigenetic influence of early-life adversity on the BDNF gene. Biol Psychiatry 65: 760-769.
344. Roth TL, Sweatt JD (2011) Epigenetic marking of the BDNF gene by early-life adverse experiences. Horm Behav 59: 315-320.
345. Laemmli UK (1970) Cleavage of structural proteins during the assembly of the head of bacteriophage T4. Nature 227: 680-685.
346. Yu Y, Zhang H, Byerly MS, Bacon LD, Porter TE, Liu GE, Song J (2009) Alternative splicing variants and DNA methylation status of BDNF in inbred chicken lines. Brain Res 1269.
347. Levenson JM, Sweatt JD (2005) Epigenetic mechanisms in memory formation. Nat Rev Neurosci 6: 108-118.
348. Sharp FR, Bernaudin M (2004) HIF1 and oxygen sensing in the brain. Nat Rev Neurosci 5: 437-448.
349. Funato H, Oda S, Yokofujita J, Igarashi H, Kuroda M (2011) Fasting and high-fat diet alter histone deacetylase expression in the medial hypothalamus. PLoS One 15: 4.
350. Plagemann A, Harder T, Rodekamp E, Kohlhoff R (2012) Rapid neonatal weight gain increases risk of childhood overweight in offspring of diabetic mothers. J Perinat Med 40: 557-563.
351. Vucetic Z, Carlin JL, Totoki K, Reyes TM (2012) Epigenetic dysregulation of the dopamine system in diet-induced obesity. J Neurochem 120: 891-898.
352. Korosi A, Shanabrough M, McClelland S, Liu ZW, Borok E, Gao XB, Horvath TL, Baram TZ (2010) Early-life experience reduces excitation to stress-responsive hypothalamic neurons and reprograms the expression of corticotropin-releasing hormone. J Neurosci 30: 703-713.
353. Tetievsky A, Cohen O, Eli-Berchoer L, Gerstenblith G, Stern MD, Wapinski I, Friedman N, Horowitz M (2008) Physiological and molecular evidence of heat acclimation memory: a lesson from thermal responses and ischemic cross-tolerance in the heart. Physiol Genomics 34: 78-87.
354. Pandolf KB (1998) Time course of heat acclimation and its decay. Int J Sports Med: S157-160.
355. Nekrasov M, Klymenko T, Fraterman S, Papp B, Oktaba K, Köcher T, Cohen A, Stunnenberg HG, Wilm M, Müller J (2007) Pcl-PRC2 is needed to generate high levels of H3-K27 trimethylation at Polycomb target genes. EMBO J 26: 4078-4088.

356. Margueron R, Justin N, Ohno K, Sharpe ML, Son J, Drury WJ, Voigt P, Martin SR, Taylor WR, De Marco V, Pirrotta V, Reinberg D, Gamblin SJ (2009) Role of the polycomb protein EED in the propagation of repressive histone marks. Nature 461: 762-767.

357. Cao R, Zhang Y (2004) SUZ12 Is Required for Both the Histone Methyltransferase Activity and the Silencing Function of the EED-EZH2 Complex. Mol Cell 15: 57-67.

358. Pasini D, Bracken AP, Jensen MR, Lazzerini Denchi E, Helin K (2004) Suz12 is essential for mouse development and for EZH2 histone methyltransferase activity. EMBO J 23: 4061-4071.

359. Chamberlain SJ, Yee D, Magnuson T (2008) Polycomb repressive complex 2 is dispensable for maintenance of embryonic stem cell pluripotency. Stem Cells 26: 1496-1505.

360. Jeanneteau FD, Lambert WM, Ismaili N, Bath KG, Lee FS, Garabedian MJ, Chao MV (2012) BDNF and glucocorticoids regulate corticotrophin-releasing hormone (CRH) homeostasis in the hypothalamus. Proc Natl Acad Sci U S A 109: 1305-1310.

361. Dambacher S, Hahn M, Schotta G (2010) Epigenetic regulation of development by histone lysine methylation. Heredity (Edinb) 105: 24-37.

362. Margueron R, Li G, Sarma K, Blais A, Zavadil J, Woodcock CL, Dynlacht BD, Reinberg D (2008) Ezh1 and Ezh2 maintain repressive chromatin through different mechanisms. Mol Cell 32.

363. Klymenko T, Muller J (2004) The histone methyltransferases Trithorax and Ash1 prevent transcriptional silencing by Polycomb group proteins. EMBO Rep 5: 373-377.

364. Smolik S, Jones K (2007) Drosophila dCBP is involved in establishing the DNA replication checkpoint. Mol Cell Biol 27: 135-146.

365. Branchi I (2009) The mouse communal nest: investigating the epigenetic influences of the early social environment on brain and behavior development. Neurosci Biobehav Rev 33: 551-559.

366. Branchi I, D'Andrea I, Fiore M, Di Fausto V, Aloe L, Alleva E (2006) Early social enrichment shapes social behavior and nerve growth factor and brain-derived neurotrophic factor levels in the adult mouse brain. Biol Psychiatry 60: 690-696.

367. Zalachoras I, Evers MM, van Roon-Mom WM, Aartsma-Rus AM, Meijer OC (2011) Antisense-mediated RNA targeting: versatile and expedient genetic manipulation in the brain. Front Mol Neurosci 4: 1-23.

368. Dias N, Stein CA (2002) Antisense oligonucleotides: basic concepts and mechanisms. Mol Cancer Ther 1: 347-355.

369. Larrouy B, Blonski C, Boiziau C, Stuer M, Moreau S, Shire D, Toulmé JJ (1992) RNase H-mediated inhibition of translation by antisense oligodeoxyribonucleotides: use of backbone modification to improve specificity. Gene 121: 189-194.

370. Cazenave C, Frank P, Bütsen W (1993) Characterization of ribonuclease H activities present in two cell-free protein synthesizing systems, the wheat germ extract and the rabbit reticulocyte lysate. Biochimie 75: 113-122.

371. Minshull J, Hunt T (1986) The use of single-stranded DNA and RNase H to promote quantitative 'hybrid arrest of translation' of mRNA/DNA hybrids in reticulocyte lysate cell-free translations. Nucleic Acids Res 14: 6433-6451.

372. Baker BF, Lot SS, Condon TP, Cheng-Flournoy S, Lesnik EA, Sasmor HM, Bennett CF (1997) 2'-O-(2-Methoxy)ethyl-modified anti-intercellular adhesion molecule 1 (ICAM-1) oligonucleotides selectively increase the ICAM-1 mRNA level and inhibit formation of the ICAM-1 translation initiation complex in human umbilical vein endothelial cells. J Biol Chem 272: 11994-12000.

373. Lai JC, Tan W, Benimetskaya L, Miller P, Colombini M, Stein CA (2006) A pharmacologic target of G3139 in melanoma cells may be the mitochondrial VDAC. Proc Natl Acad Sci U S A 103: 7494-7499.

374. Hong DS, Kurzrock R, Oh Y, Wheler J, Naing A, Brail L, Callies S, André V, Kadam SK, Nasir A, Holzer TR, Meric-Bernstam F, Fishman M, Simon G (2011) A phase 1 dose escalation, pharmacokinetic, and pharmacodynamic

evaluation of eIF-4E antisense oligonucleotide LY2275796 in patients with advanced cancer. Clin Cancer Res 17: 6582-6591.

375. Stein CA, Goel S (2011) Therapeutic oligonucleotides: the road not taken. Clin Cancer Res 17: 6369-6372.

376. Schellong K, Schulz S, Harder T, Plagemann A (2012) Birth weight and long-term overweight risk: systematic review and a meta-analysis including 643,902 persons from 66 studies and 26 countries globally. PLoS One 7: e47776.

377. Labunskay G, Meiri N (2006) R-Ras3/(M-Ras) is involved in thermal adaptation in the critical period of thermal control establishment. J Neurobiol 66: 56-70.

378. Yahav S, McMurtry JP (2001) Thermotolerance acquisition in broiler chickens by temperature conditioning early in life--the effect of timing and ambient temperature. Poult Sci 80: 1662-1666.

379. O'Carroll D, Erhardt S, Pagani M, Barton SC, Surani MA, Jenuwein T (2001) The polycomb-group gene Ezh2 is required for early mouse development. Mol Cell Biol 21: 4330-4336.

380. Smith KL, Herron B, Dowell-Mesfin N, Wu H, Kim SJ, Shain W, Hynd MR (2012) Knockdown of cortical transthyretin expression around implanted neural prosthetic devices using intraventricular siRNA injection in the brain. J Neurosci Methods 203: 398-406.

381. Lingor P, Koeberle P, Kügler S, Bähr M (2005) Down-regulation of apoptosis mediators by RNAi inhibits axotomy-induced retinal ganglion cell death in vivo. Brain 128: 550-558.

382. Manrique C, Compan V, Rosselet C, Duflo SG (2009) Specific knock-down of GAD67 in the striatum using naked small interfering RNAs. J Biotechnol 142: 185-192.

383. Nakajima H, Kubo T, Semi Y, Itakura M, Kuwamura M, Izawa T, Azuma YT, Takeuchi T (2012) A rapid, targeted, neuron-selective, in vivo knockdown following a single intracerebroventricular injection of a novel chemically modified siRNA in the adult rat brain. J Biotechnol 157: 326-333.

384. Anonymous (2013) Silencer® Select siRNAs from Ambion®. Life Technology.

385. Thakker DR, Natt F, Hüsken D, Maier R, Müller M, van der Putten H, Hoyer D, Cryan JF (2004) Neurochemical and behavioral consequences of widespread gene knockdown in the adult mouse brain by using nonviral RNA interference. Proc Natl Acad Sci U S A 101: 17270-17275.

386. Shim MS, Kwon YJ (2010) Efficient and targeted delivery of siRNA in vivo. FEBS J 277: 4814-4827.

387. Tie F, Banerjee R, Stratton CA, Prasad-Sinha J, Stepanik V, Zlobin A, Diaz MO, Scacheri PC, Harte PJ (2009) CBP-mediated acetylation of histone H3 lysine 27 antagonizes Drosophila Polycomb silencing. Development 136: 3131-3141.

388. Grimaldi G, Christian M, Steel JH, Henriet P, Poutanen M, Brosens JJ (2011) Down-regulation of the histone methyltransferase EZH2 contributes to the epigenetic programming of decidualizing human endometrial stromal cells. Mol Endocrinol 25: 1892-1903.